UNIVERSITÄT BONN

Investigating the effects of sphingosine-1-phosphate lyase (SGPL1) ablation in mouse embryonic fibroblasts and primary astrocytes

Dissertation

zur

Erlangung des Doktorgrades (Dr. rer. nat.)

der

Mathematisch-Naturwissenschaftlichen Fakultät

der

Rheinischen Friedrich-Wilhelms-Universität Bonn

vorgelegt von

Sumaiya Yasmeen Afsar

aus

Allahabad, Indien

Bonn, 2023

Angefertigt mit Genehmigung der Mathematisch-Naturwissenschaftlichen Fakultät der Rheinischen Friedrich-Wilhelms-Universität Bonn in der Zeit von Juni 2020 bis Mai 2023 am Kekulé-Institut für Organische Chemie und Biochemie unter der Leitung von Frau PD. Dr. Gerhild van Echten-Deckert.

1. Referentin: PD. Dr. Gerhild van Echten-Deckert

2. Referent: Prof. Dr. Dirk Menche

Tag der Promotion: 30.08.2023

Erscheinungsjahr: 2023

"No two things have been combined better than knowledge and patience"

Dedicated to my husband for his support throughout my pursuit of knowledge

ABSTRACT

Sphingosine-1-phosphate (S1P) is a bioactive lipid that plays a crucial role in various fundamental processes, including cellular proliferation, survival, migration, as well as inflammation. Additionally, it has been implicated in the development and progression of cancer as well. S1P metabolism, regulated by S1P-lyase (SGPL1) and its receptors, $S1PR_{1–5}$, plays a critical role in maintaining cellular homeostasis. In this study, the impact of S1P on glucose metabolism was investigated using SGPL1-deficient mouse embryonic fibroblasts (*Sgpl1*$^{-/-}$ MEFs). SGPL1 deficiency lead to accumulation of S1P which activates hypoxia-inducible factor 1 (HIF-1) and promotes the expression of glucose metabolism-related proteins through $S1PR_{1–3}$ receptors, leading to increased glucose-to-lactate conversion and cell proliferation, resembling cancer cells. Importantly, these metabolic changes did not negatively affect cellular energy status, as indicated by Akt/mTOR pathway activation and downregulation of autophagy. These results reveal a distinctive role of the S1P/$S1PR_{1–3}$ axis in glucose metabolism in SGPL1-deficient MEFs.

Moreover, the role of S1P in different neurodegenerative diseases is not yet clear, as there are contrasting findings. On the one hand it was shown to be crucial for brain development. Lack of S1P during embryonic development is extremely dangerous and can cause the failure of various essential processes, such as the closure of the front part of the neural tube. On the other hand, an excessive amount of S1P, due to mutations in the SGPL1 responsible for its cleavage, is also detrimental. It is worth mentioning that the SGPL1 gene is located in a region of the genome that is prone to mutations found in several types of human cancers. Additionally, mutations in SGPL1 can lead to a condition called S1P-lyase insufficiency syndrome (SPLIS), which is characterized by various symptoms, including neurological defects in both the peripheral and central nervous systems. This study shows the impact of S1P lyase in astrocytes derived from neural-targeted SGPL1 deficient mice ($SGPL1^{fl/fl/Nes}$). SGPL1 deficiency led to S1P accumulation, resulting in increased expression of glycolytic enzymes similar to MEFs. However, in SGPL1-deficient astrocytes, pyruvate utilization was through tricarboxylic acid (TCA) cycle via $S1PR_{2,4}$ receptors. This metabolic shift increased cellular ATP content and activated the mammalian target of rapamycin (mTOR), thus affecting autophagy in astrocytes. Furthermore, elevated extracellular ADP levels, mediated by the purinoreceptor P2Y1 (P2Y1R) in SGPL1-deficient astrocytes induced astrogliosis and

NLRP3 inflammasome activation, leading to the generation of proinflammatory cytokines.

These findings shed new light on the oncogenic implications of S1P metabolism and present opportunities for modulating membrane lipid composition as well as offer valuable insights into the interplay between astrocyte functionality and NLRP3 inflammasome. Targeting S1P metabolism and signaling pathways could potentially serve as novel therapeutic approaches and contribute to a better understanding of S1P function not only in brain pathology but also with regard to the complex phenotype of patients exhibiting mutations in SGPL1.

TABLE OF CONTENTS

1. INTRODUCTION

1.1 Lipids

Lipids are a diverse group of molecules that are composed of fatty acids and their derivatives, and they can be categorized into eight main classes: fatty acyls, glycerolipids, glycerophospholipids, sphingolipids, sterol lipids, prenol lipids, saccharolipids, and polyketides (Fahy, Subramaniam et al. 2009). Each class contains different subclasses and molecular variations which enables them to perform a wide range of critical biological functions. The role of lipids in the formation of cell membranes makes them both ligand and substrate for proteins. Besides, extensive research conducted over the past decades has revealed that certain membrane lipids also function as secondary messengers during cell signaling. These lipid second messengers interact with specific biochemical targets such as protein kinases, phosphatases, and metabolic enzymes, triggering a cascade of cellular changes (Hannun and Bell 1989, Bae, Cantley et al. 1998).

In the brain, the lipid composition possesses distinct characteristics that set it apart from other regions of the body. Membrane lipids, particularly phospholipids, are the predominant constituents and account for more than half of the solid matter in the brain. This unique lipid profile is crucial for the proper functioning of brain cells and contributes to various essential biological processes (Crawford and Sinclair 1971).

Phospholipids are a class of lipids composed of glycerol, fatty acids, and a phosphate group, which are pivotal constituents of cellular membranes. These amphipathic molecules self-assemble into lipid bilayers, forming the structural backbone of cell membranes and providing a selectively permeable barrier between the cell and its environment. However, the influence of phospholipids extends far beyond their structural role, as they actively serve as precursors for the synthesis of essential signaling molecules that regulate various cellular processes (Fahy, Subramaniam et al. 2009). One prominent example from the family of sphingolipid is known as sphingomyelin, which is the precursor for ceramide, a bioactive lipid involved in numerous cellular processes, including apoptosis, cell proliferation, and cellular stress responses. Ceramide acts as a signaling molecule, mediating diverse cellular pathways, and orchestrating cellular responses to extracellular stimuli (Taha, Mullen et al. 2006). Another notable phospholipid-derived signaling molecule is docosahexaenoic acid (DHA), an omega-3 fatty acid that plays a crucial role in brain development and function (Hannun and Obeid

2008). Furthermore, arachidonic acid, a polyunsaturated fatty acid serves as the precursor for the synthesis of diverse bioactive lipid mediators, including prostaglandins, leukotrienes, and thromboxane, which are involved in inflammation, immune responses, and vascular homeostasis (Hannun and Obeid 2008).

1.2 Sphingolipid

Discovered in the 1870s in the brain extracts, sphingolipids were named after the mythological sphinx based on their distinct and mysterious structural features (Thudichum 1884). Initially regarded mainly as a cellular building material or involved in metabolic processes (Divecha and Irvine 1995), sphingolipids have emerged as key signaling molecules, sparking ongoing investigations (Spiegel and Milstien 2000, van Echten-Deckert 2020). These intriguing compounds are prominently found in abundance within the brain, where they exert pivotal roles in its development, functionality, and serve as crucial constituents of plasma membrane at the cellular level (Olsen and Faergeman 2017).

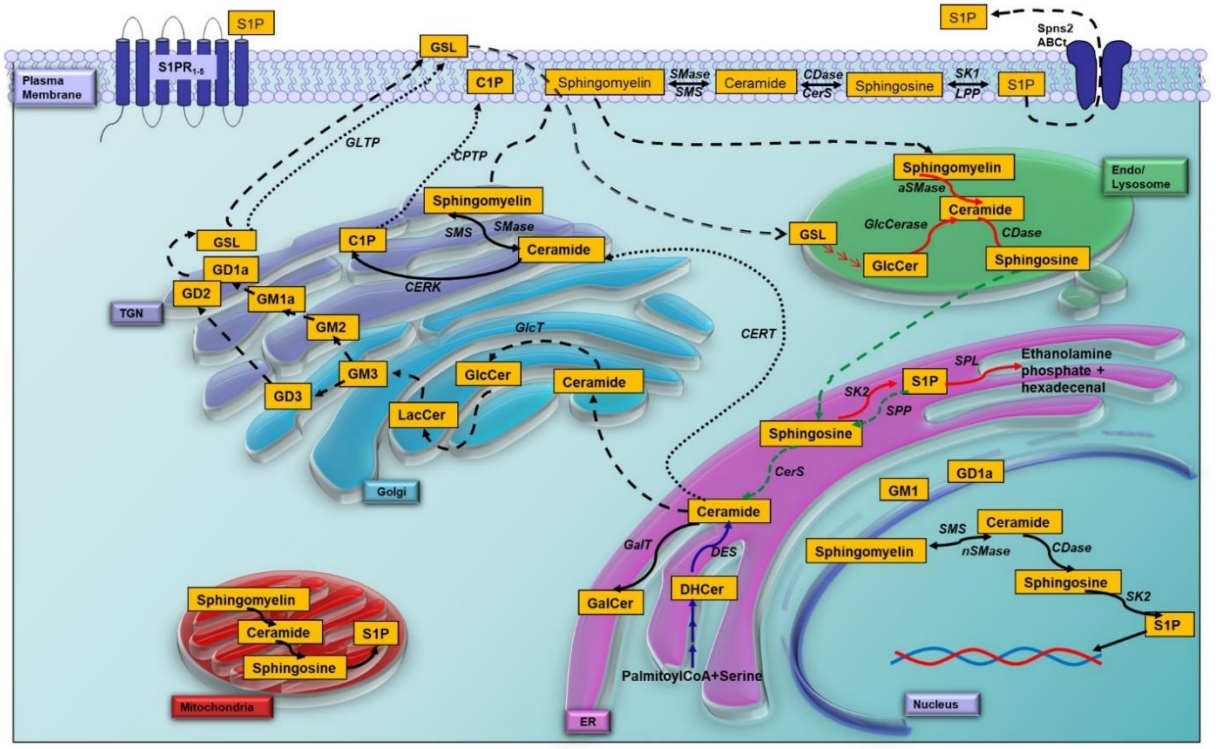

Figure 1. Schematic representation of prevalent locations and metabolic pathways of cellular sphingolipids. Ceramide is biosynthesized de novo in the ER (purple, blue arrows). It is then translocated *via* CERT, (black dotted arrows) to the site of sphingomyelin and C1P formation in the trans-Golgi network (TGN, purple) or *via* vesicular exocytotic membrane flow (black dashed arrows) to the site of glycosylation to glucosylceramide (GlcCer) in the Golgi compartment (blue) and more complex glycosphingolipids (GSL), including gangliosides (black dashed arrows). Degradation of sphingolipids down to sphingosine occurs mainly in the lysosomal compartment (red arrows). Further metabolization of sphingosine is located to the ER, where it is first phosphorylated to S1P and then cleaved into ethanolamine phosphate and hexadecenal. Alternatively, S1P can be dephosphorylated back to sphingosine and further recycled to ceramide and all other sphingolipids *via* the salvage pathway (green dashed arrows). S1P generated in the plasma membrane by SK1 can be transported into the extracellular milieu *via* ATP-binding cassette transporters (ABCt) or SPNS2 where it acts as a ligand of S1PR1-5. Transport of (glyco)

sphingolipids occurs *via* vesicles (dashed black arrows) or transport proteins (dotted arrows). Sphingolipids are metabolized also in the plasma membrane, mitochondria, and nuclei. Abbreviations used are CPTP, C1P transport protein; GlcCerase, glucocerebrosidase; GLTP, glycolipid transport protein; and LPP, lipid phosphate phosphatase. (Piazzesi, Afsar et al. 2021).

Similar to glycerolipids and sterols, sphingolipids initiate their journey in the endoplasmic reticulum (ER), with the condensation of serine and fatty acyl-CoA. A series of enzymes, namely serine palmitoyl transferase (SPT), 3-ketodihydrosphingosine reductase, dihydroceramide synthases, and dihydroceramide desaturase, work consecutively to generate ceramide (Fig. 1). Ceramidases then convert ceramide into sphingosine, while sphingosine kinases (SKs), specifically SK1 and SK2 isoforms, phosphorylate sphingosine to produce S1P (van Echten-Deckert and Herget 2006). SK1 and SK2 isoforms exhibit distinct cellular locations and functions (Kohama, Olivera et al. 1998, Maceyka, Harikumar et al. 2012). At the junction of sphingolipid and phospholipid metabolism, the degradation of S1P occurs through an irreversible cleavage catalyzed by sphingosine 1-phosphate lyase (SGPL1), located in the ER and resulting in the formation of ethanolamine phosphate (EAP) and hexadecenal. This cleavage serves as the exit point of the sphingolipid degradation pathway. As a result, SGPL1 connects the metabolism of sphingolipids with that of glycerophospholipids by generating the headgroup of phosphatidylethanolamine. S1P can also be dephosphorylated by S1P phosphatases (SPP) and subsequently traced back to ceramide *via* the salvage pathway, mediated by ceramide synthases.

Overall, the intricate actions of these enzymes, including SPPs, CerS, and SGPL1, play a crucial role in regulating the levels of S1P and maintaining the balance of sphingolipid metabolism. Additionally, sphingolipid metabolism is regulated by a variety of signaling pathways, including the sphingomyelinase-ceramide pathway, which is activated in response to stress and cell death signals. These processes are essential for proper cellular functioning and are crucial for various physiological and pathological processes in the central nervous system (CNS). Dysregulation of sphingolipid metabolism has been implicated in several human diseases, including various forms of cancer, neurodegeneration, and metabolic disorders (van Kruining, Luo et al. 2020). For instance, defects in sphingolipid metabolism have been linked to the pathogenesis of neurodegenerative diseases such as Alzheimer's and Parkinson's diseases while elevated levels of certain sphingolipids have been associated with the development of cancer (Piazzesi, Afsar et al. 2021).

1.3 Sphingosine 1-Phosphate (S1P)

S1P is an evolutionarily conserved bioactive sphingolipid molecule that regulates various biological processes, including cell signaling, immune regulation, vascular development, and inflammation (Spiegel and Milstien 2011). As mentioned before, the synthesis of sphingolipids initiates with the combination of L-serine and a fatty acid, facilitated by the enzyme serine palmitoyl transferase (SPT). This process yields 3-ketodihydrosphingosine, which is subsequently reduced to sphinganine, and it undergoes further conversion to dihydroceramide through acylation with fatty acids, employing one of six ceramide synthases (CerS1–CerS6). By means of desaturation, dihydroceramide is transformed into ceramide *via* the *de-novo* pathway (Hagen-Euteneuer, Lutjohann et al. 2012, Grassi, Mauri et al. 2019) (Fig. 2).

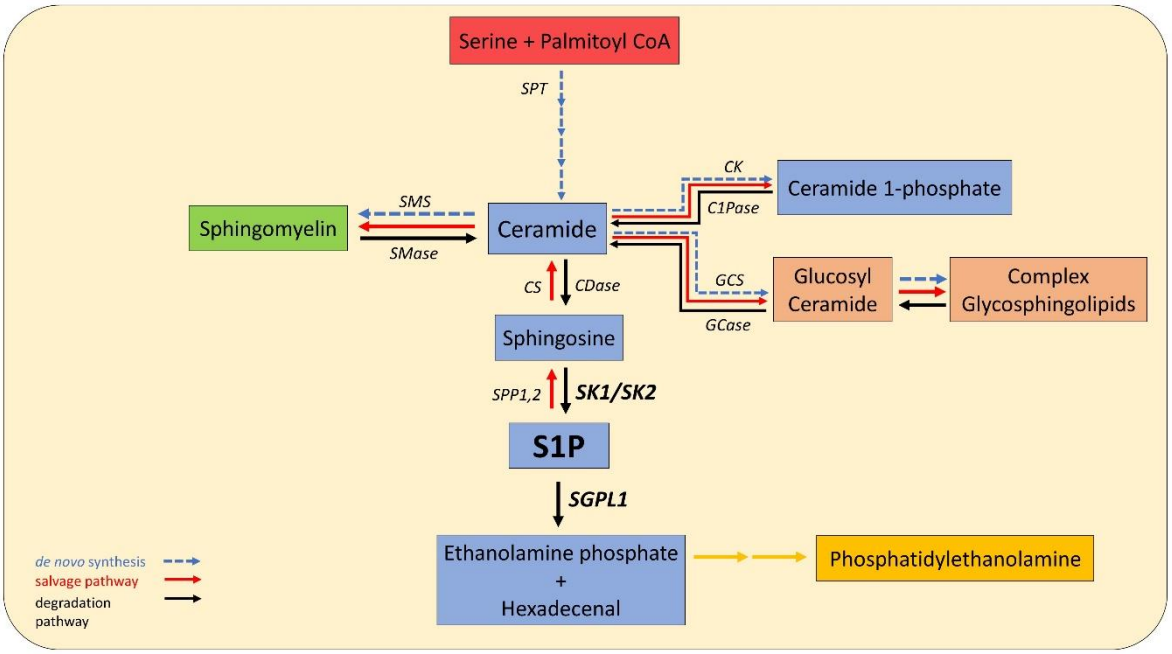

Figure 2. Scheme of sphingolipid metabolism. Ceramide formation *via* the *de novo* pathway is shown with 4 blue arrows. SPT catalyzes the first and rate-limiting condensation of serine and palmitoyl CoA. Ceramide is the starting point for *de novo* formation of sphingomyelin, C1P and all glycosphingolipids starting with glucosylceramide (blue arrows). But it is also a degradation product of all sphingolipids (black arrows). Sphingosine and S1P are exclusively catabolic products of ceramide. Finally, S1P can be dephosphorylated back to sphingosine starting an energy consuming recycling/salvage pathway (red arrows). See also (van Echten-Deckert 2023).

Additionally, ceramide has the capacity to undergo modifications and associate with different groups, leading to the formation of complex sphingolipids such as sphingomyelins, ceramide-1-phosphate, glycosyl ceramides, gangliosides (Taha, Mullen et al. 2006). Conversely, complex sphingolipids can also serve as a source of ceramide through reversible reactions in sphingomyelin metabolism. The enzyme ceramidase catalyzes the deacylation of ceramide,

resulting in the production of sphingosine (Fig. 2). Sphingosine can be employed for the resynthesis of ceramide or the generation of S1P. The balance among ceramide, sphingosine, and S1P, known as the sphingolipid rheostat, plays a vital role in maintaining organismal homeostasis (Spiegel and Milstien 2000). Sphingosine kinases (SKs) serve as the primary regulators and exist as two main isoforms, SK1 and SK2, which have been identified and characterized. While they share similar polypeptide structures, they exhibit notable distinctions in terms of kinetic properties, cellular localization, and physiological functions (Spiegel and Milstien 2000, Spiegel and Milstien 2003). S1P generated by SKs can be eliminated from the sphingomyelin cycle through the action of S1P lyase, which converts S1P into ethanolamine phosphate and hexadecenal. This process represents the sole irreversible reaction within the sphingomyelin cycle, where S1P functions as the final product.

Once formed, S1P serves as a potent signaling molecule that can bind to and activate a family of five G protein-coupled receptors known as S1P receptors ($S1PR_{1-5}$), each with distinct sub-cellular distribution and signaling properties and exerts significant regulatory effects on various biological processes. These effects include immune cell trafficking and migration (Spiegel and Milstien 2011, Thuy, Reimann et al. 2014), monitoring autophagy (Karunakaran, Alam et al. 2019), regulating cell growth (Olivera and Spiegel 1993), and apoptosis (Cuvillier, Pirianov et al. 1996). The emerging understanding of S1P's receptor independent actions highlights the complexity of S1P signaling and its multifaceted roles in cellular physiology. While our understanding of the intracellular effects of S1P is still limited, recent experimental evidence suggests that S1P can also exert receptor-independent actions in maintaining calcium levels and histone modification (Alam, Piazzesi et al. 2020). Further research is needed to unravel the precise mechanisms underlying these effects and their functional implications. Investigating the interplay between S1P receptors and the receptor-independent actions of S1P will enhance the understanding of intricate regulatory networks in which S1P participates, ultimately opening up new avenues for therapeutic interventions targeting S1P signaling pathways.

1.4 S1P in neurodegeneration

Neurodegenerative disorders are often identified by the accumulation of abnormal proteins either within the cells or outside them. These disorders include for instance Alzheimer's disease (AD), which is characterized by the presence of amyloid-β and tau proteins, Parkinson's disease (PD), associated with α-synuclein protein. In the CNS, S1P can perform protective functions and induce survival-stimulating signaling pathways or, conversely,

contribute to the development of pathological processes, including neurodegenerative disorders. The functions of S1P, the expression of its receptors, and their action depend on the type of CNS cells, the stage of their development, and the state of the whole organism. The physiological functions and pathological implications of S1P in various neurodegenerative diseases are currently being explored in scientific literature (Karunakaran and van Echten-Deckert 2017, Wang and Bieberich 2018, van Echten-Deckert 2023). Recent studies have provided evidence linking S1P to the development of brain cells in neurodegenerative conditions (Mitroi, Karunakaran et al. 2017, Moruno-Manchon, Uzor et al. 2018). Research indicates that S1P metabolism and signaling pathways differ among different types of brain cells, such as neurons, astrocytes, and microglia (Wang and Bieberich 2018). However, the role of S1P in neurodegenerative diseases remains controversial, with some studies suggesting a protective function of S1P signaling (He, Huang et al. 2010, Ceccom, Loukh et al. 2014, Couttas, Kain et al. 2014), while others, including the van Echten-Deckert group, report the detrimental effects of accumulated S1P in the brain (Hagen, Hans et al. 2011, Takasugi, Sasaki et al. 2011, Mitroi, Deutschmann et al. 2016, Lei, Shafique et al. 2017, Mitroi, Karunakaran et al. 2017, Karunakaran, Alam et al. 2019, Alam, Piazzesi et al. 2020).

The research conducted by the group of van Echten-Deckert has shed light on the diverse impact of accumulated S1P on autophagic pathways in various brain cell types, including microglia and neurons (Mitroi, Karunakaran et al. 2017, Karunakaran, Alam et al. 2019). In a study carried out by Mitroi et al. (2017), it was demonstrated that inhibiting SGPL1 resulted in impaired neuronal autophagy due to a reduction in PE production in SGPL1-deficient neurons (PE is synthesized from ethanolamine phosphate). However, the autophagy defects were restored when neurons were treated with PE. It is important to note that disrupted autophagy in the brain is considered a significant contributing factor to the development of neurodegenerative disorders. Conversely, Moruno-Manchon et al. (2015) observed that upregulating SK1, an enzyme responsible for phosphorylating sphingosine to generate S1P, promoted autophagy in neurons (Moruno Manchon, Uzor et al. 2015). In contrast, enzymes SPP and SGPL1, which degrade S1P, reduced the flux of autophagy. Another group of researchers demonstrated that SK2 played a primary role in inducing autophagy through preconditioning. By utilizing isoflurane and hypoxic preconditioning, they upregulated SK2 and induced autophagy by disrupting Bcl-2/beclin1 complexes in primary cortical neurons (Sheng, Zhang et al. 2014).

1.5 Mouse Embryonic Fibroblast (MEFs)

Mouse embryonic fibroblasts (MEFs) are a type of connective tissue cells derived from mouse embryos. They are commonly used in biomedical research as a model system to study various biological processes and functions. MEFs are derived from the mesoderm layer of the developing mouse embryo. Once obtained, MEFs can be cultured and propagated in the laboratory using standard cell culture techniques. They have a fibroblast-like morphology and exhibit characteristic properties of mesenchymal cells. MEFs are adherent cells that grow as a monolayer and display a spindle-shaped morphology. MEFs are valuable tools for studying various aspects of cell biology, including cell signaling, gene expression, cell cycle regulation, and cellular responses to different stimuli. They can be genetically manipulated using techniques such as transfection or viral transduction to investigate the functions of specific genes or pathways. In the present study the activities of S1P were investigated using fibroblasts from SGPL1 deficient mice (*Sgpl1*$^{-/-}$ MEFs) which leads to the accumulation of S1P.

Mice with a targeted deletion of SGPL1 exhibit distinct characteristics, including reduced weight gain and a shortened lifespan of around 8 weeks (Schmahl, Raymond et al. 2007, Ihlefeld, Claas et al. 2012). These mice display multiple organ defects, such as abnormalities in the vasculature, skeleton, and kidney dysfunction (Schmahl, Raymond et al. 2007). S1P lyase-deficient mice have elevated levels of S1P, sphingosine, and/or ceramide in their serum and tissues (Vogel, Donoviel et al. 2009, Ihlefeld, Claas et al. 2012). In a previous study using *Sgpl1*$^{-/-}$ MEFs, accumulation of S1P and of sphingosine (Claas, ter Braak et al. 2010) as well as of sphingomyelin (Hagen-Euteneuer, Alam et al. 2020) was also recently observed in these cultured cells. In fact, Hagen et al (2020) from the group of van Echten Deckert, have shown that the production of biosynthetic precursors of complex glycosphingolipids including ceramide, glucosylceramide and also ganglioside GM3 *via* the *de novo* synthesis and recycling pathway was substantially increased whereas the amount of more complex gangliosides dropped significantly in MEFs with SGPL1 ablation.

Moreover, *Sgpl1*$^{-/-}$ MEFs also exhibited disturbed calcium Ca^{2+} homeostasis, characterized by increased basal cytosolic free Ca^{2+} concentrations $[Ca^{2+}]_i$ enhanced agonist-induced $[Ca^{2+}]i$ increases, and elevated Ca^{2+} storage in thapsigargin-sensitive stores (Claas, ter Braak et al. 2010). Also, the same group in their later investigation, discovered high levels of S1P specifically in nuclear preparations of *Sgpl1*$^{-/-}$ MEFs and also demonstrated a reduction in both HDAC activity and the expression of HDAC isoenzymes in SGPL1-deficient MEFs

(Ihlefeld, Claas et al. 2012). Moreover, it was also shown that HDAC1 and HDAC2 regulate basal $[Ca^{2+}]_i$ levels in these cells, underscoring the role of HDACs in Ca^{2+} homeostasis regulation (Ihlefeld, Claas et al. 2012). Further exploration of the molecular mechanisms underlying the accumulation of S1P in SGPL1 deficient cells remains an area of ongoing research and is yet to be fully understood. By digging deep into these specific molecular mechanisms, namely energy metabolism and autophagy mechanisms, novel pathways, and factors can be uncovered that contribute to the regulation of S1P metabolism and its impact on cellular function. This thesis deals with the investigation of molecular mechanisms, such as energy metabolism and autophagy, that are impacted by the depletion of SGPL1 and the resulting accumulation of S1P, with a specific emphasis on *Sgpl1*$^{-/-}$ MEFs.

1.6 Astrocytes

In addition to neurons, the brain consists of a diverse population of glial cells, namely astrocytes, oligodendrocytes, and microglia, which collectively make up around 70% of the total cells (Jha, Jeon et al. 2012). Astrocytes, the specialized glial cells, surpass neurons in number by more than fivefold, strategically covering the entirety of the central nervous system (CNS) (Sofroniew and Vinters 2010). Initially regarded as supportive satellite cells, astrocytes have emerged as pivotal components of the nervous system (Nedergaard, Ransom et al. 2003). These cells seamlessly occupy and fulfill numerous crucial and intricate roles within the healthy CNS. Among their crucial functions, astrocytes provide structural and metabolic support to neurons, including energy delivery, production, utilization, and storage (Jha, Jeon et al. 2012). Their expanded repertoire of functions encompasses diverse roles, such as being critically important for the neuronal survival (Cui, Allen et al. 2001), contributing to the formation of the blood-brain barrier (BBB) (Song, Huang et al. 2021), participating in neural transmission and synapse formation (Takasugi, Sasaki et al. 2011, Allen and Eroglu 2017, Yamagata 2021), and influencing developmental synapse formation through physical support and the secretion of molecules that modulate synaptic glutamate levels, purines (ATP and adenosine), and GABA (Ullian, Sapperstein et al. 2001, Neal and Richardson 2018, Alam, Afsar et al. 2023). The direct and interactive role of astrocytes in synaptic activity is fundamental for neural circuitry and information processing, giving rise to the 'tripartite synapse' hypothesis (Magistretti and Pellerin 1999, Halassa, Fellin et al. 2007, Perea, Navarrete et al. 2009, Lalo, Koh et al. 2021). A growing body of evidence suggests that astrocytes supply energy substrates to neurons (Alle, Roth et al. 2009). In a recent report from

the group of van Echten Deckert it was shown that by importing glucose through glucose transporter 1 (GLUT1), astrocytes activate the glycolytic pathway to generate ATP (Alam, Afsar et al. 2023). Furthermore, astrocytes play a vital role in responding to CNS injury, undergoing significant changes referred to as reactive astrogliosis (Fig. 4) (Filous and Silver, 2016).

1.7 Glucose metabolism

Despite accounting for only 2% of the body's total weight, the brain exhibits a substantial demand for energy compared to other body tissues. Glucose serves as a vital energy substrate for the adult brain, with approximately 25% of glucose being utilized to sustain fundamental brain functions (Rossi, Zanier et al. 2001, Howarth, Gleeson et al. 2012). Increasing studies have found that an abnormal glucose metabolism is related to the development of neurodegenerative diseases, such as AD (Foster, Chase et al. 1983), PD (Borghammer, Chakravarty et al. 2010), ALS (Browne, Yang et al. 2006), and HD (Feigin, Leenders et al. 2001), which makes it promising to find a solution to these changes, and thereby could prolong the survival of patients with neurodegenerative diseases.

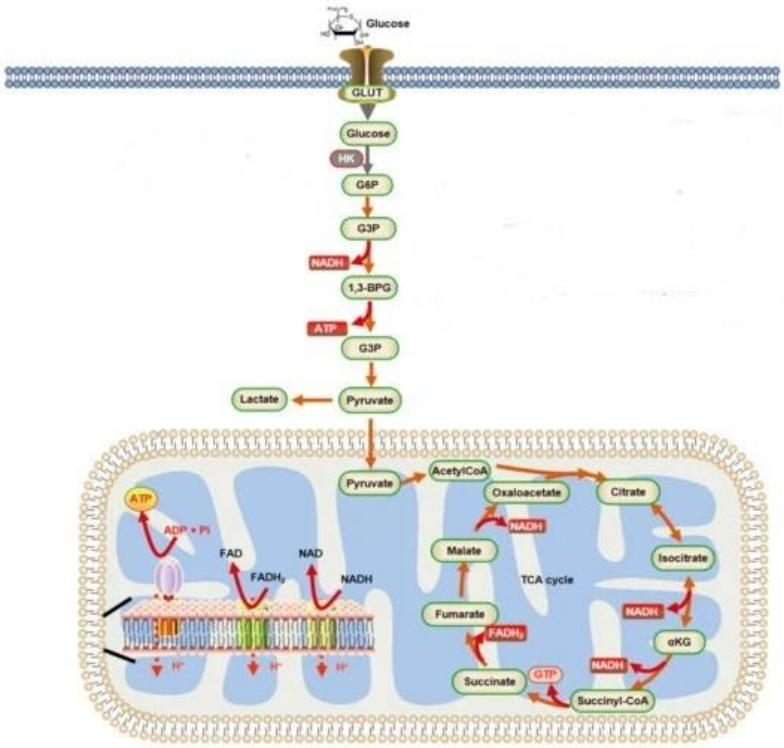

Figure 3. Glucose metabolism and energy homeostasis. Glucose enters the cell through GLUT and is converted to G6P by HK. Glycolysis (shown by red arrows), which leads to lactic acid production or the tricarboxylic acid (TCA) cycle. NADH and FADH2 are subsequently re-oxidized in ETC to produce ATP. GLUT: glucose transporters; HK: Hexokinase; G6P: glucose-6-phosphate; G1P: glucose-1-phosphate; G3P: glyceraldehyde-3-phosphate; 1,3-BPG: 1,3-bisphosphoglycerate. Image modified (Han, Liang et al. 2021).

Glucose metabolism promotes the physiological functions of the brain through glycolysis (Han, Liang et al. 2021) and mitochondrial oxidative phosphorylation, and its product, ATP, (Fig. 3) is the electrochemical basis for the maintenance of neurons and non-neuronal cells (Mergenthaler, Lindauer et al. 2013) and therefore, tight regulation of glucose metabolism is critical not only for brain physiology but for the entire organism.as well. Dysfunction in glucose metabolism, leading to a shift towards lactate production for energy needs, can have detrimental effects on the organism and increase the risk of disease development. For instance, lactate is produced as a fuel source when the demand for ATP exceeds the cellular supply. It is generated through the glycolysis pathway when the tricarboxylic acid (TCA) cycle is inhibited usually due to low oxygen levels (hypoxia). Glucose in the cytoplasm is converted to pyruvate *via* glycolysis, which is then directly converted to lactate by lactate dehydrogenase (LDH), bypassing mitochondrial oxidation.

Major brain cells, astrocytes, and neurons utilize glucose quite differently. Astrocytes, which surround neuronal synapses, primarily undergo glycolysis, while neurons mainly rely on oxidative metabolism (Magistretti and Allaman 2015). Astrocytes, positioned around neuronal synapses, play a crucial role in glucose oxidation. They consume more ATP to synthesize glutamine and package neuronal glutamate into synaptic vesicles for the glutamate-glutamine neurotransmitter cycling process (Volterra and Meldolesi 2005). Astrocytes, being glycolytic, do not extensively metabolize the end product of glycolysis, pyruvate, through the tricarboxylic acid (TCA) cycle. Instead, they preferentially generate lactate over acetyl-CoA using pyruvate dehydrogenase (PDH). Later, the lactate is transferred to neurons, where it is oxidized. This process is known as the astrocyte-neuronal lactate shuttle (ANLS), which suggests that neurons utilize lactate produced by nearby astrocytes as an energy source (Halim, McFate et al. 2010).

1.8 Autophagy

For the maintenance of metabolic homeostasis and viability, cells demonstrate remarkable ability to adapt and flourish in response to challenging circumstances, including situations where nutrient availability is limited. One crucial mechanism that enables this adaptation is autophagy, a highly conserved cellular pathway responsible for recycling nutrients and organelles (Mizushima, Levine et al. 2008). When cells detect a lack of nutrients, autophagy is rapidly induced. It begins with the formation of an autophagic membrane, known as a phagophore, which isolates itself. Subsequently, the phagophore membrane elongates and

curves around the targeted cargo, creating a closed double-membrane organelle called an autophagosome. Eventually, the autophagosome fuses with a lysosome to complete its maturation (Mizushima, Levine et al. 2008). mTOR or (mechanistic target of Rapamycin), a serine/threonine kinase, is a crucial regulator of cellular metabolism and growth. It promotes anabolic processes like cell growth in response to environmental cues while inhibiting autophagy, the catabolic pathway responsible for cellular recycling and adaptation to stress. This reciprocal relationship allows mTOR to maintain the balance between cell growth and autophagy, ensuring cellular adaptation and homeostasis in the face of changing nutrient availability and stress conditions (Dunlop and Tee 2014, Dossou and Basu 2019). Deregulation of mTOR signaling has been implicated in many human diseases, including diabetes, neurodegenerative diseases, and cancer (Laplante and Sabatini 2012). Additionally, situated upstream of mTOR, is the AKT signaling pathway which is activated *via* phosphorylation and also plays a crucial role in regulating mTOR activity and promotes cell growth, differentiation and survival (Manning and Cantley 2007). Notably, dysregulation of this pathway has been observed in neurodegenerative diseases (Jin, Sui et al. 2012) as well as many cancers (Peng, Wang et al. 2022).

While the modulation of autophagy by sphingolipids has been recognized for some time (Lavieu, Scarlatti et al. 2006, Lepine, Allegood et al. 2011), studies investigating this relationship in the brain, where autophagy is essential for recycling aggregate-prone proteins, are relatively limited (Moruno Manchon, Uzor et al. 2015, van Echten-Deckert and Alam 2018). Furthermore, the group of van Echten-Deckert established a connection between autophagy and inflammation mediated by S1P/$S1PR_2$ in microglia cultured from SGPL1-deficient mice (Karunakaran, Alam et al. 2019) where microglial inflammation was accompanied by defective microglial autophagy in SGPL1 ablated mice.

Certainly, in microglia, the signaling molecule S1P functions as a ligand for S1PR, influencing autophagy through an mTOR-dependent mechanism (Karunakaran, Alam et al. 2019). However, in neurons, the deficiency of SGPL1 leads to the accumulation of S1P alongside a decrease in phosphatidylethanolamine. This decrease in phosphatidylethanolamine has been found to hinder neuronal autophagy flux through a mechanism independent of mTOR, as observed in the study conducted by Mitroi et al., 2017 (Mitroi, Karunakaran et al. 2017). Conversely, the accumulation of S1P in neurons has been demonstrated to stimulate neuronal autophagy, as reported by Moruno Manchon et al., 2015 (Moruno Manchon, Uzor et al. 2015).

1.9 Astrogliosis (Reactive astrocytes)

When the central nervous system (CNS) faces insults, astrocytes undergo transformations and acquire novel functions and attributes. One prevalent phenomenon observed is astrogliosis or reactive astrocytosis (Sofroniew 2009). This term encompasses a wide range of functional, structural, and morphological changes experienced by astrocytes in response to CNS injury, with the severity of these alterations depending on the specific context. These changes can have both neuroprotective and neurotoxic effects, potentially leading to processes like neuroinflammation and neurodegeneration (Sofroniew 2009). Traditionally, astrogliosis was commonly understood as an upregulation of GFAP expression, often perceived as a homogeneous phenomenon. However, it is now unequivocally evident that this is not the case (Sofroniew 2015). Reactive astrogliosis represents a multifaceted process, characterized by distinct stages (Fig. 4) (Sofroniew 2009, Neal and Richardson 2018). It is an evolutionarily conserved response that entails both molecular and morphological alterations.

Morphologically, astrocytes undergo changes such as reduction in the number of primary branches and hypertrophy of the cell body and remaining processes (Neal and Richardson 2018). At the molecular level, there is a widely recognized elevation in the expression of GFAP, vimentin, nestin, and secretion of inflammatory cytokines. Astrogliosis encompasses a broad range of heterogeneous changes, determined in a context-specific manner by diverse signaling events that vary depending on the nature and severity of different CNS insults (Fig. 4).

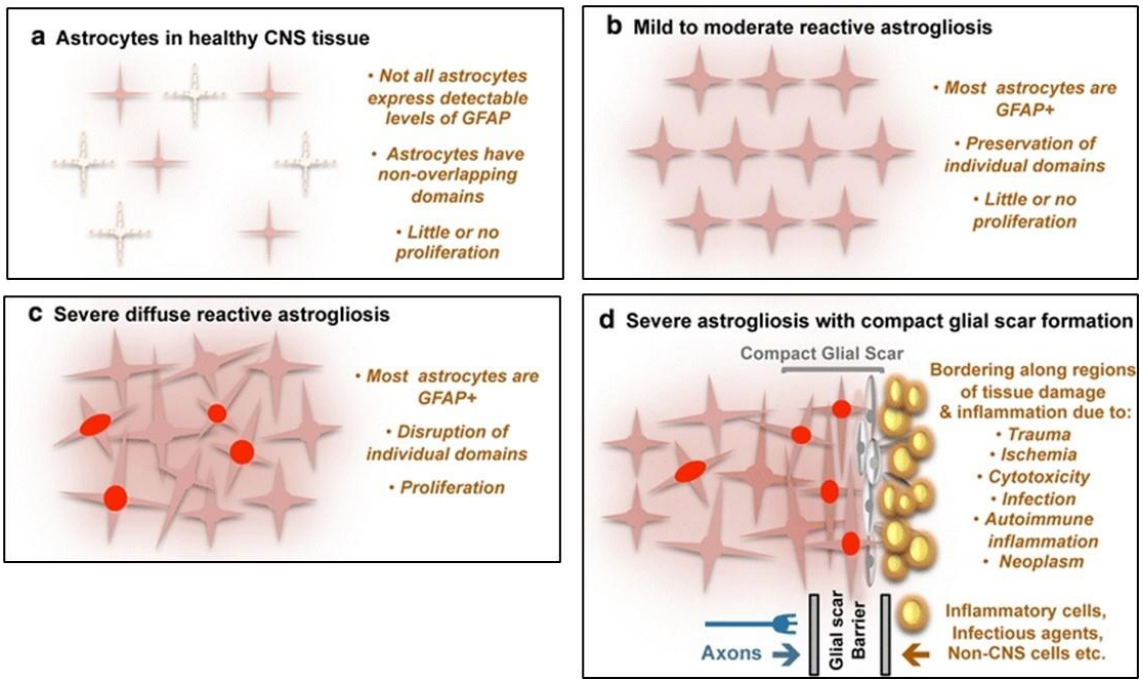

Figure 4. Schematic representation of multi-staged reactive astrogliosis. (a) Astrocytes in healthy CNS tissue. **(b)** As astrogliosis advances, there are changes in molecular expression, functional activity, and variable degrees of cellular hypertrophy observed during moderate reactive astrogliosis **(c)** In cases of severe diffuse reactive astrogliosis, there are notable alterations in molecular expression, functional activity, cellular hypertrophy, and the emergence of newly proliferated astrocytes (indicated by red nuclei in the figure). These changes disrupt astrocyte domains, leading to a long-lasting reorganization of tissue architecture. This pattern is commonly found in areas surrounding severe focal lesions, infections, or regions responding to chronic neurodegenerative triggers. **(d)** Severe reactive astrogliosis can progress into compact glial scar formation, particularly along the borders of areas with evident tissue damage and inflammation. This stage involves the proliferation of astrocytes (red nuclei in the figure) along with other cell types (depicted in gray) such as fibro meningeal cells and additional glia. The presence of a dense collagenous extracellular matrix is also observed. In the compact glial scar, astrocyte processes densely overlap. Mature glial scars tend to persist for extended periods and serve as barriers to axon regeneration, inflammatory cells, infectious agents, and non-CNS cells, effectively protecting healthy tissue from nearby areas of intense inflammation. Adapted from (Sofroniew and Vinters 2010).

1.10 Reactive astrocytes and Neuroinflammation

As mentioned before, the effects of astrocytes are highly complex and multifaceted, influenced by factors such as the type and extent of injury or disease, the surrounding microenvironment, and the interplay with other cells in the central nervous system. There is a growing body of evidence connecting reactive astrocytes to inflammatory processes, which have been implicated in the development of neurodegeneration. The relationship between astrogliosis and inflammation is bidirectional and dependent on the degree of gliosis and the specific signaling pathways involved (Fig. 5) (Sofroniew 2015, Liddelow and Barres 2017).

Recent transcriptomic studies have shed light on the interconnection between epigenetic regulation and inflammation and have reported other genes specific to reactive astrocytes, such as *Tnf* (Tumor Necrosis Factor) and *Il-1β* (Interleukin 1 beta), which exhibit higher expression levels than *Gfap* in certain types of reactive astrocytes (Liddelow and Barres 2017). With elevated histone acetylation previously reported in the SGPL1 deficient astrocytes (Alam, Piazzesi et al. 2020), a transcriptome analysis of the astrocytes derived from SGPL1 deficient murine brains revealed differential transcription of a total of 34 genes that were found to be affected of which DDX3X was most significant.

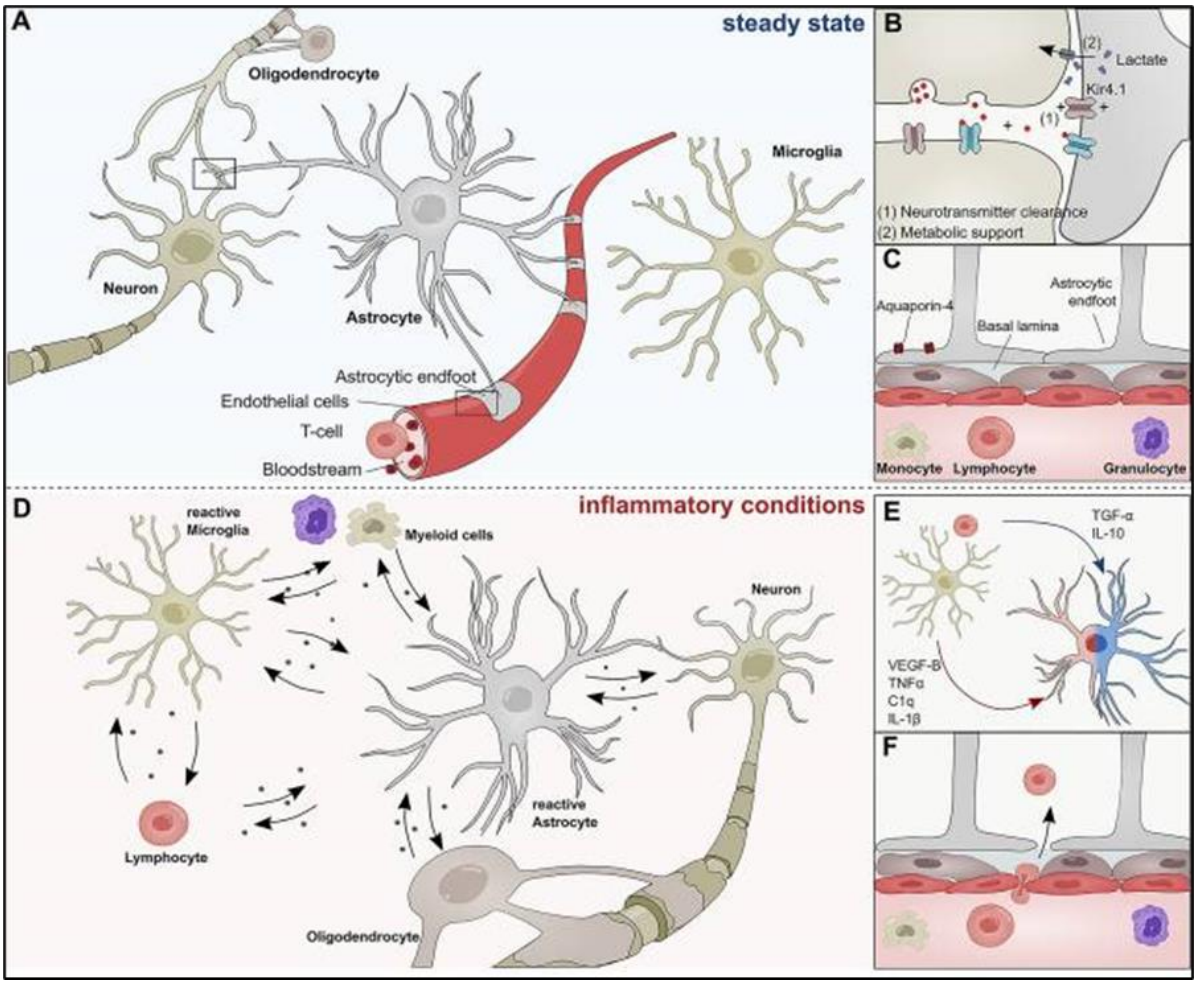

Figure 5. Astrocytes in steady state and inflammatory conditions within the CNS. (A) In steady state conditions, astrocytes establish connections and interact with neurons, oligodendrocytes, microglia, and cells of the blood-brain barrier (BBB). **(B)** They form tripartite synapses with neurons, contributing to the regulation of synaptic transmission by providing metabolic support and clearing neurotransmitters. **(C)** Astrocytic end feet line the cerebral vasculature and contribute to the BBB, limiting the entry of pathogens and peripheral immune cells into the central nervous system. These end feet express high levels of aquaporin-4 and establish close interactions with pericytes and the basal lamina of the brain parenchyma. **(D)** In inflammatory conditions, astrocytes undergo reactive changes and secrete numerous inflammatory mediators. These mediators have a regulatory impact on various cell types, including myeloid cells, lymphocytes, oligodendrocytes, neurons, and microglia. Reactive astrocytes actively participate in the immune response by modulating the functions of these cells. **(E)** Soluble inflammatory mediators derived from microglia and other immune cells can differentially induce either pathogenic (red) or protective (blue) functions in astrocytes, further influencing the outcome of the inflammatory response. **(F)** Inflammatory conditions can also lead to the infiltration of peripheral immune cells across the BBB into the central nervous system. This infiltration is facilitated by the disruption of the BBB integrity during inflammation. The presence of peripheral immune cells in the CNS can contribute to the progression and severity of neuroinflammatory processes. C1q, Complement component 1q; IL-1β, Interleukin-1 β; IL-10, Interleukin 10; TNF-α, Tumor necrosis factor α; TGF-α, Transforming growth factor α; VEGF-B, Vascular endothelial growth factor B. (Linnerbauer and Rothhammer 2020)

Inflammasomes are complex protein assemblies that detect molecular patterns associated with cellular damage or intracellular pathogens. Upon activation, they form cytosolic compartments called ASC specks, which facilitate the activation of Caspase-1. This activation leads to the secretion of interleukin IL-1β and IL-18 and drives the cell towards pyroptosis, a programmed inflammatory cell death process with significant implications in health and disease (Martinon, Burns et al. 2002). While both stress granules and inflammasomes can be triggered by cellular stress, they drive distinct cell-fate outcomes. However, the interplay

between stress granules and inflammasomes and its impact on cell fate remains poorly understood. In a recent study by Samir et al. (2019), the essential role of DDX3X, a member of the DEAD-box family and helicase, in the formation of stress granules and NLRP3 inflammasome complexes was uncovered (Samir, Kesavardhana et al. 2019). These findings shed light on the crucial role of DDX3X as a molecular switch, influencing the cell's fate by orchestrating the balance between survival and cell death in response to specific stress signals (Fig. 6).

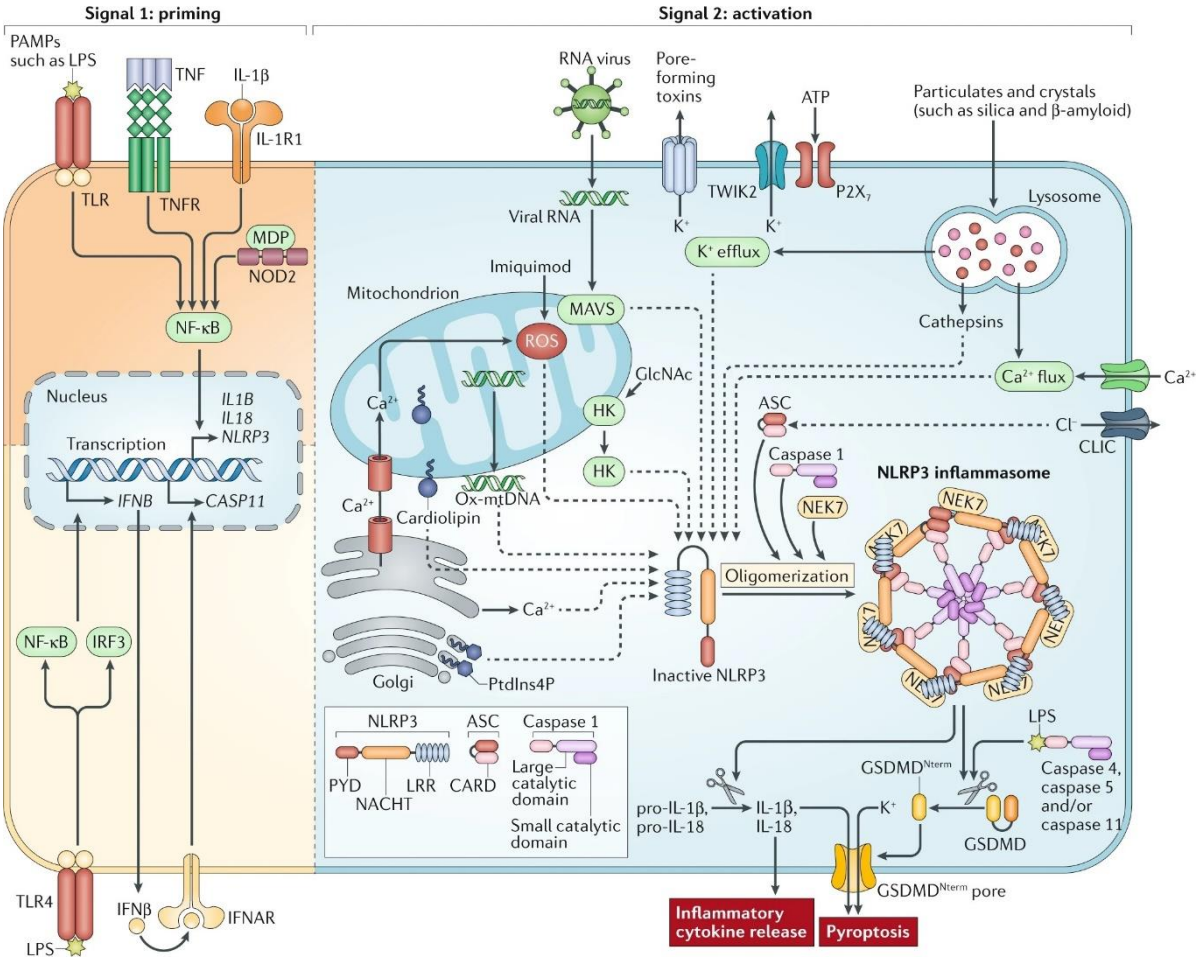

Figure 6. The priming and activation process of the NLRP3 inflammasome. Various priming signals induce the expression of pro-IL-1β and NLRP3. Activation occurs through different stimuli, resulting in the assembly of the NLRP3 inflammasome, activation of caspase-I, and cleavage of pro-IL-1β.

1.11 Purinergic Receptor signaling in astrocytes

The concept of purinergic receptors was established in 1976 (Burnstock 1976), and shortly thereafter, they were categorized into two main types: the P1 receptor, which responds to adenosine, and the P2 receptor, which responds to ATP and ADP (Burnstock, Fredholm et al. 2011). Subsequent studies explored into the classification of P2 receptors, dividing them into

two subtypes: P2X receptors, which are ligand-gated ion channels, and P2Y receptors, which are G-protein-coupled receptors (Abbracchio and Burnstock 1994). The differentiation within the P2Y receptor group is based on similarities in their evolutionary lineage and the presence of specific amino acids crucial for ligand binding and G-protein coupling selectivity (Abbracchio, Burnstock et al. 2009). The P2Y receptors can be further subdivided into two distinct subgroups with notable sequence variations. The first subgroup consists of P2Y1, P2Y2, P2Y4, P2Y6, and P2Y11, while the second subgroup includes P2Y12, P2Y13, and P2Y14 (Abbracchio, Burnstock et al. 2006, Abbracchio and Verderio 2006). Among these receptors, P2Y1R, a metabotropic receptor, is widely expressed in neurons, astrocytes, and microglia.

In astrocytes, P2Y1R plays a vital role in facilitating the propagation of short-term calcium waves throughout the astrocyte network (Abbracchio and Burnstock 1994, Abbracchio and Verderio 2006). Upon activation, astrocytes release ATP (Alam, Afsar et al. 2023), which then triggers a response *via* P2Y1R. This activation leads to an amplified propagation of intracellular calcium waves, facilitating effective communication between neighboring cells (Abbracchio and Verderio 2006, Burnstock, Fredholm et al. 2011, Delekate, Fuchtemeier et al. 2014). Moreover, an upregulation of P2Y1 receptors in glial cells across different brain regions were reported following ischemic stress (Kuboyama, Harada et al. 2011). Consequently, when activated by ATP released from injured neurons or glial cells, P2Y1 receptors on astrocytes have also been found to mediate neuroinflammatory responses in various CNS disorders (Fields and Burnstock 2006). Furthermore, the activation of astrocytic P2Y1 receptors triggers the release of proinflammatory cytokines (Fujita, Tozaki-Saitoh et al. 2009). Therefore, it is crucial to investigate the involvement of P2Y1 receptors in neuroinflammatory conditions to better understand their role.

1. AIM OF THE STUDY

The primary objective of the first study was to examine the influence of sphingosine-1-phosphate (S1P) on glucose metabolism within SGPL1-deficient mouse embryonic fibroblasts (*Sgpl1*$^{-/-}$ MEFs). The study aimed to unravel the cellular mechanisms by which accumulated S1P impacts glucose metabolism, specifically in SGPL1-deficient cells. The study sought to understand the role played by the S1P/S1PR$_{1-3}$ axis in the regulation of glucose metabolism and to gain insights into the consequent effects on other metabolic processes, such as autophagy, in SGPL1-deficient cells.

Building upon previous study by Alam et al., 2021 (Alam 2021), which demonstrated the effect of neural ablation of SGPL1 in astrocytes, the aim of the second study was to further investigate and confirm the role of S1P and its receptors in astrocytes derived from neural-targeted SGPL1-deficient mice (SGPL1$^{fl/fl/Nes}$). The specific objectives of this study were to examine the impact of S1P/S1PRs on glycolytic enzymes, pyruvate utilization, ATP content, and autophagy within SGPL1-deficient astrocytes. Additionally, the study aimed to establish a connection between SGPL1 deficiency and the activation of the NLRP3 inflammasome.

Overall, both studies aimed to deepen the understanding of the role of S1P metabolism in various cellular processes, encompassing different cell types, and to elucidate its impact on mechanisms such as glucose metabolism and autophagy. Furthermore, the studies aimed to provide valuable insights into the oncogenic consequences associated with S1P metabolism and to investigate potential therapeutic approaches that target S1P metabolism and signaling pathways specifically in the context of astrogliosis.

2. RESULTS

3.1 Studies in SGPL1-deficient mouse embryonic fibroblast (MEFs)

3.1.1 SGPL1 expression in MEFs

In this study, MEFs were used as a model system to investigate the impact of genetic elimination of SGPL1 on sphingolipid metabolism. Previous investigations on SGPL1-deficient MEFs have consistently demonstrated a notable buildup of S1P, as well as a disruption in ganglioside formation (Claas, ter Braak et al. 2010, Hagen-Euteneuer, Alam et al. 2020). Firstly, the expression of SGPL1 was examined at both the protein and mRNA levels in wild-type (WT) and SGPL1$^{-/-}$ (KO) MEFs, as depicted in fig 7A and B. The results revealed a substantial decrease of 95–98% in SGPL1 protein and mRNA expression in the KO MEFs compared to the WT controls. Image representing WT and SGPL1$^{-/-}$ MEFs as viewed under brightfield microscope (Fig. 7C), demonstrated no discernible morphological changes between the WT and SGPL1$^{-/-}$ MEFs.

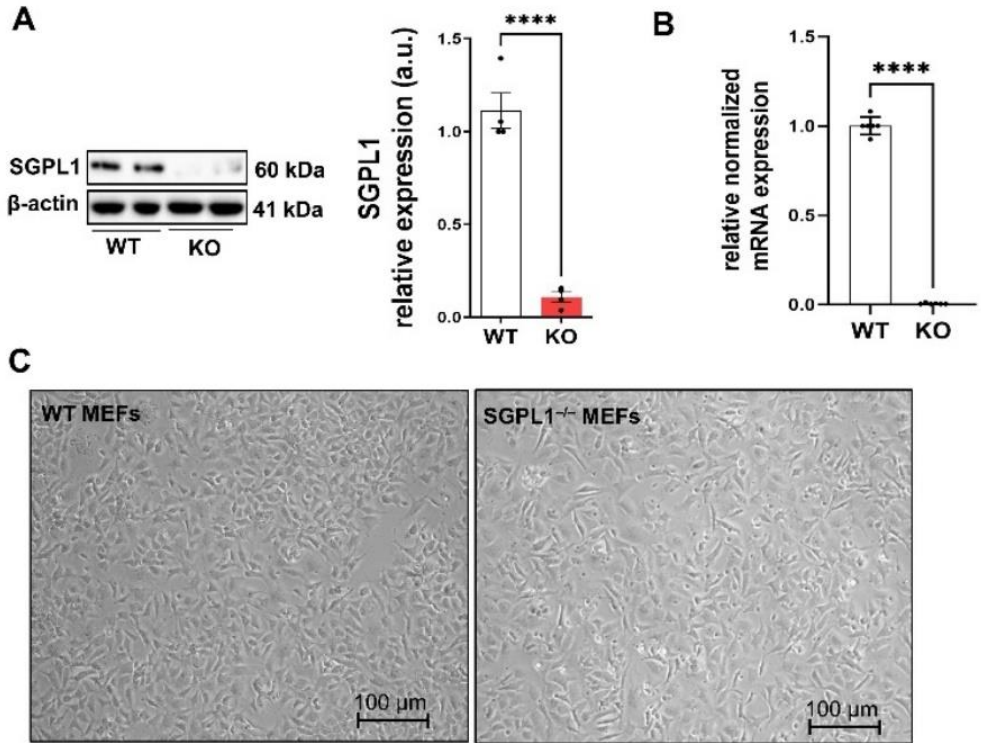

Figure 7. SGPL1 expression in MEFs. (A) Protein expression and quantification of SGPL1 examined *via* Western Immunoblotting and **(B)** mRNA expression of SGPL1 determined *via* qRT–PCR in the WT and KO MEFs. **(C)** 10X representative brightfield image of WT and SGPL1$^{-/-}$ MEFs. Shown is one representative western blot. β–actin was used as loading control (a.u., arbitrary units). Bars represent mean ± SEM (n ≥ 3, ****p < 0.00005; unpaired Student *t*–test).

3.1.2 MEFs lacking SGPL1 expression display changes in glucose uptake and metabolism.

Previous studies in the group of Dr. Gerhild van Echten–Deckert have shown that ablation of SGPL1 in non-differentiated MEFs as well as in post–mitotic terminally differentiated neurons caused a substantial increase in the amount of free and phosphorylated sphingoid bases particularly, S1P levels *via* SK1 (Hagen-Euteneuer, Lutjohann et al. 2012, Hagen-Euteneuer, Alam et al. 2020). S1P is a well–known bioactive signaling molecule that has been linked to various cellular processes, including mammalian cell growth, differentiation, and survival (Hagen-Euteneuer, Alam et al. 2020). The maintenance of systemic energy homeostasis is indispensable to growth and survival. Given the significance of energy metabolism in cellular processes, it was crucial to investigate the impact of S1P accumulation in SGPL1–deficient MEFs on glucose uptake and metabolism. GLUT1 is a glucose transporter that is ubiquitously expressed and is often upregulated in response to elevated cellular energy demands. Upon analysis of SGPL1–deficient MEFs, as shown in Fig. 8A, this study shows for the first time, a significant upregulation of GLUT1 expression in comparison to the WT controls, suggesting an increased uptake of glucose in the KO MEFs.

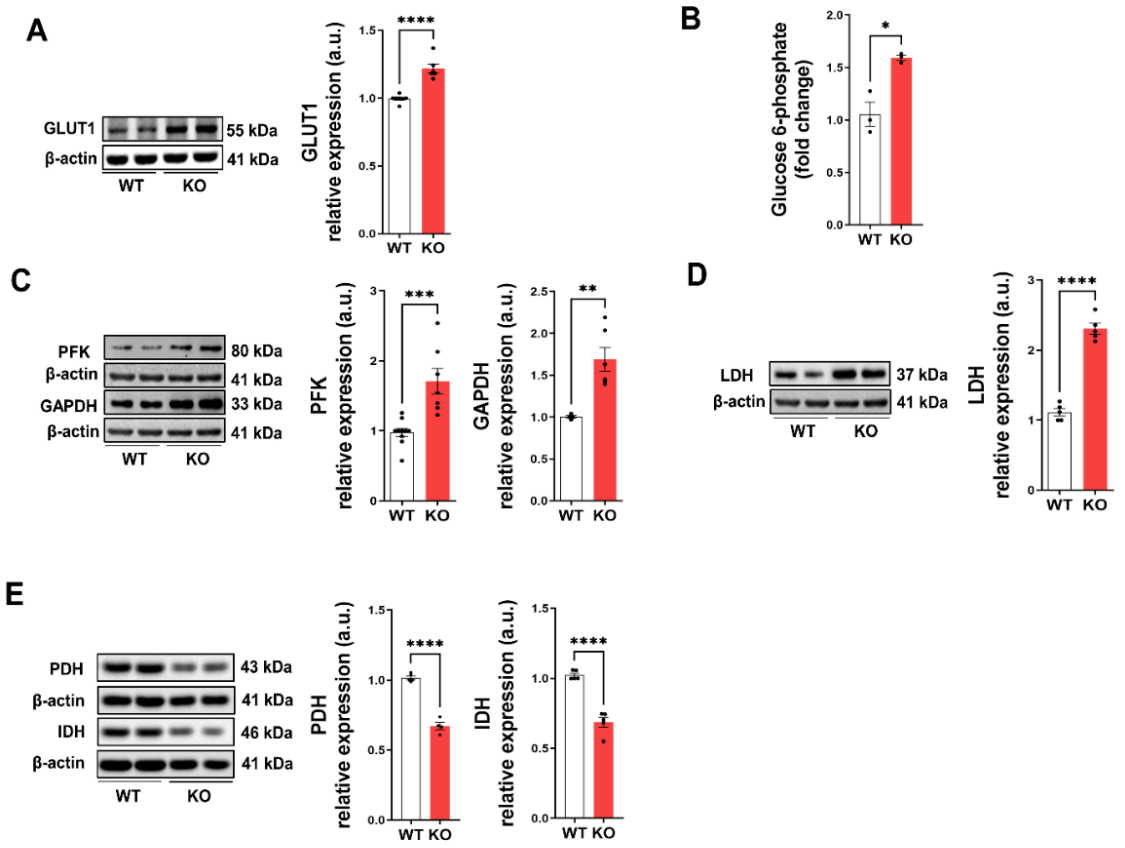

Figure 8. Remodeled glucose metabolism in SGPL1–deficient MEFs. (A) Protein quantification of GLUT1 in WT controls (white bars) and SGPL1–deficient (KO) MEFs (red bars). **(B)** Colorimetric determination of G6P shows increased levels in KO relative to WT MEFs. **(C–E)** Protein quantification of PFK, GAPDH, LDH, PDH, and IDH in WT controls and SGPL1–deficient (KO) MEFs. Shown is one representative western blot for each protein. β–actin was used as loading control

(a.u., arbitrary units). Bars represent mean ± SEM (n ≥ 3, ****p < 0.00005, ***p < 0.0005, **p < 0.005, *p < 0.05; unpaired Student *t*–test). See also (Afsar, Alam et al. 2022)

Once inside the cells, phosphorylation of glucose at the sixth carbon hydroxyl group traps the glucose within the cells by forming glucose–6–phosphate (G6P) and marks the start of the glycolysis pathway generating energy for the cells in the form of ATP. Exploring further, the quantitative analysis by colorimetric assay revealed a significant increase in the levels of G6P by approximately 30% in SGPL1$^{-/-}$ MEFs as compared to their WT counterparts (Fig. 8B).

With increased glucose uptake, the subsequent step involved assessing the indicators of glycolytic enzymes. For this, the expression of the following markers was investigated: (i) phosphofructokinase (PFK) which is the rate-limiting enzyme of glycolysis, and (ii) glyceraldehyde–3–phosphate dehydrogenase (GAPDH) which is often used as a housekeeping reference due to its consistent expression in most cell types. As depicted in Figure 8C, the immunoblots of both enzymes revealed an increased expression of approximately 40% in SGPL1–deficient MEFs implying an increased degradation of glucose in these cells. To investigate the fate of pyruvate, the final product of glycolysis, the expression of two enzymes, lactate dehydrogenase (LDH) and pyruvate dehydrogenase (PDH), were evaluated. LDH converts pyruvate to lactate, typically in the absence of oxygen, while PDH facilitates its oxidative decarboxylation into acetyl–coenzyme A, which further enters the tricarboxylic acid (TCA) cycle. It is noteworthy that the expression of LDH was considerably upregulated (by twofold), as shown in Figure 8D. In contrast, the expression of PDH was significantly downregulated by approximately 40%, in SGPL1$^{-/-}$ MEFs, as illustrated in Figure 1E. These findings suggest a shift in the fate of pyruvate towards lactate production, likely due to the decreased activity of PDH, which could affect cellular metabolism and energy production. To gain a more comprehensive understanding of the turnover of the tricarboxylic acid (TCA) cycle, the expression of isocitrate dehydrogenase (IDH) was investigated. IDH is a crucial enzyme in the Krebs cycle responsible for regulating the rate of the TCA cycle and is often found to be mutated in various types of cancer (Yan, Parsons et al. 2009). Similar to the reduction observed in PDH levels, IDH expression was also lowered by approximately 40% as depicted in Figure 8E.

Increased expression of glycolytic marker proteins and down–regulation of enzymes related to oxidative phosphorylation with a shift towards lactate production thereby enhancing glucose intake are features highly reminiscent of the Warburg effect, a typical attribute shared most in cancer cells (Vander Heiden, Cantley et al. 2009).

3.1.3 Activation of transcription factor, HIF in SGPL1 deficient MEFs

To investigate the potential involvement of transcription factors in the activation of glycolytic genes, this study focused on HIF-1, a known contributor to the Warburg effect that enhances the expression of glucose transporters and glycolytic enzymes, including PFK (Semenza 2001). In line with the elevated protein levels of these target genes as observed in SGPL1-deficient MEFs, the expression of HIF-1 was examined, as depicted in fig. 9A. Surprisingly, despite the presence of aerobic conditions, the expression of HIF-1 was found to be increased by approximately 50% in the KO MEFs compared to the WT controls. It is worth noting that the activation of HIF-1 is not solely dependent on oxygen deficiency but can also be induced through non-canonical pathways (Iommarini, Porcelli et al. 2017).

Furthermore, an intriguing observation was made regarding the growth of SGPL1$^{-/-}$ MEFs. Despite being cultured as a monolayer, the SGPL1$^{-/-}$ MEFs reached a higher cell density at confluence, indicating their enhanced proliferative capacity. To validate this, cell proliferation was assessed, as depicted in fig. 9B, and it demonstrated that the SGPL1$^{-/-}$ MEFs indeed exhibited a significantly higher rate of proliferation when compared to the WT controls.

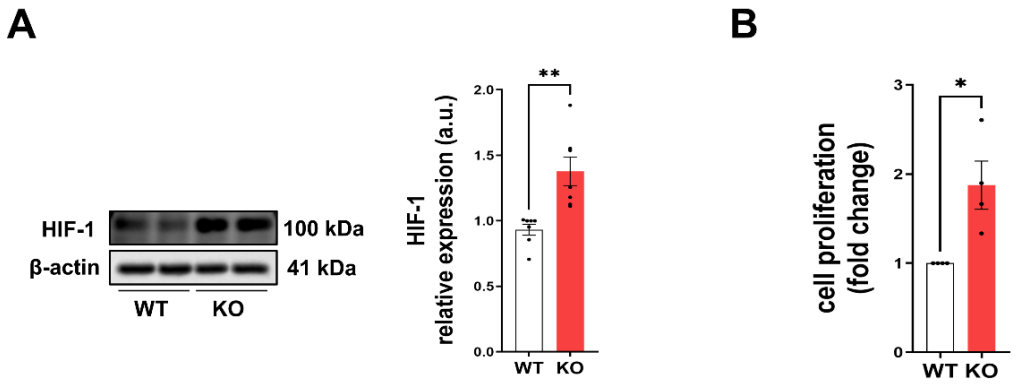

Figure 9. Activation of HIF–1 transcription factor in SGPL1–deficient MEFs. (A) Protein quantification of HIF–1 (hypoxia–inducible factor 1α) in WT controls (white bars) and SGPL1–deficient (KO) MEFs (red bars). **(B)** Rates of the proliferation of KO (red bars) are increased relative to WT (white bars) MEFs. Shown is one representative western blot for each protein. β–actin was used as loading control (a.u., arbitrary units). Bars represent mean ± SEM ($n \geq 3$, $^{**}p < 0.005$, $^{*}p < 0.05$; unpaired Student *t*–test). See also (Afsar, Alam et al. 2022)

These collective findings strongly indicate that cells lacking SGPL1 circumvent the TCA cycle and predominantly rely on glycolysis for glucose degradation. This is achieved through the activation of the HIF–1 transcription factor which allows these cells to meet the high energy demand for their rapid growth. These findings additionally support the oncogenic potential of cells lacking SGPL1, as the metabolic pattern exhibited by the SGPL1-deficient MEFs aligns with the metabolic alterations commonly observed in cancerous cells. This

highlights the significance of S1P in cellular metabolism and its potential role in making favorable environment driving oncogenesis.

3.1.4 Accumulated S1P is responsible for the elevated glucose uptake and aerobic glycolysis

To support the assumption that the accumulation of S1P is responsible for the augmented glycolysis in *Sgpl1*$^{-/-}$ MEFs, the cells were treated with FTY720, which is the S1P receptor agonist. For this, WT MEFs were treated with 10 nM of FTY720 followed by 24 h incubation and subsequently analyzed for the expression of GLUT1 and glycolytic enzymes.

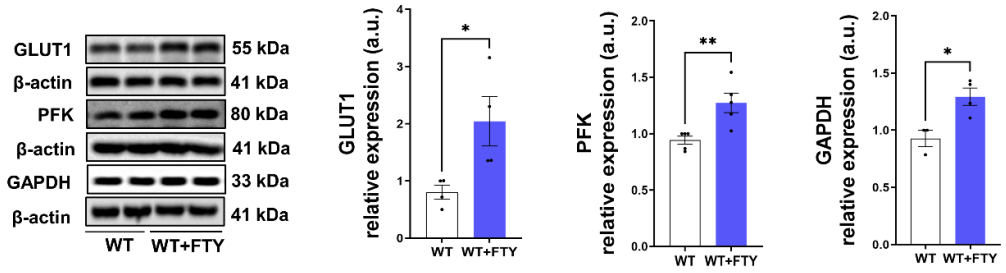

Figure 10. Recapitulation of SGPL1–deficiency by S1PR agonist (FTY–720) in MEFs. Protein quantification of GLUT1, PFK, and GAPDH in WT MEFs cultured in the absence (white bars) or presence (blue bars) of 10 nM FTY720 (WT+FTY) for 24 h. Shown is one representative western blot for each protein. β–actin was used as a loading control. Bars represent mean ± SEM ($n \geq 3$, $^{**}p < 0.005$, $^{*}p < 0.05$; one–way ANOVA with Tukey's post hoc correction). See also (Afsar, Alam et al. 2022)

The findings obtained from the treatment of WT MEFs with FTY720 exhibited similar increment to those observed in SGPL1-deficient MEFs (Fig. 10), indicating that the enhanced glycolysis observed in SGPL1-deficient MEFs were actually induced by S1P.

3.1.5 S1P stimulates glucose uptake and glycolysis via S1PR$_{1–3}$

Next, it was necessary to determine the mechanism by which accumulated levels of S1P contributed to the augmented expression of markers of aerobic glycolysis in the MEFs deficient in SGPL1. Since S1P primarily exerts its functions through the family of five G protein–coupled receptors, S1PR$_{1–5}$, it was crucial to examine their potential involvement in the altered glucose metabolism observed in *Sgpl1*$^{-/-}$ MEFs. Initially, the transcriptional expression of all five receptors was examined in the WT and KO MEFs by quantitative RT–PCR.

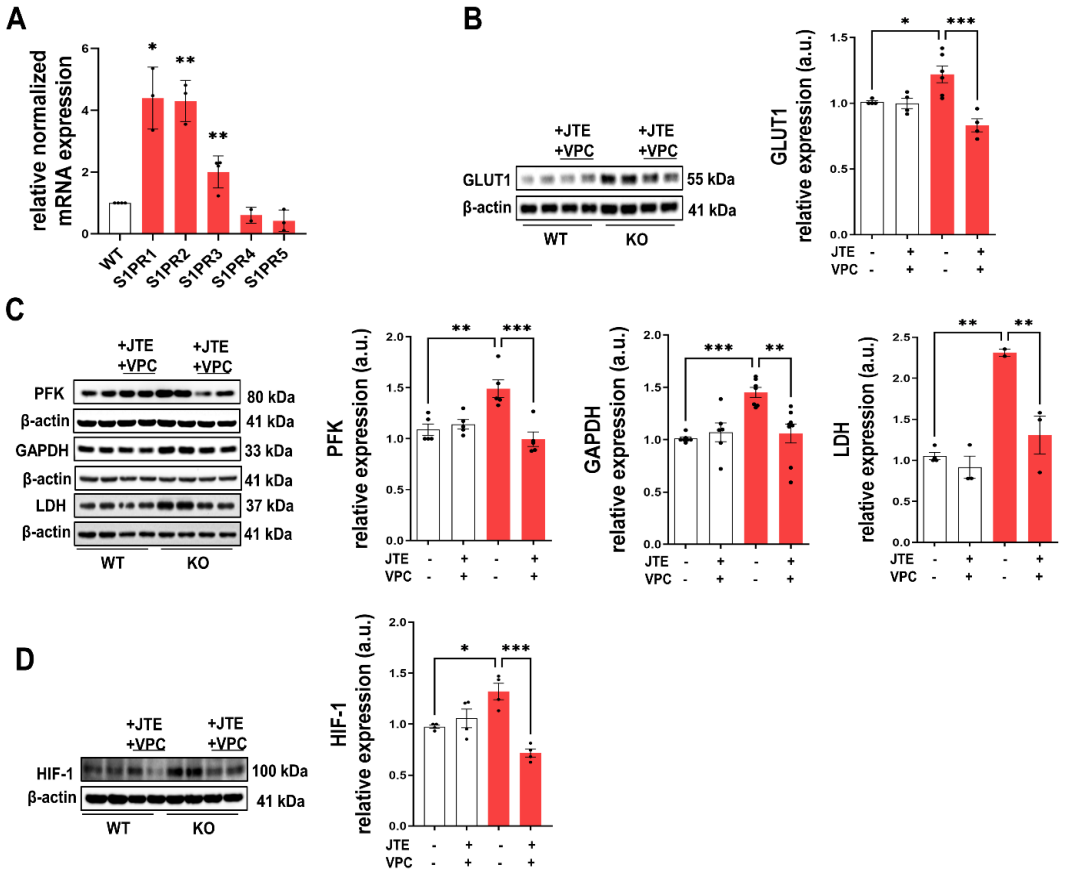

Figure 11. $S1PR_{1–3}$ mediates the effect of S1P on remodeled glucose metabolism in SGPL1–deficient MEFs. (A) Transcript amounts of S1PRs were evaluated by quantitative real-time PCR in SGPL1–deficient (KO) MEFs (red bars) relative to WT controls (white bar) as indicated. Protein quantification of **(B)** GLUT1 and of **(C)** PFK, GAPDH, and LDH and of **(D)** HIF–1 in WT controls (white bars) and SGPL1–deficient (KO) MEFs (red bars) in the presence or absence of VPC–2309 and JTE–013 as indicated. Shown is one representative western blot for each protein. β–Actin was used as loading control (a.u., arbitrary units). Bars represent means ±SEM ($n \geq 3$, for HIF–1 n = 2, ***$p < 0.0005$, **$p < 0.005$, *$p < 0.05$, Student *t*–test, one–way ANOVA with Tukey's post hoc correction). See also (Afsar, Alam et al. 2022)

The study shows in fig. 11A, that among the five known S1P receptors, the mRNA expression levels of $S1PR_1$ and $S1PR_2$ were significantly increased up to fourfold in the KO MEFs. Furthermore, the mRNA expression of $S1PR_3$ was observed to be increased by approximately twofold, while no significant changes were observed for $S1PR_4$, and $S1PR_5$ in the KO MEFs compared to their WT controls. To find out whether the increased expression of $S1PR_{1-3}$ is indicative for their potential role of the described S1P effects, MEFs were cultured in the presence of specific receptor antagonists, VPC-23019 and JTE-013, for a duration of 24 h. VPC–23019 is a competitive antagonist for $S1PR_1$ and $S1PR_3$ receptors, while JTE–013 is a specific antagonist for the $S1PR_2$ receptor. Subsequently, the expression of GLUT1 was evaluated in $S1PR_{1-3}$ inhibited MEFs and it was observed that the increased expression of GLUT1 was reduced to normal levels in MEFs deficient in SGPL1, whereas the expression of

GLUT1 in the WT controls was unaltered as shown in fig. 11B. Similar results were obtained for the glycolytic marker proteins, PFK and GAPDH as well as LDH (Fig. 11C).

Interestingly, targeted inhibition of $S1PR_{1–3}$ also had a significant impact on reversing the effects of SGPL1 deficiency by reducing the expression levels of HIF–1 to even lower levels than the controls as shown in fig. 11D. The results of the study revealed that despite the inhibition of S1PRs, the reduced expression of PDH and IDH detected in SGPL1–deficient MEFs could not be restored. This indicates that the S1PRs were not responsible for the regulation of PDH and IDH expression in SGPL1–deficient MEFs. Furthermore, when each S1PR was independently inhibited, there was no restorative effect observed, suggesting that the three S1PRs may act as substitutes for each other in the context of glucose metabolism (result not shown).

Taken together, these findings suggest that an S1P–induced molecular mechanism, mediated by $S1PR_{1–3}$, is responsible for the increased glucose uptake and subsequent aerobic glycolytic degradation observed in SGPL1–deficient MEFs.

3.1.6 SGPL1 deficiency in MEFs resulted in activation of the Akt/mTOR pathway

The results obtained above strongly demonstrate that MEFs with significant accumulation of S1P exhibit increased glycolysis thereby increasing the energy load within the cell. Furthermore, several studies have established that an increase in energy levels within the cell can trigger the activation of the Akt signaling pathway, which plays a pivotal role in numerous cellular processes, such as cell growth, survival, and proliferation (Abdel-Wahab, Mahmoud et al. 2019).

Therefore, the expression of phosphorylated Akt was analyzed in SGPL1-deficient MEFs and as seen in fig. 12A, the level of activated Akt was nearly 2 times higher in *Sgpl1*$^{-/-}$ MEFs than in WT controls.

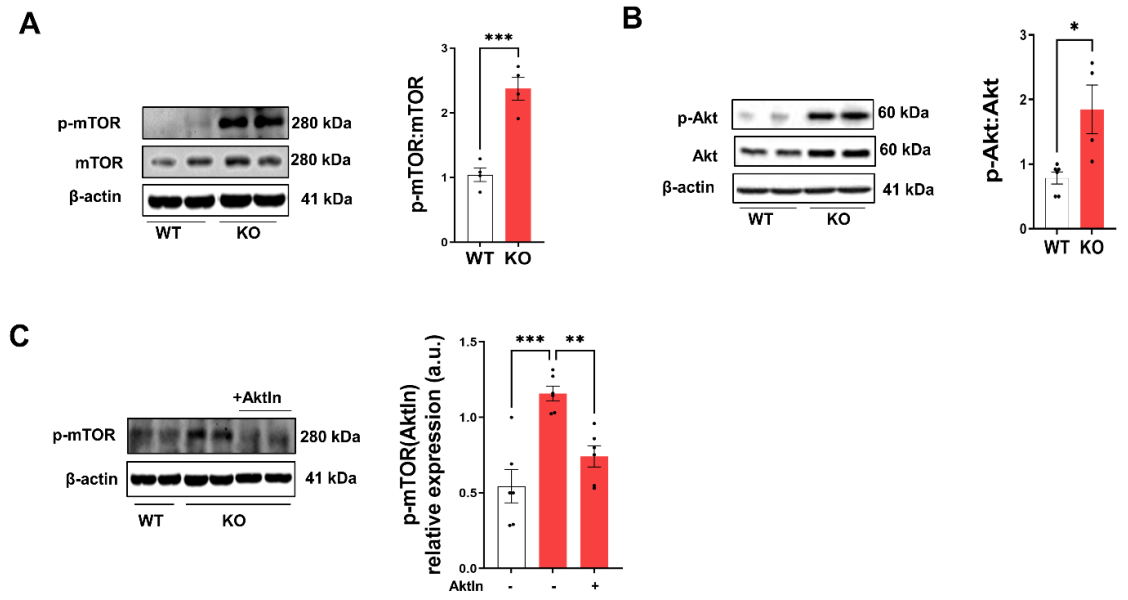

Figure 12. Activation of AKT/mTOR signaling pathway in *Sgpl1*$^{-/-}$ MEFs. Protein quantification of **(A)** the ratio of p-mTOR and of mTOR, **(B)** the ratio of p-Akt and Akt evaluated by Western Immunoblotting in SGPL1–deficient (KO) MEFs (red bar) relative to WT controls (white bar) as indicated, and **(C)** quantification of p-mTOR in the absence (-) and presence (+) of AktIn (Akt inhibitor) in WT and in KO MEFs. Shown is one representative western blot for each protein. β–actin was used as loading control (a.u., arbitrary units). Bars represent means ±SEM ($n \geq 3$, ***$p < 0.0005$, **$p < 0.005$, *$p < 0.05$, one–way ANOVA with Tukey's post hoc correction). See also (Afsar, Alam et al. 2022)

Once activated, Akt further signals its downstream activator known as mTOR which acts as a nutrient-sensing molecule adjusting nutrient availability with cell growth and survival (Laplante and Sabatini 2009). Therefore, to check for the activation of mTOR, the expression of its phosphorylated active form was investigated in WT and *Sgpl1*$^{-/-}$ MEFs. As shown in fig. 12B the ratio of phosphorylated mTOR to total mTOR was observed to be twice as high in the KO MEFs than in the WT controls. Furthermore, to validate that mTOR was being activated *via* Akt signaling, the knockout MEFs were treated with the Akt inhibitor, AktIn (5µM), for 24 h. As shown in fig 12C, AktIn treatment reversed the expression of mTOR in the KO MEFs, bringing it back to the levels of the WT controls. This clearly demonstrates the activation of the AKT/mTOR signaling axis in SGPL1-deficient MEFs.

Moreover, the addition of AktIn did not eliminate the enhanced expression of GLUT1, PFK, and GAPDH (result not shown), indicating that there was no glucose degradation *via* Akt/mTOR signaling pathway.

3.1.7 mTOR dependent impaired autophagy in SGPL1-deficient MEFs

Maintaining metabolic homeostasis and viability in cells relies on their ability to adapt to variations in nutrient availability. One vital cellular response to the depletion of nutrients is the activation of autophagy which is a natural recycling process needed by the cells to

maintain nutrient homeostasis (Dunlop and Tee 2014). As glucose metabolism was altered in KO MEFs, we investigated the autophagy mechanism by assessing the expression of the following autophagy markers: (1) p62/sequestosome 1, which is a specific autophagy substrate that recognizes and removes autophagy cargo, and (2) 1A/1B-light chain 3, LC3. The second marker, LC3, occurs in two variations: LC3-I and LC3-II. Following lipidation, LC3-I transforms into LC3-II and attaches to the developing autophagosomal vesicle, ultimately promoting its elongation and maturation.

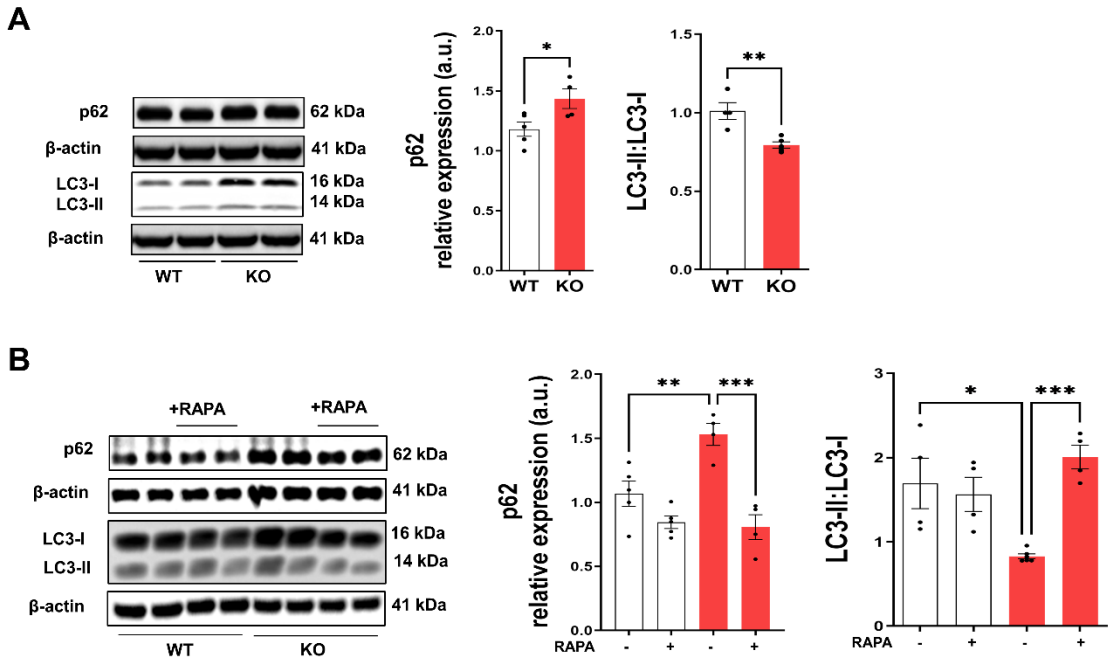

Figure 13. mTOR dependent impaired autophagy in SGPL1–deficient MEFs. (A) Protein quantification of autophagy marker proteins, p62/SQSTM1 (sequestome 1), and the ratio of LC3-II:LC3-I in SGPL1-deficient KO (red bars) and WT (white bars) MEFs **(B)** Quantification of p62, and of the ratio LC3-II:LC3-I in the absence (-) and presence (+) of rapamycin (RAPA) in WT and in KO MEFs. Bars represent means ±SEM (n ≥ 3, ***p< 0.0005, **p< 0.005, *p< 0.05, one-way ANOVA with Tukey's post hoc correction). For all blots β-actin was used as the loading control. See also (Afsar, Alam et al. 2022)

The immunoblots presented in fig. 13A, demonstrate a notable decrease in the LC3-II:LC3-I ratio, along with a modest yet statistically significant increase in p62 expression in SGPL1 deficient MEFs. These observations suggest a marked decrease in autophagic activity within these cells and may contribute to a better understanding of the role of S1P in regulating autophagy.

Additionally, mTOR is also known as a master regulator of autophagy (Dossou and Basu 2019) and an activated mTOR expression argues for reduced autophagy in the cells. Therefore, with its elevated expression in SGPL1-deficient MEFs, it was essential to investigate the regulatory function of mTOR in relation to autophagy in SGPL1-deficient MEFs. Rapamycin is well established as an inhibitor of mTOR (Benjamin, Colombi et al.

2011), therefore in order to look for the dependency of autophagy on mTOR, WT and *Sgpl1*$^{-/-}$ MEFs were treated with 1 µM of rapamycin for 24 h. As shown in fig. 13B treatment with rapamycin restored the expression of both p62 and the ratio of LC3II:LC3I to control levels, clearly indicating that impaired autophagy in SGPL1-deficient MEFs is indeed mediated *via* mTOR.

Moreover, to rule out the possibility of glycolysis being influenced due to the high expression of mTOR and activated Akt, the expression of PFK and GAPDH were also analyzed in the presence of rapamycin. As shown in fig. 14, with the addition of rapamycin (1 µM, 24 h) the expression of PFK and GAPDH remained elevated, indicating that mTOR did not have an effect on their expression levels and confirming again that the increased levels of p-mTOR as well as the activation of Akt are not responsible for the increased levels of glycolytic enzymes.

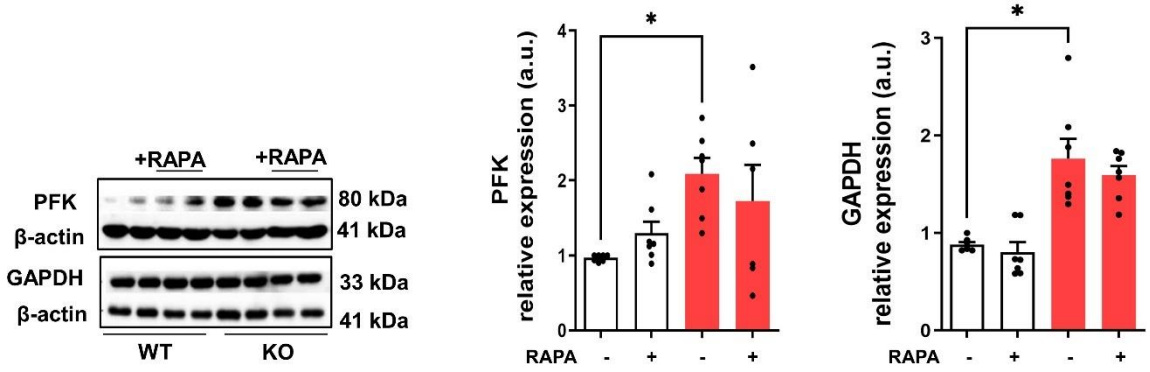

Figure 14. Increased glycolysis is independent of mTOR activation in SGPL1–deficient MEFs. Protein quantification of glycolytic marker proteins PFK and GAPDH in the absence (-) and presence (+) of rapamycin (RAPA, 1 µM, 24 h) in controls (WT, white bars) and in SGPL1-deficient (KO) MEFs (red bars). Bars represent means ±SEM ($n \geq 3$, *$p < 0.05$, one-way ANOVA with Tukey's post hoc correction). For all blots β-actin was used as the loading control (a.u., arbitrary units). Shown is one representative western blot. See also (Afsar, Alam et al. 2022)

In conclusion, this study demonstrates a significant link between the deficiency of SGPL1 and cellular processes, including energy metabolism and autophagy. The findings of this study underscore the pivotal role of the SGPL1/S1P/S1PR$_{1\text{-}3}$ axis in governing these essential cellular mechanisms within MEFs. These insights highlight the significance of SGPL1 and S1P signaling in both normal cellular functions and disease states, presenting potential avenues for targeted interventions in various pathological conditions, including cancer.

3.2 Studies in SGPL1-deficient astrocytes

3.2.1 SGPL1 expression in SGPL1$^{fl/fl/Nes}$ murine brain

Astrocytes show similarity with fibroblasts regarding their sphingolipid pattern (van Echten-Deckert and Herget 2006). Moreover, a mouse model (SGPL1$^{fl/fl/Nes}$), had been generated in the group of Dr. Gerhild van Echten Deckert in which SGPL1 was ablated in neural cells derived from murine brain (Mitroi, Deutschmann et al. 2016) as described in the section 7.1. It was therefore interesting to ascertain if SGPL1-deficiency similarly affects glucose metabolism as it did with the SGPL1 deficient MEFs. Previous reports on SGPL1$^{fl/fl/Nes}$ mouse model have shown that the expression of SGPL1 was reduced considerably by about 75-80% in brain tissue as well as in primary cultured astrocytes derived from SGPL1-deficient mice (Mitroi, Deutschmann et al. 2016, Alam, Piazzesi et al. 2020).

3.2.2 Effect of SGPL1-deficiency in astrocyte via exogenous stimulation of S1P

Similar to the MEFs, astrocytes also displayed a significant increased expression of the key glycolytic marker proteins i.e., PFK and GAPDH. Moreover, the fate of pyruvate was also examined and unlike in the MEFs, astrocytes deficient in SGPL1 revealed a marked decrease in the expression of LDH, which was accompanied by a twofold increase in PDH expression. (Alam, Afsar et al. 2023). Furthermore, investigation of TCA cycle revealed significantly increased activity of IDH which is the key enzyme of TCA cycle (Alam, Afsar et al. 2023) giving strong indication of aerobic degradation of glucose in SGPL1-deficient astrocytes unlike in the MEFs which relied more on glucose degradation by the production of lactate. It was therefore not surprising that similar results regarding the glucose degradation was observed in both MEFs and astrocytes, but their fate of pyruvate was different since astrocytes are predominantly glycolytic (Magistretti and Allaman 2015). Consequently, SGPL1-deficient astrocytes exhibited significantly higher amount of ATP levels (more than two-fold), as the TCA cycle generates ATP more efficiently (30 ATP per glucose molecule) than glycolysis (2 ATP per glucose) (Alam, Afsar et al. 2023).

To ascertain the role of S1P in regulating glycolysis, control astrocytes were incubated with exogenous S1P (10 nM) for 24 h. As shown in fig.14, the expression of PFK, GAPDH, LDH as well as PDH in the control astrocytes stimulated by exogenous S1P was similar to that of the SGPL1-deficient astrocytes. These findings provide strong evidence that S1P signaling is

the predominant factor responsible for the observed increase in glucose metabolism *via* aerobic degradation through TCA cycle in SGPL1-deficient astrocytes.

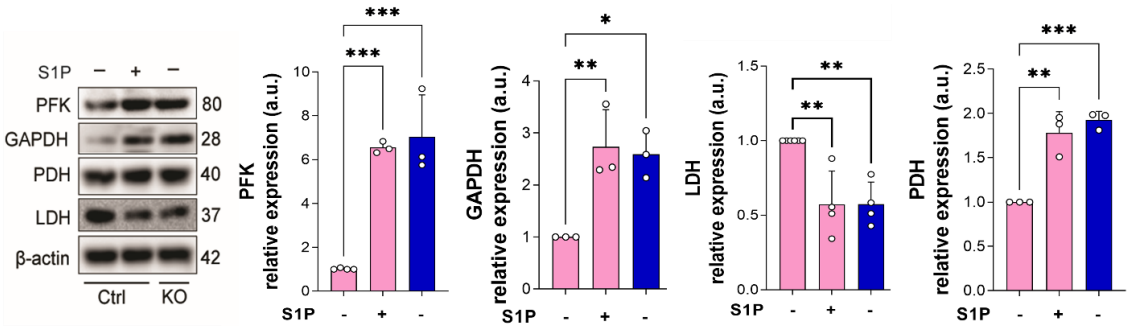

Figure 14. Recapitulation of SGPL1–deficiency by exogenously applied S1P (10 nM) to control astrocytes. Protein quantification of PFK, GAPDH, LDH and PDH in control astrocytes (pink bars) cultured in the absence (-) or presence (+) of 10 nM S1P for 24 h compared to the SGPL1-deficient astrocytes (blue bars). Shown is one representative western blot for each protein. β–actin was used as loading control (a.u., arbitrary units). Bars represent mean ± SEM ($n \geq 3$, ***$p < 0.0001$, **$p < 0.001$, *$p < 0.05$; one–way ANOVA with Bonferroni multiple comparison test). See also (Alam, Afsar et al. 2023)

3.2.3 S1P receptor 2 and 4 mediate the effect of S1P on glucose degradation in SGPL1-deficient astrocytes

To identify which S1P receptors out of the five known G-protein coupled receptors, were responsible for the alteration in glucose metabolism in SGPL1-deficient astrocytes, it was crucial to investigate the specific S1P receptors involved. It was found that out of five, $S1PR_{2,4}$ were strongly expressed in astrocytes with SGPL1 ablation (Alam, Afsar et al. 2023). To assess the possible impact of S1P signaling through these two receptors, CYM520 and CYM50300 were used as specific agonists for $S1PR_2$ and $S1PR_4$, respectively. For this, control astrocytes were incubated with both $S1PR_2$ and $S1PR_4$ receptor agonists simultaneously at a concentration of 5 µM each for 24 h. As shown in fig. 15, the expression of PFK, GAPDH and PDH in the control astrocytes treated with the $S1PR_{2,4}$ agonist produced similar effect to those observed in SGPL1-deficient astrocytes. It was also found that the combined addition of each agonist was required to replicate the effects of S1P suggesting that these two receptors may function as replacements for one another in eliciting glucose degradation in astrocytes.

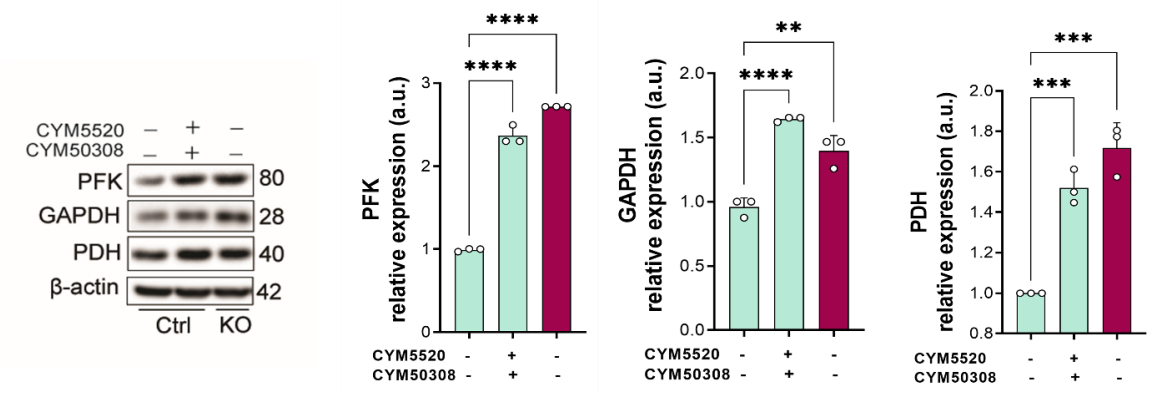

Figure 15. S1P receptors 2 and 4 mediate the effect of S1P on glucose degradation in SGPL1–deficient astrocytes. Protein quantification of PFK, GAPDH, and PDH following stimulation (+) of control astrocytes (blue bar) with a combination of specific agonists of $S1PR_2$ (CYM5520, 5 µM) and $S1PR_4$ (CYM50308, 5 µM) for 24 h compared to the SGPL1-deficient (purple bar) astrocytes. Shown is one representative western blot for each protein. β–actin was used as loading control (a.u., arbitrary units). Bars represent mean ± SEM ($n \geq 3$, ****$p < 0.0001$, ***$p < 0.001$, **$p < 0.01$; one–way ANOVA with Bonferroni multiple comparison test). See also (Alam, Afsar et al. 2023)

3.2.4 Increased glucose degradation is linked to the impaired autophagy in SGPL1-deficient astrocytes via S1P/$S1PR_{2,4}$ signaling

As discussed previously in section 3.1.6, cellular energy metabolism and autophagy are intimately linked processes. Therefore, similar to MEFs, with increase in glucose metabolism, the expression of mTOR which acts as a nutrient sensing molecule was evaluated and found to be significantly increased in SGPL1-deficient astrocytes (Alam, Afsar et al. 2023). Since mTOR functions as a master regulator of autophagy, the expression of autophagy marker genes, p62 and LC3 were analyzed which revealed a considerable increase in the expression of p62 on one hand and a considerable decrease in the ratio of LC3-II:LC3-I, suggesting a dysfunctional cargo processing and the obstruction in the autophagic flux, similar to that in the MEFs (Alam, Afsar et al. 2023).

Therefore, with established impaired autophagy in SGPL1-deficient astrocytes, it was crucial to explore the potential involvement of S1P receptors. To investigate this, control astrocytes were incubated in the presence of both CYM520 and CYM50300, specific agonists of $S1PR_2$ and $S1PR_4$, respectively, at a concentration of 5 µM each for 24 h. As depicted in fig. 16, the expression of p62 and the expression of the ratio of LC3-II:LC3-I, following the administration of the $S1PR_{2,4}$ agonist to control astrocytes resulted in comparable effects to those observed in the astrocytes lacking SGPL1. This finding was also confirmed by treatment of control and SGPL1-deficient astrocytes with specific inhibitors of $S1PR_2$ and $S1PR_4$ (Alam, Afsar et al. 2023).

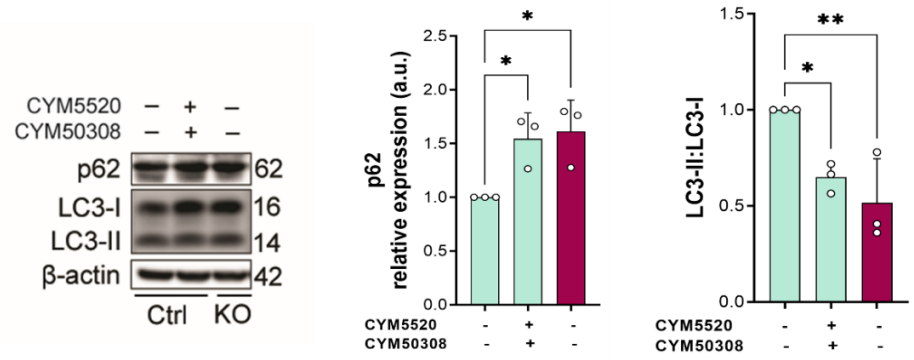

Figure 16. S1P signaling *via* S1PR$_{2,4}$ regulates autophagy in SGPL1-deficient astrocytes. Protein quantification of p62 and the ratio of LC3-I and LC3-II following stimulation (+) of control astrocytes (blue bar) compared to the SGPL1-deficient astrocytes (purple bar) with a combination of specific agonists of S1PR$_2$ (5 µM CYM5520) and S1PR$_4$ (5 µM CYM50308, 24 h), (-) represents without stimulation. For all, representative immunoblots are shown with β-actin as loading control. Bars represent mean ±SEM ($n \geq 3$, $^{**}p < 0.001$, $^{*}p < 0.05$, one-way ANOVA with Bonferroni multiple comparison test). See also (Alam, Afsar et al. 2023)

3.2.5 SGPL1 deficiency triggers astrogliosis in murine brains

Astrocytes play a vital role in promoting neuronal communication and upholding cellular balance and integrity of the CNS. As highlighted in section 1.7, alterations in metabolic processes, such as glucose degradation, can significantly impact their functioning. Building on previous findings that demonstrated significant accumulation of S1P in all brain regions of SGPL1$^{fl/fl/Nes}$ mice (Mitroi, Deutschmann et al. 2016), the current objective was to specifically investigate the potential impact of S1P accumulation in astrocytes. Astrocytes are capable of reacting to different types of brain injuries, leading to a condition known as astrogliosis where they become highly active (Sofroniew and Vinters 2010). Since GFAP is known as a marker for astrogliosis (Sofroniew and Vinters 2010), the expression of GFAP was investigated. Immunostaining of cortical slices from 12–month old mice and primary cultured astrocytes derived from SGPL1$^{fl/fl/Nes}$ mice revealed a considerable increased GFAP expression as depicted in fig. 17 A and B. Furthermore, the protein expression of GFAP from the cortex of SGPL1$^{fl/fl/Nes}$ mice was found to be more pronounced with an age-dependent increase when compared to the controls (Alam, Afsar et al., 2023 manuscript submitted).

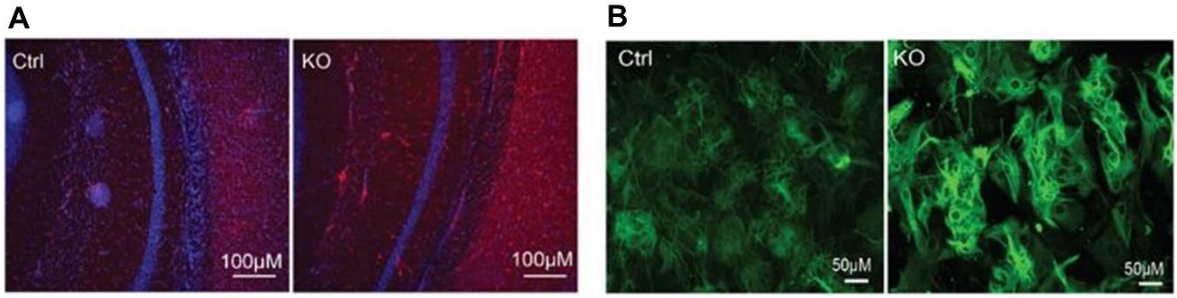

Figure 17. Validation of GFAP expression *via* immunostaining. Representative images of **(A)** cortical slices and **(B)** primary cultured astrocytes stained for GFAP from Ctrl and KO mice.

3.2.6 S1P accumulation triggers astrogliosis via activation of purinergic receptor, P2Y1R

As mentioned earlier, the buildup of S1P triggers an upsurge in glucose breakdown, resulting in a higher amount of cellular ATP in the SGPL1-deficient astrocytes. Subsequently, the level of extracellular ADP and ATP were also examined, where on one hand the level of ADP was found to be significantly higher as opposed to the reduced level of ATP in the media of SGPL1-deficient astrocytes compared to the control levels (Alam, Afsar et al., 2023 manuscript submitted). To ascertain the role of S1P/$S1PR_{2,4}$ axis to be responsible for the increased extracellular ADP, astrocytes were treated separately with exogenous addition of S1P (10 nM) and specific agonist of $S1PR_2$ (CYM5520) and $S1PR_4$ (CYM50308) 5 µM each respectively for 24 h. The administration of S1P and agonist of $S1PR_{2,4}$ respectively to the control astrocytes yielded similar results to those observed in the SGPL1-depleted cells (Fig. 18). These results thereby confirm that in SGPL1-deficient astrocytes, S1P signaling *via* its receptors $S1PR_2$ and $S1PR_4$ triggers the elevated extracellular ADP level.

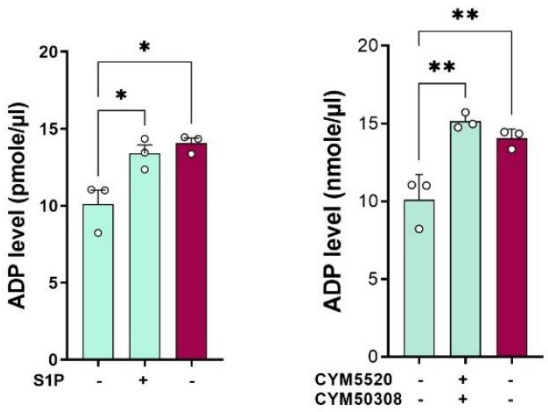

Figure 18. S1P/$S1PR_{2,4}$ axis is responsible for the increased extracellular ADP level in S1P–deficient astrocytes. Quantification of extracellular ADP level in the presence (+) and absence (-) of S1P (10 nM, 24h) and of $S1PR_{2/4}$ agonist (CYM5520 and CYM50308, 5 µM each) as indicated in the culture media of astrocytes derived from Ctrl and KO mice. Bars represent means ± SEM, ($n \geq 3$; $^{**}p < 0.001$, $^{*}p < 0.0$; one way ANOVA with Bonferroni multiple comparison test).

An elevated level of extracellular ATP in the brain can be a warning signal, indicating vulnerability to damage in the central nervous system (Rodrigues, Tomé et al. 2015). The activation of purinergic P2X receptors by ATP or P2Y adenosine receptors following the breakdown of extracellular ATP by ecto-nucleotidases into ADP is responsible for this effect (Rassendren and Audinat 2016). In particular, P2Y1R, which is a metabotropic receptor predominantly activated by ADP, is often implicated in the development of pathological conditions, primarily in astrocytes, by promoting astrocytic hyperactivity and astrogliosis (Delekate, Fuchtemeier et al. 2014, Franke and Illes 2014).

Upon investigation the expression of purinergic P2Y1R was found to be indeed higher in the cortex as well as in the primary cultured astrocytes from SGPL1-deficient murine brains (Alam 2021). To verify if the observed effect was indeed caused by the accumulation of S1P, which functions through its receptors $S1PR_{2,4}$, the control astrocytes were treated with $S1PR_2$ and $S1PR_4$ agonists simultaneously at a concentration of 5 µM each for 24 h and looked for the expression of P2Y1R. As shown in fig. 19, the administration of $S1PR_{2,4}$ agonist to control astrocytes resulted in a similar effect to that observed in the SGPL1-deficient astrocytes. These results suggest that the hyperactivation of SGPL1-deficient astrocytes induced by P2Y1R is triggered by S1P signaling through $S1PR_{2,4}$ leading to an increase in ATP levels and the subsequent production of extracellular ADP, which acts on the P2Y1R. These findings highlight the complex interplay between S1P and purinergic signaling pathways in astrocytes.

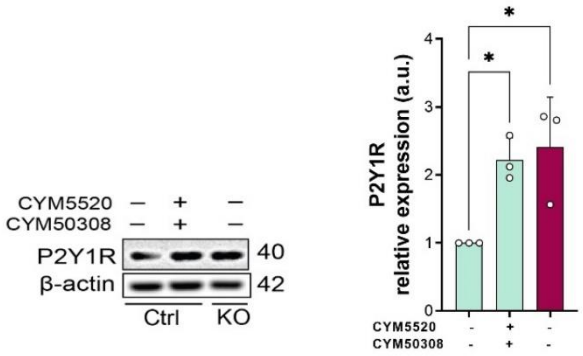

Figure 19. S1P/$S1PR_{2,4}$ signaling axis is responsible for the activation of purinergic receptor P2Y1R. Protein quantification of P2Y1R in the presence (+) and absence (-) of $S1PR_{2,4}$ agonist (CYM5520 and CYM50308, 5 µM each) for 24 hours as indicated in the primary cultured astrocytes derived from Ctrl (blue bar) and KO (purple bar) mice. Representative immunoblots are shown with β–actin as loading control. Bars represent means ± SEM, ($n \geq 3$; $^*p < 0.05$, one way ANOVA with Bonferroni multiple comparison test).

As mentioned above, the activation of P2Y1R is known to contribute to pathological processes in reactive astrocytes, such as astrocytic hyperactivity and astrogliosis (Delekate, Fuchtemeier et al. 2014). Additionally, GFAP serves as a well-established hallmark and specific marker for reactive astrocytes (Eng and Ghirnikar 1994). To provide further evidence regarding the functional connection between astrogliosis and the purinergic mechanism mediated by P2Y1R in SGPL1-deficient astrocytes, the expression of GFAP was examined in control astrocytes that had been exposed to a specific P2Y1R agonist, MRS2905, at a concentration of 5 nM for 24 h.

As depicted in fig. 20, a significant and almost identical increase in GFAP expression was observed in both the treated control astrocytes and SGPL1-deficient astrocytes. These findings support the idea that P2Y1R plays a critical role in promoting astrogliosis in SGPL1-deficient astrocytes.

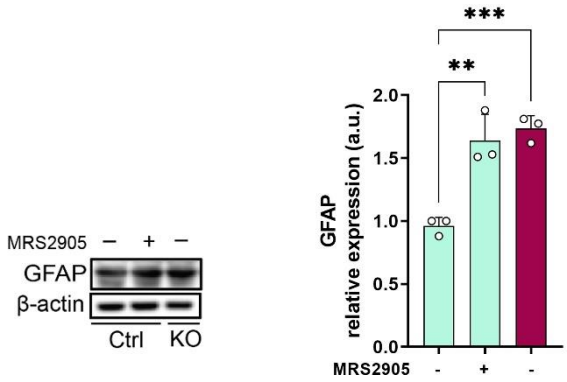

Figure 20. Activation of GFAP *via* P2Y1R in SGPL1 deficient astrocytes. Protein quantification of GFAP in the presence (+) and absence (-) of P2Y1R agonist (MRS2905, 5 nM each) for 24 hours as indicated in the primary cultured astrocytes derived from control (Ctrl, blue bar) and SGPL1$^{fl/fl/Nes}$ (KO, purple bar) mice. Representative immunoblots are shown with β–actin as loading control. Bars represent means ± SEM, ($n \geq 3$; **$p < 0.001$, ***$p < 0.0001$, one way ANOVA with Bonferroni multiple comparison test).

3.2.7 Transcriptional and epigenetic alterations in SGPL1-deficient murine brains

Previous studies on neural targeted SGPL1 deficient mice demonstrated that accumulation of S1P increases histone acetylation in astrocytes derived from SGPL1-deficient murine brains (Alam, Piazzesi et al. 2020). This points towards a functional role of S1P metabolism in eliciting epigenetic responses which could possibly contribute to neurodegenerative conditions.

Hence, there was a compelling interest in investigating the epigenetic regulatory effects resulting from the accumulation of S1P in astrocytes lacking SGPL1. To accomplish this, the first step involved a comprehensive analysis of the entire transcriptome using RNA sequencing, and examining the epigenetic status was conducted *via* CUT&Tag sequencing in hippocampal and cortical astrocytes. The analysis in Fig. 21 showcased transcriptional variation in a pool of 34 impacted genes, spanning categories such as PSD scaffolding proteins (*Begain, Dlgap3, Shank1*), synapse-associated proteins (*Dnd, Nsmf, Plppr2*), neurodegenerative disease-related proteins (*Plp1, Serpina3n*), and inflammation activating proteins (*Gja1, Ddx3x*). Notably, CUT&Tag sequencing identified significant alterations in only 2 genes, *Ddx3x* and *Nes*. Intriguingly, both RNA sequencing and CUT&Tag sequencing demonstrated downregulated expression of *Ddx3x*, highlighting its significance for further exploration (Fig. 21 B and E) (Alam, Afsar et al., 2023, manuscript submitted).

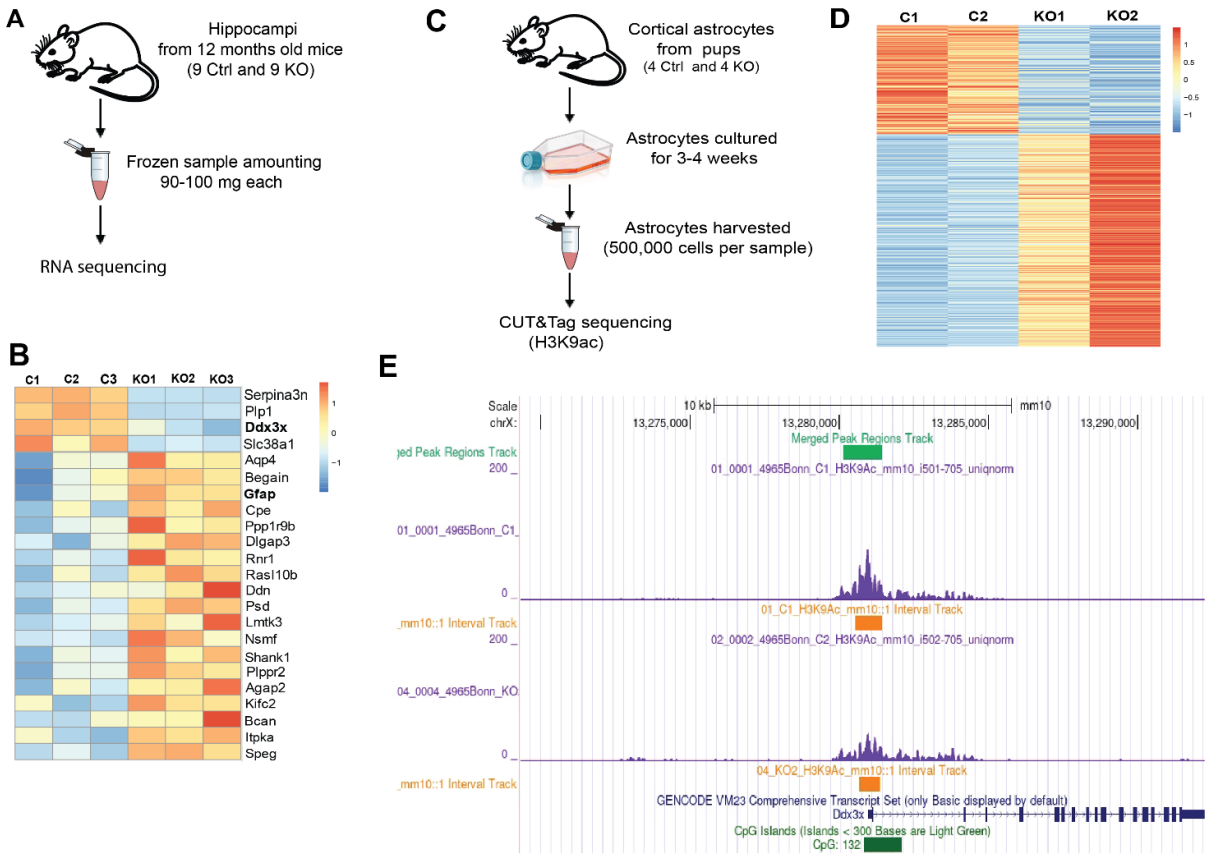

Figure 21. Transcriptome analysis in hippocampi and CUT&Tag chromatin profiling for histone H3K9ac in astrocytes. (A) Overview of RNA Sequencing **(B)** Heat map of differentially transcribed genes (see also Supplementary data 1) **(C)** Summary of CUT&Tag Sequencing **(D)** Heat map showing the intensity of H3K9ac signals across the astrocytic genome **(E)** Visualization of a 10kb chromatin segment of the Ddx3x promotor region showing the H3K9ac occupancy, using Integrated Genome Browser. (Alam, Afsar et al., 2023, manuscript submitted)

3.2.8 Activation of NLRP3 inflammasome in SGPL1-deficient murine brains

As shown in the RNA-Seq and CUT&Tag results, significant differences were observed in both the transcription and H3K9ac occupancy particularly at the promoter of *Ddx3x* between the control and SGPL1-deficient samples. However, immunoblot experiments revealed a significant increase in DDX3X protein level (Fig. 22). These results suggest high DDX3X protein levels may lead to downregulated transcription of the respective gene, implying a potential feedback loop. Despite discrepancies in the epigenomic and transcriptomic findings, the absence of SGPL1 and S1P accumulation have a significant impact on gene regulation and protein expression levels.

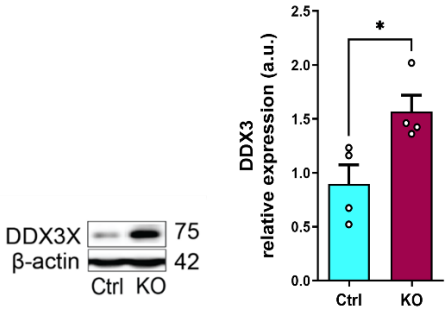

Figure 22. Expression of DDX3X in astrocytes derived from control and SGPL1 deficient murine brains. Protein quantification of DDX3X in the primary cultured astrocytes derived from control (Ctrl, blue bars) and SGPL1$^{fl/fl/Nes}$ (KO, purple bars) mice. Representative immunoblots are shown with β–actin as loading control. Bars represent means ± SEM, (n ≥ 3; *p < 0.05; unpaired Student *t* test).

Furthermore, recent studies have recognized the significance of DDX3X as a key contributor in signaling pathways associated with inflammation (Kesavardhana, Samir et al. 2021). Therefore, it was necessary to verify whether NLRP3 was activated due to the high level of DDX3X protein expression. Indeed, the expression of NLRP3 was significantly increased more than 50% in cortices from 12–month old SGPL1$^{fl/fl/Nes}$ mice (Fig. 23).

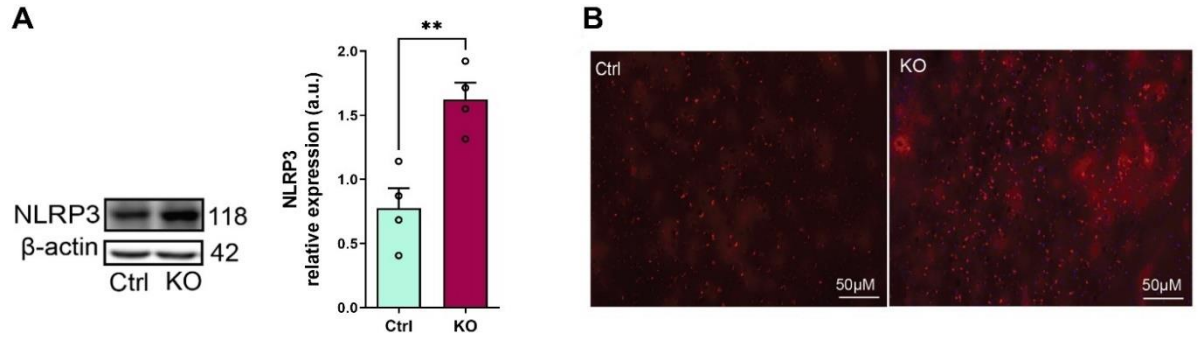

Figure 23. Increased expression of NLRP3 in cortex derived from SGPL1-deficient murine brain.(A) Protein quantification of NLRP3 and **(B)** Representative image derived from the cortical slices of control (Ctrl) and SGPL1$^{fl/fl/Nes}$ (KO) mice. Representative immunoblots are shown with β–actin as loading control. Bars represent means ± SEM, (n ≥ 3; **p < 0.001; unpaired Student *t* test).

NLRP3 inflammasome consists of three components: a sensor (NLRP3), an adaptor (ASC or PYCARD) and an effector (caspase1) (Swanson, Deng et al. 2019). Moreover, for the activation of the NLRP3 inflammasome it is necessary to undergo priming which involves assembly and increased expression of inflammasome component caspase1 which further cleaves pro-IL-1β into its mature activated form IL-1β (Kelley, Jeltema et al. 2019). Therefore, in order to validate an activated NLRP3 inflammasome it was necessary to look for the expression of NLRP3 along with caspase1 and IL-1β as well. Immunoblots from control and SGPL1-depleted astrocytes depicted increased expression of both caspase1 as well as a significant increase in the expression of pro IL–1β and IL–1β (Fig. 24) suggesting a strongly activated NLRP3 inflammasome.

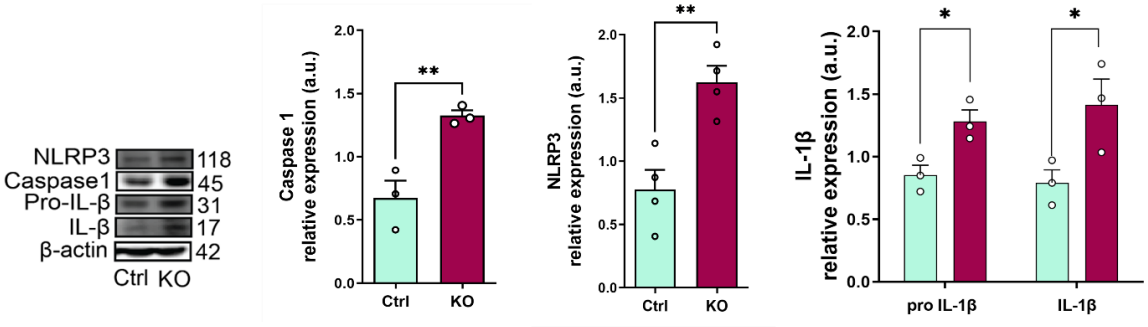

Figure 24. Activated NLRP3 inflammasome derived from SGPL1-deficient astrocytes. (A) Protein quantification of NLRP3, Caspase1, Pro IL-1β and IL–1β in primary cultured astrocytes of control (Ctrl, blue bar) and SGPL1$^{fl/fl/Nes}$ (KO, purple bar) mice. Representative immunoblots are shown with β–actin as loading control. Bars represent means ± SEM, (n ≥ 3; **p < 0.001, *p < 0.05; unpaired Student *t* test).

3.2.9 Activation of NLRP3 inflammasome in SGPL1-deficient murine brains via purinergic *P2Y1R-mediated signaling*

In order to establish a correlation between astrogliosis and inflammation in SGPL1 deficient astrocytes, the expression of NLRP3 in the astrocytes was examined in the presence of P2Y1R specific agonist (MRS2905, 10 nM) for 24 h. Interestingly, administration of P2Y1R agonist to the control astrocytes recapitulated the effect seen in the SGPL1$^{fl/fl/Nes}$ astrocytes (Fig. 25).

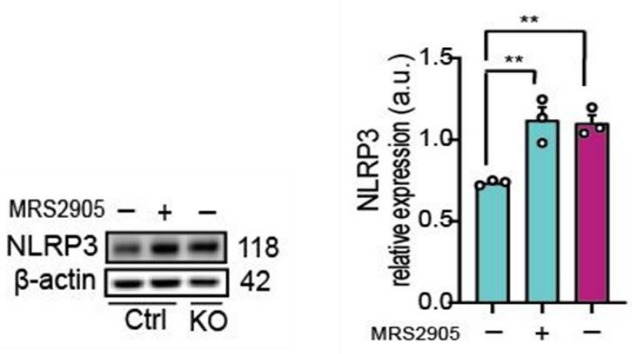

Figure 25. Increased expression of NLRP3 in SGPL1-deficient astrocytes with P2Y1R agonist treatment. Protein quantification of NLRP3 in the presence (+) and absence (-) of P2Y1R agonist, MRS2905 (10 nM, 24 h) in primary cultured astrocytes of control (Ctrl, blue bar) and SGPL1$^{fl/fl/Nes}$ (KO, purple bar) mice. Representative immunoblots are shown with β–actin as loading control. Bars represent means ± SEM, (n ≥ 3; **p < 0.001; one way ANOVA with Bonferroni multiple comparison test).

In order to validate the association between NLRP3 and P2Y1R, the expression of NLRP3 inflammasome markers was assessed in the presence of a specific antagonist of P2Y1R, MRS2179 (100 μM, 24h). The results demonstrated that the increased expression of NLRP3, caspase-1, and IL-1β in SGPL1-deficient astrocytes was effectively reversed back to control values upon treatment with MRS2179, confirming the link between NLRP3 and P2Y1R (Fig. 26).

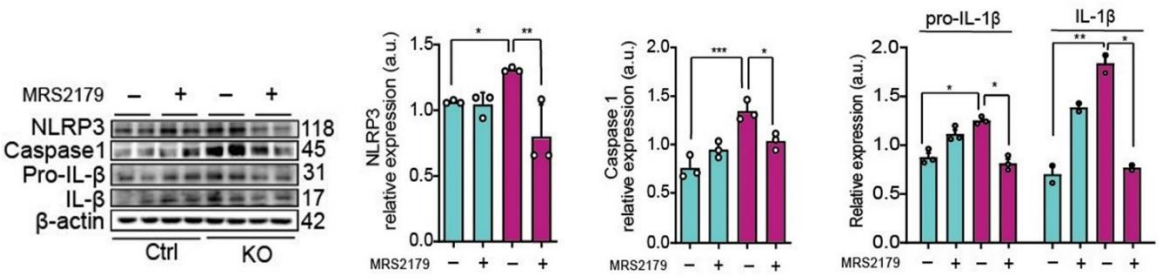

Figure 26. Activated NLRP3 inflammasome is P2Y1R dependent in SGPL1-deficient astrocytes. Protein quantification of NLRP3, Caspase1, Pro IL-1β and IL–1β in the presence (+) and absence (-) of P2Y1R antagonist, MRS2179 (100 µM, 24 h) in primary cultured astrocytes of control (Ctrl, blue bar) and SGPL1$^{fl/fl/Nes}$ (KO, purple bar) mice. Representative immunoblots are shown with β–actin as loading control. Bars represent means ± SEM, (n ≥ 3; ***p < 0.0001 **p < 0.001, *p < 0.05; one way ANOVA with Bonferroni multiple comparison test).

Likewise, the increased expression of DDX3X was also reversed back to control levels in the presence of P2Y1R antagonist (Fig. 27). Subsequently, the mRNA expression of proinflammatory cytokine IL-1β induces maturation of IL-1 family cytokines such as IL-18, IL-15, IL-11 as well as TNFα was found to be increased in the astrocytes deficient of SGPL1 (Alam, Afsar et al., 2023 manuscript submitted).

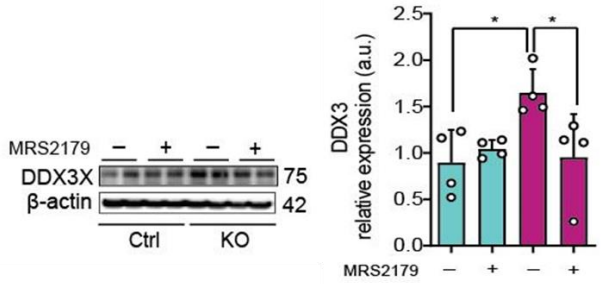

Figure 27. Rescue of DDX3X expression with P2Y1R antagonist treatment in SGPL1-deficient astrocytes. Protein quantification of DDX3X in the presence (+) and absence (-) of P2Y1R antagonist, MRS2179 (100 µM, 24 h) in primary cultured astrocytes of control (Ctrl, blue bar) and SGPL1$^{fl/fl/Nes}$ (KO, purple bar) mice. Representative immunoblots are shown with β–actin as loading control. Bars represent means ± SEM, (n ≥ 3; *p < 0.05; one way ANOVA with Bonferroni multiple comparison test).

Together, the findings of this study illustrate the critical role of P2Y1R signaling in driving astrogliosis and subsequent activation of NLRP3 inflammasome in SGPL1 deficient murine brains.

3. DISCUSSION

S1P has gathered significant attention due to its diverse signaling properties in a wide range of cellular processes. While considerable progress has been made in understanding its functions, there is still much to reveal about the intricate molecular mechanisms that drive S1P-mediated signaling. This study aimed to address this knowledge gap by investigating the accumulation of S1P and its influence on critical cellular pathways, like glucose metabolism, autophagy and inflammation leading to the development of pathophysiological conditions particularly neurodegeneration and cancer.

4.1 Effect of S1P Accumulation on SGPL1-deficient MEFs

Previous research conducted by the group of van Echten Deckert showed that the depletion of SGPL1 in MEFs leads to alterations in sphingolipid metabolism, resembling the characteristics favoring growth of cancer cells. The absence of SGPL1 is also associated with increased cell proliferation in vitro and oncogenesis in vivo. Building upon this, we hypothesized that the accumulation of S1P in SGPL1-deficient MEFs could impact glucose metabolism acting *via* its receptors. In a first attempt, our results demonstrated an elevation in glucose uptake along with increased expression of GLUT 1. Consistently, higher expression level of glycolytic marker proteins such as PFK and GAPDH strongly argues in favor of higher glucose degradation in SGPL1 deficient MEFs. Moreover, substantial increase in the expression of LDH while a considerable down regulated expression of markers of TCA cycle provided evidence favoring a shift to aerobic glycolysis in SGPL1 deficient MEFs. Notably, one of the key factors that contributes to the enhanced aerobic glycolysis particularly observed in cancer cells is the activation of HIF-1α. This activation is also responsible for upregulating the expression of glucose transporters and glycolytic enzymes, and also plays a crucial role in facilitating cellular adaptation to low oxygen levels thereby promoting malignancy in cancer cells (Semenza 2001). Interestingly in the case of SGPL1-deficient MEFs, a significant increase in the expression of HIF-1α was observed even under aerobic conditions since activation of HIF-1 is not exclusively dependent on the lack of oxygen and can also be triggered through non-canonical pathway (Iommarini, Porcelli et al. 2017). The upregulation of HIF-1 in SGPL1-deficient MEFs induced by S1P/S1PR1-3 signaling (Fig. 28) occurs independently of oxygen levels and bears resemblance to the activation of HIF-1 by insulin and insulin-like growth factors (IGFs) (Ren, Accili et al. 2010). Besides, MEFs

deficient in SGPL1 exhibited higher proliferative capacity despite growing as a monolayer. Overall, SGPL1 deficient MEFs demonstrated considerably increased reliance on aerobic glycolysis as their primary glucose degradation pathway by evading TCA cycle, facilitated by the activation of HIF-1 transcription factor, enabling these cells to meet the substantial energy demands required for their rapid growth. These findings strongly support the notion that MEFs lacking SGPL1 activity exhibit cancer-like properties, further underscoring their resemblance to cancer cell.

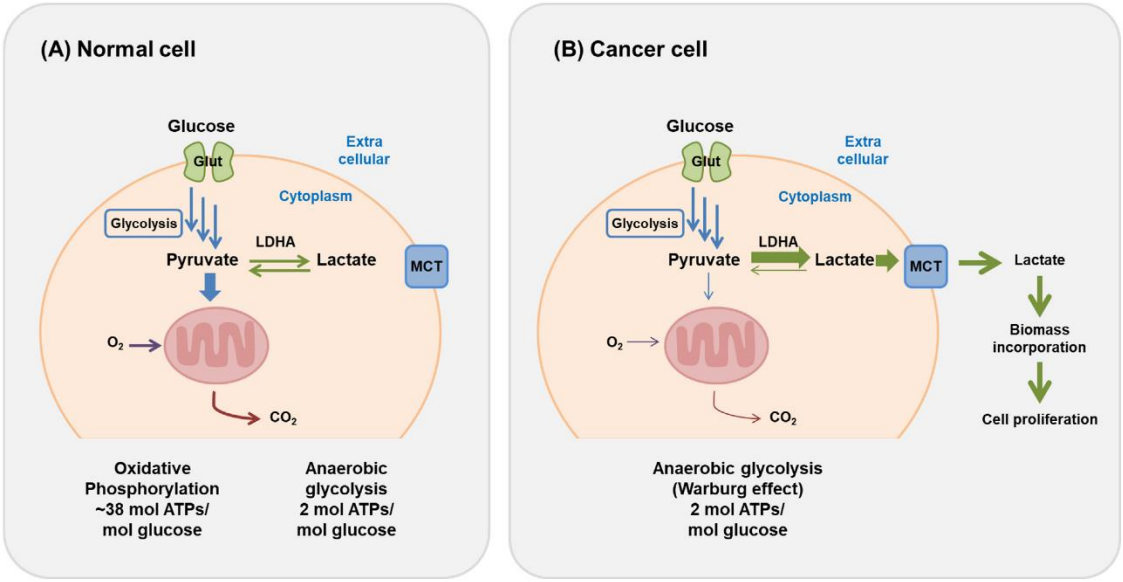

Figure 28. Representative image of glucose metabolism. (A) In the presence of oxygen, normal cells efficiently utilize glucose through glycolysis, the TCA cycle, and the electron transport system, producing up to 38 ATP molecules per glucose molecule. However, under low oxygen conditions, normal cells accumulate pyruvate as it cannot enter the TCA cycle. This accumulated pyruvate is converted to lactic acid, resulting in the production of only 2 ATP molecules. This anaerobic glycolysis pathway yields a limited amount of energy compared to aerobic conditions. **(B)** Cancer cells exclusively rely on glycolysis as their primary energy-producing pathway, regardless of the presence or absence of oxygen. This metabolic strategy leads to the production of only 2 ATP molecules per glucose molecule. As a result, cancer cells require a greater amount of glucose compared to normal cells in order to meet their energy demands. (Kim and Baek 2021)

Since MEFs with substantial accumulation of S1P, exhibited an upregulation of glycolysis, leading to an increased energy load within the cells. This elevation in cellular energy levels has been shown in multiple studies to activate the Akt signaling pathway, which plays a critical role in various cellular processes including cell growth, survival, and proliferation (Abdel-Wahab, Mahmoud et al. 2019). Therefore, to gain more insights of the energy status in SGPL1-deficient MEFs, an investigation was conducted to check for the activation of the Akt and its downstream activator, mTOR pathway. The mTOR protein, a serine/threonine kinase, plays a critical role in sensing ATP and amino acid levels, thereby regulating nutrient availability, cell growth, and survival (Manning and Cantley 2007, Laplante and Sabatini 2009). It is activated by pathways responsive to mitogens that signal energy and nutrient availability. The PI3K/Akt pathway, known for its role in promoting cell proliferation and

survival, is considered the primary mechanism by which mTOR is regulated (Laplante and Sabatini 2009). In this context, the phosphorylation-driven activation of Akt and the heightened expression of mTOR in SGPL1-deficient MEFs indicate that the metabolic alterations occurring in the absence of SGPL1 are advantageous for meeting the cellular energy demands. These findings suggest that the changes in cellular metabolism resulting from SGPL1 deficiency create a favorable environment for maintaining the necessary energy load within the cells.

Furthermore, mTOR, a crucial regulator of autophagy, is known to be affected by rapamycin, which induces autophagy (Dunlop and Tee 2014, Dossou and Basu 2019). However, the role of mTOR in autophagy regulation is intricate, influencing not only the initiation but also subsequent steps of the autophagy process (Dossou and Basu 2019). In the case of SGPL1-deficient MEFs, the elevated phosphorylation-driven activation of mTOR indicates a defective autophagy within these cells. The findings in this study provide compelling evidence for a decrease in autophagy in *Sgpl1*$^{-/-}$ MEFs, which can be restored to normal levels through the use of rapamycin treatment (Fig. 29).

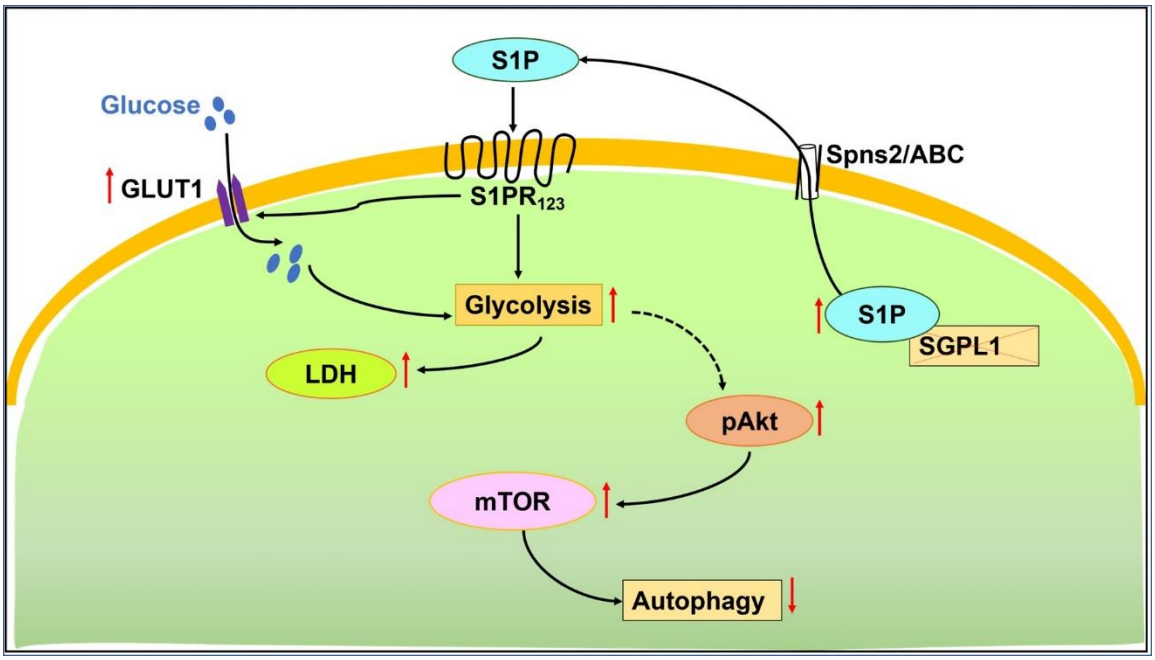

Figure 29. Scheme illustrating the effects of SGPL1 depletion in MEFs. In the absence of SGPL1, accumulated S1P is released by the cells [55]. S1P binds to S1PR1–3 receptors, initiating signaling pathways that enhance the expression of proteins involved in glucose uptake and utilization through aerobic glycolysis. This metabolic shift, along with the elevated energy state, triggers the activation of the Akt/mTOR pathway, resulting in reduced autophagy. The figure indicates the affected targets by S1PR antagonists (VPC and JTE), Akt inhibitor (AktIn), and mTOR inhibitor (rapamycin). ABC, ATP-binding cassette transporters; HIF-1, hypoxia-inducible factor 1; p-Akt, phosphorylated Akt; p-mTOR, phosphorylated mTOR; Spns2, spinster 2. See also (Afsar, Alam et al. 2022)

It is intriguing that a previous study did not observe any changes in autophagy in SGPL1-deficient MEFs compared to their wild-type counterparts (Colie, Van Veldhoven et al. 2009), and the reason for this inconsistency remains unknown. However, it is important to highlight

that the same study reported an increase in the levels of the antiapoptotic proteins Bcl-2 and Bcl-xL in SGPL1-deficient MEFs, which conferred protection against apoptosis induced by chemotherapy drugs. Interestingly, Bcl-2 not only has antiapoptotic properties but also hinders the process of autophagy through its interaction with Beclin1, a crucial protein involved in autophagy (Pattingre, Tassa et al. 2005). Moreover, the inhibitory effect of Bcl-2 on apoptosis can be counteracted by rapamycin, suggesting the involvement of mTOR and its upstream activator, Akt (Asnaghi, Calastretti et al. 2004). These findings provide further evidence supporting the notion that cells lacking SGPL1 possess oncogenic characteristics, as they exhibit altered regulation of autophagy and enhanced resistance to apoptosis.

4.2 Impact of S1P accumulation on SGPL1-deficient astrocytes

The effect of S1P signaling mediated *via* its receptor as seen in non-neural fibroblasts was recapitulated in astrocytes derived from SGPL1 deficient murine brain in this study focusing on investigating the impact of S1P metabolism on astrocytes, and exploring into its significant implications for glucose breakdown, autophagy and inflammation.

As already mentioned in the introduction section, astrocytes are often overlooked in favor of neurons but are in fact key players in the central nervous system (CNS). They surpass neurons in number by more than fivefold (Sofroniew and Vinters 2010) and promptly respond to various forms of brain injury (Carter, Herholz et al. 2019, Ravi, Paidas et al. 2021) and contribute significantly to crucial neurodevelopmental processes (de Oliveira Figueiredo, Cali et al. 2022).

The initial aim of this study was to investigate whether the accumulation of S1P has any impact on glucose metabolism in astrocytes lacking SGPL1. Glucose, a fundamental energy source for the brain, is essential for sustaining crucial processes such as maintaining membrane ion gradients and facilitating synaptic transmission (Attwell and Laughlin 2001). While neurons primarily rely on oxidative glucose degradation to produce ATP (Goyal, Hawrylycz et al. 2014), astrocytes predominantly employ glycolysis (Choi and Chun 2013). This glycolytic preference allows astrocytes to efficiently extract glucose from the bloodstream or mobilize glycogen stores, all under the guidance and regulation of neighboring neurons (Goyal, Hawrylycz et al. 2014). This study specifically investigated the impact of S1P signaling, mediated by $S1PR_2$ and $S1PR_4$, on the upregulation of critical glycolytic enzymes such as PFK and GAPDH. Furthermore, it revealed that S1P signaling promoted the expression of PDH while simultaneously reducing the expression of LDH. Similar to the non-neural cells such as MEFs lacking SGPL1, the accumulation and release of S1P also resulted

in the signaling through $S1PR_{1-3}$ leading to an enhanced glucose uptake and breakdown *via* glycolysis (Afsar, Alam et al. 2022). However, in the case of astrocytes lacking SGPL1, upregulated expression of PFK and subsequent elevation of glycolytic flux may serve as a protective mechanism, shielding them from toxic depositions that have been observed in SGPL1-deficient neurons (Mitroi, Karunakaran et al. 2017). It is significant to highlight that despite its lower efficiency in ATP production compared to oxidative phosphorylation, aerobic glycolysis plays a beneficial role in providing intermediary compounds necessary for the synthesis of lipids, nucleic acids, and amino acids (Vander Heiden, Cantley et al. 2009). Nonetheless, the preferential degradation of glucose *via* the TCA cycle induced by S1P poses potential drawbacks for astrocytes. This metabolic shift could lead to a reduction in lactate generation, which has crucial implications for brain health (Vardjan, Chowdhury et al. 2018, Cai, Wang et al. 2022). Lactate, generated by astrocytes through aerobic glycolysis despite sufficient oxygen levels, serves a dual purpose as a vital energy source for neurons and an intercellular messenger (Barros 2013, Cai, Wang et al. 2022). Its contribution to brain development is undeniable, as it supports the biosynthetic demands of synaptic growth and remodeling and also plays a role in memory formation (Barros 2013, Alberini, Cruz et al. 2018).

As shown previously, in SGPL1-deficient fibroblasts, a metabolic shift was observed from the TCA (tricarboxylic acid) cycle, which is the main pathway for glucose oxidation, to aerobic glycolysis, where glucose is broken down into lactate even in the presence of sufficient oxygen which is famously known as Warburg effect and commonly associated with cancer cells promoting cell growth (Pavlova and Thompson 2016, Afsar, Alam et al. 2022). However, in SGPL1-deficient astrocytes, a different metabolic response was observed. Instead of relying on aerobic glycolysis, pyruvate, the end product of glycolysis, was preferentially directed towards the TCA cycle. This shift allows astrocytes to generate more ATP through oxidative phosphorylation, which is a more efficient process of ATP production. ATP, apart from being the energy currency of cells, plays a crucial role in various cellular functions, including neuronal activity in the brain. ATP and adenosine are involved in regulating oligodendrocyte differentiation and myelination (Agresti, Meomartini et al. 2005, Rivkees and Wendler 2011) and also modulate the functioning of astrocytes and sustain calcium waves, which are crucial for the excitability of glial cells and communication between them (Koizumi 2010). Moreover, ATP primarily acts as a synaptic neuromodulator by regulating the release of neurotransmitters at the presynaptic level and influencing other receptors or the intrinsic excitability of neurons at the postsynaptic level. These actions of

ATP have significant implications for synaptic plasticity, which refers to the ability of synapses to change and adapt (Cunha and Ribeiro 2000, Khakh 2001, Halassa, Fellin et al. 2009). Accordingly, it has been shown that metabolic agents that increase ATP levels can have positive effects on cognitive functioning (Owen and Sunram-Lea 2011). However, studies involving $SGPL1^{fl/fl/Nes}$ mice have revealed cognitive deficits, including impairments in spatial and associative learning as well as memory (Mitroi, Deutschmann et al. 2016). By preferentially utilizing the TCA cycle, SGPL1-deficient astrocytes enhanced their ATP production, which can support the energy demands of brain cells and contribute to normal brain functioning (Alam, Afsar et al. 2023). This metabolic adaptation in astrocytes may serve as a compensatory mechanism to overcome the metabolic deficiencies caused by SGPL1 deficiency.

Conclusively, the study reveals that S1P signaling has complex effects on astrocytic glucose metabolism. It enhances ATP production through $S1PR_{2,4}$ activation while concurrently reducing lactate formation, as indicated by decreased LDH levels (Alam, Afsar et al. 2023). These findings highlight the intricate changes induced by S1P signaling in astrocytic glucose metabolism.

4.3 Interplay of S1P accumulation and autophagy in astrocytes

As shown in previous section, studies examining the relationship between glucose metabolism and cellular autophagy in SGPL1-deficient cells, such as fibroblasts, have demonstrated that the absence of SGPL1 leads to enhanced glucose metabolism *via* $S1P/S1PR_{1-3}$ signaling axis. This alteration in glucose metabolism subsequently impairs mTOR-dependent autophagy. Building on these findings, further investigations were conducted to elucidate the connection between glucose metabolism and cellular autophagy in SGPL1-deficient astrocytes. Indeed, elevated glucose breakdown through the TCA cycle led to mTOR dependent impaired autophagy. Conversely, in neurons lacking SGPL1 activity, autophagic flux was disrupted due to a decrease in phosphatidylethanolamine (PE), and this disruption was independent of mTOR signaling (Mitroi, Karunakaran et al. 2017). Notably, previous findings on SGPL1 deficient murine brains demonstrated that SGPL1-depleted astrocytes did not experience alterations in PE levels (Karunakaran, Alam et al. 2019). The significance of autophagy in the survival of postmitotic neurons is well-established (Nixon 2013). Additionally, impaired neuronal autophagy is strongly associated with various neurodegenerative diseases (Nixon 2013). The compromised autophagic process contributes to the pathogenesis of these diseases

by impeding the clearance of intracytoplasmic aggregates of protein prone to forming aggregates (Menzies, Fleming et al. 2015).

Previous reports on neurons derived from SGPL1$^{fl/fl/Nes}$ mice demonstrated that impaired neuronal autophagy in mice leads to the accumulation of aggregate-prone proteins, such as amyloid precursor protein (APP) and α-synuclein (SNCA), which are associated with cognitive deficits in these mice (Mitroi, Deutschmann et al. 2016, Mitroi, Karunakaran et al. 2017). Impaired neuronal autophagy is also a characteristic feature of inherited congenital disorders known as "lysosomal storage" disorders, which are characterized by severe neurodegenerative symptoms (Nixon 2004, Nixon, Yang et al. 2008). Similar results have been observed in astrocytes affected by lysosomal storage disorders, indicating that impaired autophagosomal maturation in astrocytes affects the survival of cortical neurons and contributes to various neurological manifestations of the disease (Di Malta, Fryer et al. 2012). Furthermore, the significance of astrocytic autophagy in systemic metabolism has been emphasized (van Echten-Deckert and Alam 2018). Therefore, it is possible that down-regulated autophagy in astrocytes of SGPL1$^{fl/fl/Nes}$ mice may have a negative impact. However, the impaired autophagy could not be restored using rapamycin, a neuroprotective agent known to counteract the pathological effects of mTOR (Schmeisser and Parker 2019). Understanding the consequences of SGPL1 deficiency on glucose degradation and autophagy in astrocytes can provide valuable insights not only into S1P function in brain pathology but also into the complex phenotype observed in patients with mutations in SGPL1.

4.4 Impact of S1P accumulation on astrogliosis

The various functions performed by astrocytes, such as providing support to neurons, regulating the blood-brain barrier, modulating the extracellular environment, managing immune cells, and influencing synapse formation and function, are crucial in determining how the brain fares during and following injury (Pekny and Nilsson 2005, Sofroniew 2009). The results from this study reveals that in the astrocytes of SGPL1$^{fl/fl/Nes}$ murine brains, elevated levels of ATP (Alam, Afsar et al. 2023) can act as a warning sign, indicating an increased vulnerability to CNS damage (Rodrigues, Tome et al. 2015). The observed elevation of extracellular ADP levels in this study is likely attributed to the release of ATP into the extracellular environment, followed by its breakdown by ectonucleotidases, resulting in the generation of ADP. This effect is attributed to the activation of purinergic P2X receptors by ATP or P2Y adenosine receptors, which occurs subsequent to the breakdown of extracellular ATP into ADP facilitated by ecto-nucleotidases (Rassendren and Audinat 2016). In response

to disruptions in brain homeostasis caused by injury or disease within the CNS, astrocytes activate a defense mechanism known as reactive astrogliosis which serves as a sensitive indicator for various brain pathologies, including ischemia, infections, stroke, and neurodegenerative disorders (Sofroniew 2009, Sofroniew 2014, Neal and Richardson 2018). Notably, the P2Y1R receptor, which is primarily activated by ADP, is frequently associated with the development of pathological conditions, particularly in astrocytes thereby promoting excessive astrocytic activity and contributing to astrogliosis (Delekate, Fuchtemeier et al. 2014). A recent study conducted by Delekate et al., in a mouse model of Alzheimer's disease emphasized the significance of purinergic signaling through P2Y1R in disrupting the functioning of astroglial networks (Delekate, Fuchtemeier et al. 2014). The study revealed the upregulated expression of P2Y1Rs in reactive astrocytes surrounding senile plaques, indicating their involvement in promoting astrocytic hyperactivity, while ruling out the role of P2X receptors. Consistently, a significant increase in ADP levels was observed in the culture medium of astrocytes lacking SGPL1, underscoring the importance of ADP signaling mediated by P2Y1R in the absence of SGPL1. In primary cultured astrocytes derived from $SGPL1^{fl/fl/Nes}$ mice, the increased extracellular ADP levels were found to be dependent on S1P signaling *via* its receptors, specifically $S1PR_2$ and $S1PR_4$ (Alam, Afsar et al. 2023) and thereby suggests that SGPL1 deficiency affects S1P signaling, leading to altered ADP release in astrocytes.

4.5 Astrogliosis and neuroinflammation

Astrogliosis and neuroinflammation have long been recognized as significant factors contributing to the onset and progression of numerous neurological disorders. When astrogliosis and scar formation occur, inflammation serves as an acute response triggered by cellular injury or insult (Iglesias, Morales et al. 2017). The prototypic neuroinflammatory neurodegenerative disorder characterized by astrogliosis is multiple sclerosis (MS). In chronic MS lesions, there is a notable and pronounced astrogliosis that is distinct from other CNS disorders. The earliest descriptions of these lesions referred to them as "sclerotic patches," which ultimately led to the name "multiple sclerosis" (Hostenbach, Cambron et al. 2014). Apart from this, dysregulated S1P metabolism has often been associated as a significant factor in the pathogenesis of inflammatory conditions, contributing to the development of neurodegenerative diseases. For instance, aberrant S1P signaling, particularly through the $S1PR_1$, has been implicated in the induction of astrogliosis and neuroinflammation (Choi, Gardell et al. 2011, Kim, Bielawski et al. 2018). Moreover, studies employing simulated

inflammation in primary cultured murine astrocytes identified $S1PR_3$ as the key mediator of the S1P-induced inflammatory response (Dusaban, Chun et al. 2017). Additionally, upregulation of astrocytic $S1PR_1$ and $S1PR_3$ has also been observed in multiple sclerosis lesions (Van Doorn, Van Horssen et al. 2010, Fischer, Alliod et al. 2011). Consistently, in $SGPL1^{fl/fl/Nes}$ murine brains, S1P produced by astrocytes, activates microglia through the $S1PR_2$, resulting in the release of inflammatory cytokines and contributing to the induction of neuroinflammation (Karunakaran, Alam et al. 2019). To further elucidate the underlying molecular mechanism linking astrocyte activation and inflammation, this study implicates the role of the S1P/$S1PR_{2,4}$ signaling axis in SGPL1-deficient astrocytes. The findings demonstrate that this signaling pathway stimulates the purinoreceptor P2Y1R, which in turn activates the NLRP3 inflammasome—a key player in neuroinflammation (Gombault, Baron et al. 2012). The NLRP3 inflammasome plays a crucial role in the innate immune system by activating caspase-1 and facilitating the release of proinflammatory cytokines such as IL-1β when there is microbial infection or cellular damage (Kelley, Jeltema et al. 2019). Typically, the NLRP3 inflammasome is activated through two signals: a priming signal and an activation signal (Swanson, Deng et al. 2019). The priming signal is triggered by various factors, including damage or pathogen-associated molecular patterns (DAMPs/PAMPs), as well as cytokines, leading to increased expression of *Nlrp3, Caspase-1, pro-IL-1β,* and *IL-1β* (Kelley, Jeltema et al. 2019). In astrocytes lacking SGPL1, the production of different inflammasome components may be primed by cytokines released by microglia (Karunakaran, Alam et al. 2019). However, our findings suggest that purine nucleotides likely play a role in this mechanism which was further supported by the use of specific P2Y1R agonists and antagonists (Swanson, Deng et al. 2019). Nevertheless, ATP, much like beta-amyloid (the primary constituent of senile plaques found in Alzheimer's disease), as well as various other factors, functions as a stimulator for the activation signal that initiates the formation and active state of the inflammasome (Swanson, Deng et al. 2019). This activation signal subsequently prompts caspase-1 to cleave pro-IL-1β, resulting in the release of IL-1β (Kelley, Jeltema et al. 2019).

Our findings also demonstrate that in SGPL1 deficient astrocytes, presence of sustained upregulated expression of the stress protein DDX3X, plays a significant role in triggering the activation of the NLRP3 inflammasome. This observation aligns with previous studies conducted on primary bone marrow-derived macrophages (Samir, Kesavardhana et al. 2019). Importantly, DDX3X is a highly adaptable protein with multiple functions, particularly in regulating the translation process during inflammation caused by infections and injuries (Ku,

Lai et al. 2019). Furthermore, recent research has established a connection between DDX3X and the degeneration of motor neurons seen in amyotrophic lateral sclerosis (Chen, Wang et al. 2017). While the exact mechanisms driving the activation of the NLRP3 inflammasome remain elusive at present, in a cohort study conducted on astrocytopathy patients, the levels of NLRP3 inflammasome and inflammatory cytokine were found to be elevated (Luo, Yan et al. 2019). Consistently, our study revealed an increased level of not only IL-1β but also other proinflammatory cytokines, including IL-6, IL-11, and TNFα (Fig. 30). Moreover, this study underlines the involvement of the metabotropic purinoreceptor P2Y1R in directly controlling both GFAP expression and NLRP3 activation in SGPL1-deficient astrocytes. Consistently, the use of P2Y1R antagonist to restore the elevated levels of DDX3X expression could potentially elucidate the relationship between purinergic-dependent inflammation induction in SGPL1 deficient astrocytes (Fig. 30).

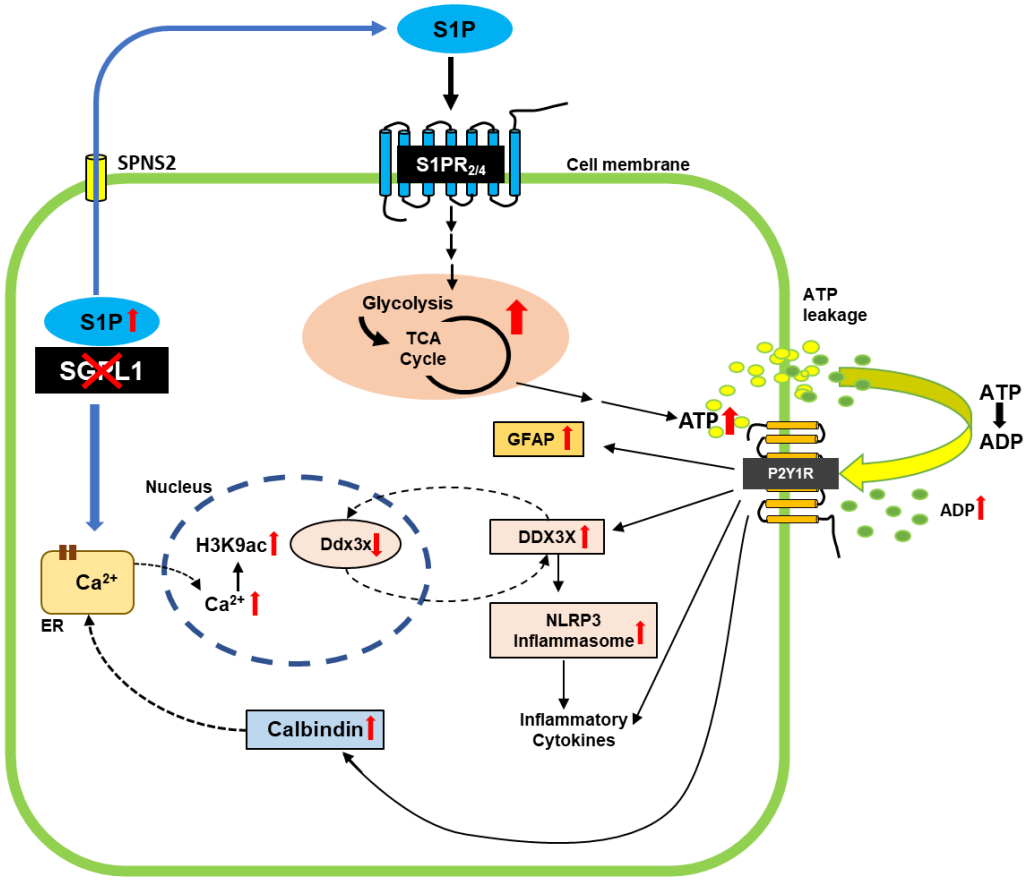

Figure 30 . Scheme summarizing the effect of SGPL1 ablation in astrocytes. With SGPL1 deficiency, accumulated S1P is released from the cells (Karunakaran, Alam et al. 2019). This S1P then binds to $S1PR_{2,4}$, initiating signaling pathways that enhance the production of proteins involved in glucose breakdown through glycolysis and the TCA cycle (Alam, Afsar et al. 2023). Consequently, the levels of extracellular ADP, which acts as a ligand for P2Y1R, increase. This receptor's involvement in the gliotic response of SGPL1-deficient astrocytes, leading to a proinflammatory reaction, is highlighted. Additionally, P2Y1R signaling induces the expression of calbindin, which binds to cytosolic Ca^{2+} released from the endoplasmic reticulum due to S1P accumulation (Ghosh, Bian et al. 1994). Moreover, nuclear Ca^{2+} promotes H3K9 acetylation (Alam, Piazzesi et al. 2020), impacting the transcription of *Ddx3x*. The elevated expression of DDX3X implies a potential feedback loop between protein levels and transcriptional regulation.

4. CONCLUSION

The present study highlights the significant role of S1P accumulation in various cellular processes, particularly in glucose metabolism, autophagy, and inflammation. The findings indicate that in MEFs lacking SGPL1, the accumulation of S1P leads to alterations in sphingolipid metabolism, resulting in enhanced glucose uptake and utilization through aerobic glycolysis. This metabolic shift is associated with the activation of HIF-1α and the Akt/mTOR pathway, promoting cell proliferation and survival. Additionally, autophagy is impaired in SGPL1-deficient MEFs, suggesting a defective cellular recycling process.

In astrocytes lacking SGPL1, S1P signaling also promotes glucose uptake and glycolysis through $S1PR_2$ and $S1PR_4$ activation. However, unlike in MEFs, pyruvate is preferentially directed towards the TCA cycle, leading to increased ATP production through oxidative phosphorylation. This metabolic adaptation may serve as a compensatory mechanism to overcome the metabolic deficiencies caused by SGPL1 deficiency. Furthermore, the study reveals that S1P signaling influences ATP levels, which have crucial implications for neuronal activity, synaptic plasticity, and cognitive functioning. In astrocytes, S1P signaling enhances ATP production while reducing lactate formation, indicating complex effects on glucose metabolism.

Overall, this study provides valuable insights into the molecular mechanisms and functional consequences of S1P accumulation in different cell types. Understanding S1P-mediated signaling in cellular processes and its impact on neurodegeneration and cancer has important therapeutic implications. The study also highlights the activation of NLRP3 inflammasome in SGPL1-deficient brains, with P2Y1R signaling playing a central role.

The study elucidates the critical involvement of the SGPL1/S1P/S1PR pathways in fundamental cellular processes, such as energy metabolism and autophagy, which may contribute to the diverse array of anomalies observed in cancer and brain pathologies.

5. MATERIALS

6.1 Chemical reagents

Chemical	Company	Source
Acrylamidmix 37,5:1, 30%	Carl Roth	Karlsruhe, Germany
Ammonium persulfate	Merck	Darmstadt, Germany
Tris–HCl	TH.GEYER	Renningen, Germany
SDS	Carl Roth	Karlsruhe, Germany
TEMED	Thermo Scientific	IL, USA
Glycine	TH.GEYER	Renningen, Germany
PVDF membrane	Merck Millipore	Tullagreen, Ireland
BSA	Thermo Scientific	IL, USA
Agarose	MJ Research/Biozym	Oldendorf, Germany
DMSO	Applicem	Darmstadt, Germany
Ethidiumbromide	Applicem	Darmstadt, Germany
Tween–20	Sigma	Taufkirchen, Germany
Protease inhibitor	Carl Roth	Karlsruhe, Germany
RIPA lysis buffer	Thermo Fischer Scientific	IL, USA
Laemmli buffer	BioRad	CA, USA
Stripping Buffer	TAKARA	Saint-Germain-en-Laye, France,

6.2 Cell culture reagents

Media	Catalogue Number	Company	Source
DMEM	31966	Gibco TM	Paisley, UK
FBS	P40–47100	PAN Biotech	Aidenbach, Germany
PBS	70077–044	Gibco TM	Neew York, USA
HBSS	14170–088	Gibco TM	Paisley, UK
Trypsin–EDTA	59418C	Sigma–Aldrich	Taufkirchen, Germany
Pennicillin/Streptomycin	15140122	Life Technologies	Darmstadt, Germany

6.3 Antibodies

Name	Catalogue Number	Company	Source
HRP–linked anti–mouse	7076S	Cell Signaling Technology	MA, USA
HRP–linked anti–rabbit	7074S	Cell Signaling Technology	MA, USA
B–actin	4967S	Cell Signaling Technology	MA, USA
GAPDH	5174S	Cell Signaling Technology	MA, USA
PDH	3205S	Cell Signaling Technology	MA, USA
LDH	2012S	Cell Signaling Technology	MA, USA
PFK	8164S	Cell Signaling Technology	MA, USA
mTOR	2972S	Cell Signaling Technology	MA, USA
p62	5114S	Cell Signaling Technology	MA, USA
LC3	12741S	Cell Signaling Technology	MA, USA
Akt	9272S	Cell Signaling Technology	MA, USA
p–Akt	193H12	Cell Signaling Technology	MA, USA
GFAP	3670S	Cell Signaling Technology	MA, USA
Calbindin	13176S	Cell Signaling Technology	MA, USA
NLRP3	15101S	Cell Signaling Technology	MA, USA
Caspase1	3866S	Cell Signaling Technology	MA, USA
IL–1β	12242S	Cell Signaling Technology	MA, USA
P2Y1R	BS–1204R	Thermo Fisher Scientific	MA, USA
DDX3X	2635S	Cell Signaling Technology	MA, USA
IDH	HPA007831	Sigma–Aldrich	MO, USA
GLUT–1	MA5–31960	Invitrogen	CA, USA
p–MTOR	129718–41	Invitrogen	CA,USA
HIF–1α	sc–13 515	Santa Cruz Biotechnology	TX, USA
SGPL1	ABS528	Sigma–Aldrich	MO, USA

6.4 Inhibitors

Name	Company	Source
JTE–013	Sigma–Aldrich (J4080)	MO, USA
VPC–2309	Cayman Chemical Company	MI, USA
Rapamycin	Cayman Chemical Company	MI, USA

CYM–55380	Sigma–Aldrich (SML–1066)	IL, USA
Akt1/2 kinase inhibitor	Abcam	Cambridge, UK
MRS2179	Tocris (0900)	Wiesbaden–Norderstedt, Germany

6.5 Agonists

Name	Company	Source
FTY–720	Cayman Chemical Company	MI, USA
S1P-SML2709	Sigma-Aldrich	MO, USA
CYM–5520 ($S1PR_2$)	Cayman Chemical Company	MI, USA
CYM–50308 ($S1PR_4$)	Cayman Chemical Company	MI, USA
MRS–2905 (P2Y1R)	Tocris (5633)	Wiesbaden–Norderstedt, Germany

6.6 Assay kit

Name	Catalogue Number	Company	Source
RNA isolation	EMB30–200	EXTRAzol (Blirt)	Gdansk, Poland
cDNA synthesis	E6560L	ProtoScript II First Strand (New England Biolabs)	MA, USA
MTT Assay	ab197010	Abcam	Cambridge, UK
G6P Assay	MAK014	Merck	Darmstadt, Germany

6.7 Primers

Gene	Primer sequence (forward and reverse)
β–actin	5′–CTTTGCAGCTCCTTCGTTGC–3′ 3′–CCTTCTGACCCATTCCCACC–5′
S1PR1	5′–CTACACAACGGGAGCAACAG–3′ 3′–CCCCAGGATGAGGGAGAGAT–5′
S1PR2	5′–CAGGATCTACTCCTTGGTCAGG–3′ 3′–GAGATGTTCTTGCGGAAGGT–5′
S1PR3	5′–CCCAACTCCGGGACATAGA–3′

	3′–ACAGCCAGTGGTTGGTTTTG–5′
S1PR4	5′–TTCCATATGATGGACACTCC–3′ 3′–TGGACAAATGAACGCAGGT–5′
S1PR5	5′–GCTTTCTGTGTACAGTTGACAAATACT–3′ 3′–CCAACTGTTCCAACTGTATGCT–5′

6.8 Apparatus

Name	Company	Source
Agarose gel imager	Alpha Innotech	Kasendorf, Germany
Immunoblot imager	Bio–RAD VersaDoc Imaging System	CA, USA
SDS–PAGE	Bio–RAD Mini PROTEAN Tetra cell	CA, USA
Fluorescence Microscope	Nikon–U2000	CA, USA
pH–meter	PH537, WTW	Weilheim, Germany
Pipette	Eppendorf research	Hamburg, Germany
qRT–PCR	Bio–RAD, CFX96 Real–Time System	CA, USA
Spectrophotometer	Bio–RAD SmartSpec Plus	CA, USA
Thermocycler	PTC–200, MJ Research/Biozym	Oldendorf, Germany
Nanodrop	Thermo Fischer Scientific ND–2000	DE, USA
Microplate reader	FLUOstar Omega BMG Labtech	Ortenberg, Germany
Fluorescence microscope	Keyence microscope BZ–X series	Neu–Isenburg, Germany

6. METHODOLOGY

7.1 Mouse model

In order to study the effect of S1P accumulation, particularly in the brain, a neural–specific *Sgpl1* knockout mouse model was generated by Dr. Nadine Hagen (in the group of Dr. van–Echten Deckert, 2013). In this mouse model SGPL1 floxed ($SGPL1^{fl/fl}$) was defined as control and neural–specific *SGPL1* transgenic mice ($SGPL1^{fl/fl/Nes}$, neural–specific *SGPL1* deleted mice) was used as SGPL1–deficient KO mice. Floxed mice were kindly provided by Prof. Dr. Julie D. Saba (University of California, USA) while, Prof. Dr. Martin Theiß (previously from Uniklinikum Bonn, Germany) contributed to the nestin–Cre transgenic mice.

The generation of $SGPL1^{fl/fl/Nes}$ mice was based on the Cre–lox recombinase technique which employs a Cre recombinase and its recognition site, *loxP* for the purpose of mammalian gene editing. Cre recombinase is an enzyme produced from *cre* gene (cyclization recombinase) of bacteriophage P1 which specifically binds to DNA sequences called *loxP* sites (locus of x–over, P1) and mediates site specific deletion of DNA sequences between two *loxP* sites.

In mice, the exons between 9/10 and 12/13 encode for the binding site of the SGPL1 cofactor, pyridoxal phosphate (PLP). These sites, flanked by the loxP sites led to the creation of "floxed" mice ($SGPL1^{fl/fl}$). In order to obtain neural–specific transgenic mice, it was necessary to generate neural–specific *cre* strain in which cre recombinase was expressed by a promoter that specifically targets neural cells. Nestin is an intermediate filament protein expressed by embryonic cells of neuronal origin and is used as a marker for central nervous system progenitor cells. A nestin–cre transgenic mice, therefore, controls the cre activation in a cell specific manner targeting only the cells with neural origin. Finally, to produce neural SGPL1–deficient mice ($SGPL1^{fl/fl/Nes}$), a nestin–cre transgenic mice line was crossbred with the "floxed" mice line ($SGPL1^{fl/fl}$) in which SGPL1 gene was inactive explicitly in cells of neural origin like neurons, astrocytes, and oligodendrocytes. $SGPL1^{fl/fl/Nes}$ mice displayed no phenotypic differences, and their lifespan was comparable to that of their wild–type littermates. In this respect, the $SGPL1^{fl/fl/Nes}$ mice line presented a promising model for the study of S1P–induced signaling pathways in brain and neural cells.

7.2 Ethical statement

Each animal experimental procedures were conducted in accordance with the guidelines of the Animal Care Committee of the University of Bonn. The experimental protocols were approved by Landesamt für Natur, Umwelt und Verbraucherschutz Nordrhein–Westfalen (LANUV) (LANUV NRW, Az. 87–51.04. 2011. A049).

7.3 Mouse genotyping

As previously discussed in this study, the "floxed" mice ($SGPL1^{fl/fl}$) served as controls and neural–specific *SGPL1* transgenic mice ($SGPL1^{fl/fl/Nes}$) were used as KO. The differences in the genetic makeup of control and KO mice were confirmed through genotyping using standard PCR.

7.4 Tissue harvesting

Mice between the ages of 10 and 15 months were killed *via* cervical dislocation. The neck was decapitated with a surgical scissor, and both skull and skin were removed following the midline with an iris scissor. The skull was removed with curved forceps, and the brain was transferred into a separate petri dish with ice cold HBSS buffer, instructions were followed, as shown in European Journal for Neuroscience's protocol video (EJNeuroscience 2014). Control and SGPL–lyase deficient brains were separately stored in cryovials and kept at –80°C until further use.

7.5 Primary astrocyte culture

Astrocyte culture was performed using P1 to P4 mouse pups. The pups' neck was decapitated with a surgical scissor; both skull and skin were removed following the midline with an iris scissor. The skull was removed with curved forceps, and the brain was transferred with the help of a micro scoop into a separate petri dish with ice cold Ca^{2+} and Mg^{2+} free HBSS buffer. Following this, the cerebellum and meninges were removed using forceps with straight tips. Similarly, the rest of the brain hemispheres were prepared and transferred with the micro scoop into a 15 mL tube containing 1–2 ml HBSS and kept on ice until all control and SGPL1 deficient mice brain were dissected. Thereafter, HBSS was carefully aspirated, and 1–2 mL of 0.05% Trypsin–EDTA was added in each tube. The tubes were incubated in a water bath at

37°C for 10 min with constant shaking. 1–2 ml of prewarmed cell culture medium was added to neutralize the effect of Trypsin–EDTA. The tubes were centrifuged for a short time, followed by adding 1–2 ml prewarmed cell culture medium after carefully removing Trypsin–EDTA. Cortices were mechanically dissociated by pipetting up and down with a sterile 10 mL pipette. The cell suspension was loaded on T25 cell culture flasks containing 5 ml of prewarmed complete medium and incubated in the incubator at 37°C with 5% CO_2 overnight. Next day, after removing the cell culture medium, the cells were washed with prewarmed sterile PBS to remove all cell debris and 5 ml of fresh cell culture medium was then added. Cells were further incubated for 2–3 days in the incubator . The medium of the growing cells was freshly replaced every 2–3 days. After about 10 days, a confluent layer of astrocytes was formed, along with microglia and oligodendrocytes loosely growing on this astrocyte layer. Astrocytes were used for experiments after about 25 days in culture. Before astrocytes were used for experiments, microglia, and oligodendrocyte precursor cells (OPC) were detached by vigorous shaking. The medium was then removed, and astrocytes were used for experiments as needed.

7.6 Cell culture

Mouse embryonic fibroblasts (wild–type, WT controls, and SGPL1–deficient, Sgpl1$^{-/-}$, KO) were originally provided by P.P. van Veldhoven (KU Leuven, Belgium) and characterized by the group of Dagmar Meyer zu Heringdorf (Ihlefeld, Claas et al. 2012). Briefly, cells were cultured and maintained in Dulbecco's Modified Eagle Medium complete media containing 10% fetal bovine serum supplemented with 100 units ml^{-1} penicillin and 100 mg (ml^{-1}) streptomycin. Cells were grown in 25 cm^2 (T25) flasks and maintained in a humidified incubator with 5% CO_2 at 37°C.

7.7 Cell harvesting

The experiments were conducted at a confluency of 70–80% of the cell layer in a T25 flask following passages every 2–3 days prior to confluence. Cells were harvested by trypsinization using 1ml of 0.05% Trypsin–EDTA. An equal amount of complete media was added to neutralize trypsin followed by centrifugation at 1000 rpm for 5 mins at RT. The cell pellet in the tube was stored at -80°C until further use to extract protein or DNA.

7.8 Protein extraction and lysate preparation

Cellular proteins were extracted using freshly prepared RIPA lysis buffer and Laemmli buffer was used to prepare lysates. For protein extraction, a working stock of 1X RIPA lysis buffer was diluted from 50X stock solution in which one tablet of protease inhibitor cocktail was dissolved. After thawing the cell pellets on ice for approximately 3–4 mins, the pellet was dissolved in 150 µl of 1X RIPA lysis buffer while incubating for 1 hr. Samples were frequently vortexed at maximum speed during the incubation period. Lysed samples were transferred into fresh prechilled eppendorf tubes and centrifuged at 14,000 rpm for 45 minutes at 4°C and clear supernatant (lysates) was transferred into a fresh tube.

Thereafter, total protein concentration was measured using Nanodrop where a direct measurement of protein concentration of the cell sample was conducted using the Protein 280 application of the Nanodrop. Lysates were prepared by adding Laemmli buffer (4X Laemmli buffer) to the extracted protein in a 4:1 ratio. Protein in the samples was denatured by heating for 5 min at 95°C before loading on SDS–PAGE gel for protein quantification.

7.9 SDS–PAGE

Proteins or charged molecules are separated according to their molecular weight by the SDS–PAGE method. In the preparation of polyacrylamide gels, acrylamide is mixed with bisacrylamide in order to create a crosslinked polymer network with the addition of ammonium persulfate (APS). By stimulating the production of free radicals by APS, TEMED catalyzes the polymerization reaction. As a result, polyacrylamide gel is formed. The amount of bisacrylamide decides the gel percentage to separate different molecular weight proteins as shown in the table below:

Table 1. SDS–PAGE gel percentage

Gel percentage	Range of molecular weight of the protein
6%	50 kDa–500 kDa
10%	20 kDa–300 kDa
12%	10 kDa–200 kDa

In this process, proteins are initially concentrated in a stacking gel with a neutral pH, and then they need to migrate into a separating gel with a basic pH, where the actual separation is performed. The concentration of the following components needed to prepare 5ml stacking gel is given below:

Table 2. Stacking gel composition

Stacking gel	
Water	2.975 ml
Acrylamide/Bis–acrylamide	0.67 ml
0.5M Tris–HCl, pH 6.8	1.25 ml
10% (w/v) SDS	50 µl
10% (w/v) Ammonium persulfate (APS)	50 µl
TEMED	5 µl

Below is the concentration of each component needed to prepare 5 ml of separating gel:

Table 3. Separating gel composition

Gel percentage	6%	8%	10%	12%
Water	5.2 ml	4.6 ml	3.2 ml	2.2 ml
Acrylamide/Bis–acrylamide	2 ml	2.6 ml	3.4 ml	5 ml
1.5M Tris–HCl, pH 8.8	2.6 ml	2.6 ml	2.6 ml	2.6 ml
10% (w/v) SDS	100 µl	100 µl	100 µl	100 µl
10% (w/v) Ammonium persulfate (APS)	100 µl	100 µl	100 µl	100 µl
TEMED	10 µl	10 µl	10 µl	10 µl

7.10 Sample preparation

During sample preparation, the samples were heated at 95°C for 5 min to denature the protein. As a result of heating, the secondary and tertiary structures of the protein are disrupted by the breaking of hydrogen bonds and the molecules becoming linearized. As soon as the samples have cooled to RT, they are pipetted into the respective wells in the gel immersed in the electrophoresis buffer. Along with the samples, a known molecular weight size marker was also loaded which allows for the estimation of the size of the proteins. A final concentration of 2 µg/µl (5–15 µl) of protein was used for loading during electrophoresis.

7.11 Electrophoresis

As part of the separation process, the gel was immersed in the electrophoresis running buffer of the following components to enable separation.

Table 4. Running buffer composition

10X SDS running buffer (1l stock)	
Tris base	30.23 g
Glycine	144 g
SDS	10 g

ddH_2O	make up the volume to 1 liter
Diluted to 1X with ddH_2O for electrophoresis	

The assembly was filled with running buffer and the gel was placed in the electrode clamp. Powerpack was initially set at 50 V for 10–15 min for proper stacking. Afterward, the run was speeded up to 150 V for 90 min. Once the dye reaches the end, the powerpack was switched off and the gel was prepared for western blot transfer.

7.12 Western immunoblotting

After the SDS–PAGE, the proteins were transferred to the PVDF (Polyvinylidene fluoride) membrane. Prior to use, the PVDF membrane was activated in methanol for 2 min. The gel casting was removed, and the gel was arranged on transfer clamps with gel stacked in between scratch pads, filter paper wicks, and PVDF membrane. The assembly was filled with the transfer buffer of the following composition and the whole assembly was placed at a constant 400 mA for 2 h at 4°C.

Table 5. 10X Transfer buffer composition

10X Transfer buffer (1l stock)	
Tris base 25 mM	30.23 g
Glycine 190 mM	144 g
ddH_2O	make up the volume to 1 liter

A stock of 10X was made, and a fresh 1X buffer of the following composition was made from it to be used as needed.

Table 6. 1X Transfer buffer composition

1X Transfer buffer (1l)	
10X Transfer buffer stock	100 ml
Methanol	200 ml
ddH_2O	700 ml

Table 7. TBST buffer

10X TBST buffer (1l)	
Tris 20 mM (pH 7.5)	24.3 g
NaCl 150 mM	87.66 g
0.1% Tween20	10 ml
Diluted to 1X with ddH2O to use as the washing buffer	

Table 8. Blocking buffer

Blocking buffer (50 ml)	
5% BSA or milk powder	2.5 g
Tween–20	25 µl
1X TBST buffer	make up to 50 ml

Following the complete transfer of protein on to PVDF membrane, the membrane was blocked with 5% non–fat milk powder or 5% BSA (for phosphorylated proteins) in TBST buffer for 1h and washed 2 times (2 min each) with TBST wash buffer. Then after, the membrane was incubated overnight with the primary antibody at 4°C on a shaking rocker. After that, the membrane was washed with TBST washing buffer, three times for 7 min each at RT. HRP–conjugated secondary antibody was added and kept on a rotator for about 1 h. The membrane was again washed with TBST three times for 7 min each to remove excess secondary antibodies. The PVDF membrane was then exposed to Western BLoTChemiluminescence HRP Substrate, and the bands were visualized using the VersaDoc 5000 imaging system. ImageJ and Prism GraphPad were used to perform quantification and statistical analysis.

7.13 RNA isolation

Isolation of total RNA was performed using the EXTRAzol kit according to the manufacturer's instructions. Briefly, cells were homogenized in 800 µl EXTRAzol by pipetting it up and down a few times and incubated for 5 min at RT. For phase separation, 200 µl chloroform was added per 1ml EXTRAzol and vigorously shaken by hand for 15 seconds and kept at RT for 3 min. Samples were then centrifuged for 15 min at 10000 rpm at 4°C which enabled phase separation into a pale–yellow phase, turbid interphase, and a colorless upper aqueous phase that contained RNA. Colorless RNA was transferred carefully to another tube and 500 µl of ice–cold isopropyl alcohol was added per 1ml EXTRAzol and further incubated to precipitate the RNA for 10 min. Afterward, samples were centrifuged for 10 mins at 12000 rpm at 4°C. A very small white pellet of unpurified RNA collects at the bottom of the tube. Further, 1 ml of 75% ethanol was added, and the content was vortexed and then centrifuged at 7500 rpm for 5 mins at 4°C to purify the RNA. Ethanol was discarded and the pellet was air–dried to remove any trace of ethanol (additionally heated at 60°C for 1 min) and the pellet was dissolved in 25 µl of PCR grade or RNase–free water. Isolated RNA was kept on ice for a short period and stored at -80°C for later use.

The concentration of the total purified RNA samples was measured using the Nucleic acid application of the Nanodrop One. This spectrophotometer measures the concentration of purified RNA, dsDNA, or ssDNA at a wavelength of 260 nm using the modified Beer–Lambert equation. The method requires selecting RNA from the Nucleic acid option on the home screen. After blank reading, RNA concentration was measured in µg/ml. Along with the concentration, the spectrophotometer displays an $A_{260/280}$ ratio, which indicates the purity status of the isolated RNA. An $A_{260/280}$ ratio of ~2.0 for RNA is generally accepted as "pure". A lower $A_{260/280}$ ratio indicates the presence of DNA and protein contamination.

7.14 cDNA SYNTHESIS

Using reverse transcription, complementary DNA or cDNA was synthesized from the isolated RNA template using the TAKARA kit. Following the manufacturer's instruction, up to 1 µg RNA was used (max 8 µl), and 2 µl of the 5X master mix was mixed (total volume 10 µl) and incubated at 37°C for 15 min. Synthesized cDNA was stored at -80°C for long term storage or -20°C for short term storage, as needed for further experiments. The cDNA thus produced was further used as a template for the quantitative polymerase chain reaction, qPCR.

7.15 Primer design

Using the NCBI–Nucleotide database, the FASTA sequence of each gene of interest was retrieved which was used to design primers for real–time qPCR using the Primer–BLAST tool from NCBI. The primers were obtained from Invitrogen and were designed to have an optimum melting temperature, T_m of 60°C ± 3°C, and to be of a maximum length of 250 bp. Besides, primers tend to bind at the junction of exons, preventing them from binding to genomic DNA. Therefore, primers were specifically designed to either span an exon–exon junction or the forward and reverse primers were located on different exons, separated by an intron.

7.16 Quantitative Real–Time PCR

A real–time polymerase chain reaction, (qPCR) is a technique based on the detection of PCR products in real–time used to study the gene expression in a particular sample. Real–time PCR was carried out in a CFX96 Real–Time System thermal cycler from Bio–Rad. In general, PCR comprises a series of 20–50 recurring temperature changes, called cycles. These cycles normally consist of the following primary stages:

- Initialization or activation stage at around 94–98°C, which allows for the separation of the nucleic acid's double chain.
- Next is the denaturation stage at a temperature of around 94–98°C, which allows the binding of the primers with the DNA template.
- The third is the annealing stage between 50–65°C, which facilitates the polymerization carried out by the DNA polymerase.
- The extension or elongation stage depends on the temperature for the activity of the DNA polymerase used.
- Last is the final hold between 4–15°C, to cool the reaction chambers containing the final product for an indefinite time.

The following table gives the specification of the program used for the amplification.

Table 9. Specifications of the qPCR program

Temperature	Process	Duration
95°C	activation and denaturation	30 sec
95°C	denaturation	5 sec
60°C	annealing and extension	1 min
10°C	holding	indefinite

In order to amplify a small amount of dsDNA, a fluorescent DNA binding dye (SYBR Green) which binds to all dsDNA, is added to the mixture containing a specific pair of primers, DNA polymerase, and enzyme mix along with the target dsDNA. The sensors inside the thermal cycler detect the intensity of the fluorescence emitted by the dye when bound to the dsDNA product after each cycle.

7.17 Immunohistochemistry

Microscopic slides containing cryosections of the brain tissue were prepared and stored by Dr. Shah Alam in the -80°C. Next, the frozen brain sections were thawed and subsequently fixed with ice–cold 4 % *(v/v)* paraformaldehyde in PBS for 5 min. Sections were then permeabilized with 0.1 % *(v/v)* Triton X–100 in PBS for 30 min at RT and blocked in 20 % *(v/v)* normal goat serum in PBS for 30 min. A subsequent incubation in the desired primary antibody was done for overnight in 4°C. For primary antibody the dilution used was in the ratio 1:200 in PBS containing 0.5% lambda–carrageenan and 0.02% sodium azide. Following overnight incubation, the slides with brain sections were washed 3 times with PBS and were incubated with Cy3–conjugated anti–rabbit/mouse Alexa Fluor 488 secondary antibody

diluted in the ratio of 1:300 in PBS for 1 hour at RT. Finally, antibody–labeled brain sections were embedded in Fluoromount G medium with DAPI for microscopic analysis with Keyence microscope (BZ-X series).

7.18 Immunocytochemistry

Astrocytes were grown in T25 flasks for approximately 18 days prior to being transferred to a coverslip to grow further for 5–10 days. Cells on the coverslip were fixed in methanol (chilled at -20°C) and incubated for 5 min and washed 3 times with cold PBS. After this, a 30 min blocking step was followed in which cells were incubated in 20% *(v/v)* goat serum (made in PBS) for the next 30 min. The coverslips were then incubated overnight with primary antibody at 4°C diluted in the ratio of 1:200 with PBS. Next, cells were washed 3 times with PBS and were incubated with anti–rabbit/mouse Alexa Fluor 488–conjugated secondary antibodies (1:300) for 50 min at RT. Lastly, cells were embedded in Fluoromount G medium with DAPI for microscopic analysis with Keyence microscope (BZ-X series).

7.19 Cell proliferation assay

The proliferative potential of MEFs (WT and KO cells) was monitored using the MTT (3–(4,5– Dimethylthiazol–2–yl–2,5–Diphenyltetrazolium Bromide) assay from. About 5 X 10^3 cells per well were seeded in 96 well plates in DMEM containing 10% FBS and cultured for 24 h. Then the medium was changed, and 50 µl of MTT reagent was added in 50 µl of serum–free DMEM as indicated by the provider, and the plate was kept in the incubator for 3 h to form the formazan crystals. The medium with MTT reagent was then discarded, and the experiment was terminated by adding 150 µl of MTT solvent in each of the wells. The 96–well plate was kept on the shaker for 10–15 min so that the crystals were completely dissolved. Absorbance was recorded at 590 nm using microplate reader. Obtained data were expressed relative to their WT controls.

7.20 Glucose–6–phosphate determination

Glucose–6–phosphate was determined by colorimetric detection at 450 nm using the G6P Assay kit. The total protein concentration of each sample was used as a reference. The deproteination step was performed by adding an equal volume of ice cold 0.5 M $HClO_4$ and incubating on ice for 5 min (Zhu, Romero et al. 2011). Thereafter to remove protein, the

mixture was centrifuged at 10,000 g for 5 min, and the supernatant was collected. Two hundred microliter of the supernatant was neutralized with 10 µl of 2.5 M K_2CO_3 at 4°C. Samples were further degassed and briefly centrifuged for 5 min. A clear supernatant was collected and used for the G6P assay following the instructions provided by the manufacturer.

7.21 RNA Sequencing

Total RNA was isolated from the cells using the Qiagen RNeasy Mini Kit (Qiagen 74104). For each sample, 700 ng of total RNA was then used in Illumina's TruSeq Stranded mRNA Library kit (20020594). Libraries were sequenced on Illumina NextSeq 550 as paired–end 42–nt reads. Sequence reads were analyzed with the STAR alignment – DESeq2 software pipeline described in the Supplementary Data 2.

7.22 Active Motif CUT&Tag

Samples were sent to Active Motif for CUT&Tag. Briefly, cells were incubated overnight with Concanavalin A beads and 1 µl of the primary anti–H3K9Ac antibody per reaction (Active Motif, 39917). After incubation with the secondary anti–rabbit antibody (1:100), cells were washed and tagmentation was performed at 37°C using protein–A–Tn5. Tagmentation was halted by the addition of EDTA, SDS and proteinase K at 55°C, after which DNA extraction and ethanol purification was performed, followed by PCR amplification and barcoding (Active Motif CUT&Tag kit, 53160). Following SPRI bead cleanup (Beckman Coulter), the resulting DNA libraries were quantified and sequenced on Illumina's NextSeq 550 (8 million reads, 38 paired end).

Reads were aligned using the BWA algorithm (mem mode; default settings) (Li and Durbin 2009). Duplicate reads were removed, and only reads that mapped uniquely (mapping quality >= 1) and as matched pairs were used for further analysis. Alignments were extended in silico at their 3'–ends to a length of 200 bp and assigned to 32–nt bins along the genome. The resulting histograms (genomic "signal maps") were stored in bigWig files. Peaks were identified using the MACS 2.1.0 algorithm at a cutoff of p–value 1e–7, without control file, and with the –nomodel option. Peaks that were on the ENCODE blacklist of known false ChIP–Seq peaks were removed. Signal maps and peak locations were used as input data to Active Motifs proprietary analysis program, which creates Excel tables containing detailed information on sample comparison, peak metrics, peak locations, and gene annotations. For

differential analysis, reads were counted in all merged peak regions (using Subread), and the replicates for each condition were compared using DESeq2 (Love, Huber et al. 2014).

Other key software used: bcl2fastq2 (v2.20) (processing of Illumina base–call data and demultiplexing), Samtools (v0.1.19) (processing of BAM files), BEDtools (v2.25.0) (processing of BED files), wigToBigWig (v4) (generation of bigWIG files), Subread (v1.5.2) (counting of reads in BAM files for DESeq2).

7.23 Treatment of cells

7.23.1 JTE–013 and VPC–23019 Treatment

For the glycolysis rescue experiments, JTE–013 (JTE) and VPC–23019 (VPC) were used, which block S1P receptor 2 and receptor 1,3 respectively. WT and SGPL1–deficient MEFs were incubated with 10 μM each of JTE and VPC for 24 hrs. JTE and VPC were added from a stock prepared in ethanol and DMSO, respectively, that ensured final ethanol and DMSO concentration of less than 1% in the medium to avoid toxicity. Exact amounts of ethanol and DMSO were added to untreated WT and KO MEFs cultures.

7.23.2 FTY–720 treatment

To validate the S1PR dependent effect on glucose metabolism, the results obtained in SGPL1–deficient MEFs were recapitulated by extracellular administration of S1PR agonist, FTY–720. For this, WT MEFs were incubated with 10 nM of FTY–720 for 24 h. FTY–720 stock was prepared in DMSO and the exact amount of DMSO was added to the untreated MEFs.

7.23.3 Rapamycin Treatment

In order to perform autophagy rescue experiments, WT and KO MEFs were incubated with 1 μM of Rapamycin for 24 hrs. Rapamycin was added from a stock prepared in ethanol that ensured a final ethanol concentration of less than 1% in the medium to avoid toxicity. Exact amounts of ethanol were added to the untreated WT and KO MEFs cultures.

7.23.4 S1P and S1PR$_{2,4}$ Agonist Treatment

To confirm the role of S1P signaling, the results obtained in SGPL1–deficient astrocytes were recapitulated by extracellular administration of S1P. For this, control astrocytes were incubated with 10 nM of S1P for 24 hr. S1P stock solution was prepared in water.

Additionally, to confirm the role of $S1PR_2$ and $S1PR_4$ in the activation of P2Y1R signaling, control astrocytes were treated with the specific agonist of $S1PR_2$ and $S1PR_4$. For this, the control astrocytes were incubated with 5 µM of CYM–5520 ($S1PR_2$ agonist) and 5 µM of CYM–50308 ($S1PR_4$ agonist) for 24 hr. CYM–5520 and CYM–50308 were both dissolved in DMSO and so the exact amount of DMSO was added to the untreated control astrocyte culture.

7.23.5 $P2Y_1R$ Inhibitor Treatment

For the rescue experiments of astrocytic hyperactivity, control and SGPL1 deficient KO astrocytes were treated with 100 µM of MRS2179 for 24 hr to block the $P2Y_1$ receptor. MRS2179 stock solution was prepared in water.

7.23.6 $P2Y_1R$ Agonist Treatment

In order to confirm the role of $P2Y_1R$ in mediating astrogliosis, a specific agonist of $P2Y_1R$ was used. For this, control astrocytes were treated with the $P2Y_1R$ specific agonist, MRS2905 (5 nM) for 24 hr.

7.23.7 P2Y1R antagonist treatment

The rescue experiment of astrocytic hyperactivity was conducted by treating astrocytes with 100 µM of the specific P2Y1R antagonist, MRS2179 for 24 hours. MRS2179 stock solution was prepared in water.

7.24 Statistical analysis

For the statistical analysis, GRAPHPAD PRISM 9 software was used. Each result expressed as means ± SEM was based on at least three independent experiments if not otherwise stated. The significance of differences between the experimental groups and controls was assessed by either unpaired Student *t*–test with false discovery rate (FDR) correction or One–way Analysis of Variance (ANOVA) with Bonferroni multiple comparison test, as appropriate. Values with $p < 0.05$ were considered statistically significant (*$p < 0.05$; **$p < 0.001$; ***$p < 0.0001$; ****$p < 0.00001$; compared with the respective control group).

7. REFERENCES

Abbracchio, M. P. and G. Burnstock (1994). "Purinoceptors: are there families of P2X and P2Y purinoceptors?" Pharmacol Ther **64**(3): 445-475.

Abbracchio, M. P., G. Burnstock, J. M. Boeynaems, E. A. Barnard, J. L. Boyer, C. Kennedy, G. E. Knight, M. Fumagalli, C. Gachet, K. A. Jacobson and G. A. Weisman (2006). "International Union of Pharmacology LVIII: update on the P2Y G protein-coupled nucleotide receptors: from molecular mechanisms and pathophysiology to therapy." Pharmacol Rev **58**(3): 281-341.

Abbracchio, M. P., G. Burnstock, A. Verkhratsky and H. Zimmermann (2009). "Purinergic signalling in the nervous system: an overview." Trends Neurosci **32**(1): 19-29.

Abbracchio, M. P. and C. Verderio (2006). "Pathophysiological roles of P2 receptors in glial cells." Novartis Found Symp **276**: 91-103; discussion 103-112, 275-181.

Abdel-Wahab, A. F., W. Mahmoud and R. M. Al-Harizy (2019). "Targeting glucose metabolism to suppress cancer progression: prospective of anti-glycolytic cancer therapy." Pharmacol Res **150**: 104511.

Afsar, S. Y., S. Alam, C. Fernandez Gonzalez and G. van Echten-Deckert (2022). "Sphingosine-1-phosphate-lyase deficiency affects glucose metabolism in a way that abets oncogenesis." Mol Oncol **16**(20): 3642-3653.

Agresti, C., M. E. Meomartini, S. Amadio, E. Ambrosini, C. Volonte, F. Aloisi and S. Visentin (2005). "ATP regulates oligodendrocyte progenitor migration, proliferation, and differentiation: involvement of metabotropic P2 receptors." Brain Res Brain Res Rev **48**(2): 157-165.

Alam, S. (2021). Effect of neural ablation of sphingosine-1-phosphate lyase (SGPL1) in glial cells.

Alam, S., S. Y. Afsar and G. J. I. J. o. M. S. Van Echten-Deckert (2023). "S1P Released by SGPL1-Deficient Astrocytes Enhances Astrocytic ATP Production via S1PR2/4, Thus Keeping Autophagy in Check: Potential Consequences for Brain Health." **24**(5): 4581.

Alam, S., A. Piazzesi, M. Abd El Fatah, M. Raucamp and G. van Echten-Deckert (2020). "Neurodegeneration Caused by S1P-Lyase Deficiency Involves Calcium-Dependent Tau Pathology and Abnormal Histone Acetylation." Cells **9**(10).

Alberini, C. M., E. Cruz, G. Descalzi, B. Bessieres and V. Gao (2018). "Astrocyte glycogen and lactate: New insights into learning and memory mechanisms." Glia **66**(6): 1244-1262.

Alle, H., A. Roth and J. R. Geiger (2009). "Energy-efficient action potentials in hippocampal mossy fibers." Science **325**(5946): 1405-1408.

Allen, N. J. and C. Eroglu (2017). "Cell Biology of Astrocyte-Synapse Interactions." Neuron **96**(3): 697-708.

Asnaghi, L., A. Calastretti, A. Bevilacqua, I. D'Agnano, G. Gatti, G. Canti, D. Delia, S. Capaccioli and A. Nicolin (2004). "Bcl-2 phosphorylation and apoptosis activated by damaged microtubules require mTOR and are regulated by Akt." Oncogene **23**(34): 5781-5791.

Attwell, D. and S. B. Laughlin (2001). "An energy budget for signaling in the grey matter of the brain." J Cereb Blood Flow Metab **21**(10): 1133-1145.

Bae, Y. S., L. G. Cantley, C. S. Chen, S. R. Kim, K. S. Kwon and S. G. Rhee (1998). "Activation of phospholipase C-gamma by phosphatidylinositol 3,4,5-trisphosphate." J Biol Chem **273**(8): 4465-4469.

Barros, L. F. (2013). "Metabolic signaling by lactate in the brain." Trends Neurosci **36**(7): 396-404.

Benjamin, D., M. Colombi, C. Moroni and M. N. Hall (2011). "Rapamycin passes the torch: a new generation of mTOR inhibitors." Nat Rev Drug Discov **10**(11): 868-880.

Borghammer, P., M. Chakravarty, K. Y. Jonsdottir, N. Sato, H. Matsuda, K. Ito, Y. Arahata, T. Kato and A. Gjedde (2010). "Cortical hypometabolism and hypoperfusion in Parkinson's disease is extensive: probably even at early disease stages." Brain Struct Funct **214**(4): 303-317.

Browne, S. E., L. Yang, J. P. DiMauro, S. W. Fuller, S. C. Licata and M. F. Beal (2006). "Bioenergetic abnormalities in discrete cerebral motor pathways presage spinal cord pathology in the G93A SOD1 mouse model of ALS." Neurobiol Dis **22**(3): 599-610.

Burnstock, G. (1976). "Purinergic receptors." J Theor Biol **62**(2): 491-503.

Burnstock, G., B. B. Fredholm and A. Verkhratsky (2011). "Adenosine and ATP receptors in the brain." Curr Top Med Chem **11**(8): 973-1011.

Cai, M., H. Wang, H. Song, R. Yang, L. Wang, X. Xue, W. Sun and J. Hu (2022). "Lactate Is Answerable for Brain Function and Treating Brain Diseases: Energy Substrates and Signal Molecule." Front Nutr **9**: 800901.

Carter, S. F., K. Herholz, P. Rosa-Neto, L. Pellerin, A. Nordberg and E. R. Zimmer (2019). "Astrocyte Biomarkers in Alzheimer's Disease." Trends Mol Med **25**(2): 77-95.

Ceccom, J., N. Loukh, V. Lauwers-Cances, C. Touriol, Y. Nicaise, C. Gentil, E. Uro-Coste, S. Pitson, C. A. Maurage, C. Duyckaerts, O. Cuvillier and M. B. Delisle (2014). "Reduced sphingosine kinase-1 and enhanced sphingosine 1-phosphate lyase expression demonstrate deregulated sphingosine 1-phosphate signaling in Alzheimer's disease." Acta Neuropathol Commun **2**: 12.

Chen, Y., Q. Wang, Q. Wang, H. Liu, F. Zhou, Y. Zhang, M. Yuan, C. Zhao, Y. Guan and X. Wang (2017). "DDX3 binding with CK1epsilon was closely related to motor neuron degeneration of ALS by affecting neurite outgrowth." Am J Transl Res **9**(10): 4627-4639.

Choi, J. W. and J. Chun (2013). "Lysophospholipids and their receptors in the central nervous system." Biochim Biophys Acta **1831**(1): 20-32.

Choi, J. W., S. E. Gardell, D. R. Herr, R. Rivera, C. W. Lee, K. Noguchi, S. T. Teo, Y. C. Yung, M. Lu, G. Kennedy and J. Chun (2011). "FTY720 (fingolimod) efficacy in an animal model of multiple sclerosis requires astrocyte sphingosine 1-phosphate receptor 1 (S1P1) modulation." Proc Natl Acad Sci U S A **108**(2): 751-756.

Claas, R. F., M. ter Braak, B. Hegen, V. Hardel, C. Angioni, H. Schmidt, K. H. Jakobs, P. P. Van Veldhoven and D. M. zu Heringdorf (2010). "Enhanced Ca2+ storage in sphingosine-1-phosphate lyase-deficient fibroblasts." Cell Signal **22**(3): 476-483.

Colie, S., P. P. Van Veldhoven, B. Kedjouar, C. Bedia, V. Albinet, S. C. Sorli, V. Garcia, M. Djavaheri-Mergny, C. Bauvy, P. Codogno, T. Levade and N. Andrieu-Abadie (2009). "Disruption of sphingosine 1-phosphate lyase confers resistance to chemotherapy and

promotes oncogenesis through Bcl-2/Bcl-xL upregulation." Cancer Res **69**(24): 9346-9353.

Couttas, T. A., N. Kain, B. Daniels, X. Y. Lim, C. Shepherd, J. Kril, R. Pickford, H. Li, B. Garner and A. S. Don (2014). "Loss of the neuroprotective factor Sphingosine 1-phosphate early in Alzheimer's disease pathogenesis." Acta Neuropathol Commun **2**: 9.

Crawford, M. A. and A. J. Sinclair (1971). "Nutritional influences in the evolution of mammalian brain. In: lipids, malnutrition & the developing brain." Ciba Found Symp: 267-292.

Cui, W., N. D. Allen, M. Skynner, B. Gusterson and A. J. Clark (2001). "Inducible ablation of astrocytes shows that these cells are required for neuronal survival in the adult brain." Glia **34**(4): 272-282.

Cunha, R. A. and J. A. Ribeiro (2000). "ATP as a presynaptic modulator." Life Sci **68**(2): 119-137.

Cuvillier, O., G. Pirianov, B. Kleuser, P. G. Vanek, O. A. Coso, S. Gutkind and S. Spiegel (1996). "Suppression of ceramide-mediated programmed cell death by sphingosine-1-phosphate." Nature **381**(6585): 800-803.

de Oliveira Figueiredo, E. C., C. Cali, F. Petrelli and P. Bezzi (2022). "Emerging evidence for astrocyte dysfunction in schizophrenia." Glia **70**(9): 1585-1604.

Delekate, A., M. Fuchtemeier, T. Schumacher, C. Ulbrich, M. Foddis and G. C. Petzold (2014). "Metabotropic P2Y1 receptor signalling mediates astrocytic hyperactivity in vivo in an Alzheimer's disease mouse model." Nat Commun **5**: 5422.

Di Malta, C., J. D. Fryer, C. Settembre and A. Ballabio (2012). "Autophagy in astrocytes: a novel culprit in lysosomal storage disorders." Autophagy **8**(12): 1871-1872.

Divecha, N. and R. F. Irvine (1995). "Phospholipid signaling." Cell **80**(2): 269-278.

Dossou, A. S. and A. Basu (2019). "The Emerging Roles of mTORC1 in Macromanaging Autophagy." Cancers (Basel) **11**(10).

Dunlop, E. A. and A. R. Tee (2014). "mTOR and autophagy: a dynamic relationship governed by nutrients and energy." Semin Cell Dev Biol **36**: 121-129.

Dusaban, S. S., J. Chun, H. Rosen, N. H. Purcell and J. H. Brown (2017). "Sphingosine 1-phosphate receptor 3 and RhoA signaling mediate inflammatory gene expression in astrocytes." J Neuroinflammation **14**(1): 111.

Eng, L. F. and R. S. J. B. p. Ghirnikar (1994). "GFAP and astrogliosis." **4**(3): 229-237.

Fahy, E., S. Subramaniam, R. C. Murphy, M. Nishijima, C. R. Raetz, T. Shimizu, F. Spener, G. van Meer, M. J. Wakelam and E. A. Dennis (2009). "Update of the LIPID MAPS comprehensive classification system for lipids." J Lipid Res **50 Suppl**: S9-14.

Feigin, A., K. L. Leenders, J. R. Moeller, J. Missimer, G. Kuenig, P. Spetsieris, A. Antonini and D. Eidelberg (2001). "Metabolic network abnormalities in early Huntington's disease: an [(18)F]FDG PET study." J Nucl Med **42**(11): 1591-1595.

Fields, R. D. and G. Burnstock (2006). "Purinergic signalling in neuron-glia interactions." Nat Rev Neurosci **7**(6): 423-436.

Fischer, I., C. Alliod, N. Martinier, J. Newcombe, C. Brana and S. Pouly (2011). "Sphingosine kinase 1 and sphingosine 1-phosphate receptor 3 are functionally upregulated on astrocytes under pro-inflammatory conditions." PLoS One **6**(8): e23905.

Foster, N. L., T. N. Chase, P. Fedio, N. J. Patronas, R. A. Brooks and G. Di Chiro (1983). "Alzheimer's disease: focal cortical changes shown by positron emission tomography." Neurology **33**(8): 961-965.

Franke, H. and P. Illes (2014). "Nucleotide signaling in astrogliosis." Neurosci Lett **565**: 14-22.

Fujita, T., H. Tozaki-Saitoh and K. Inoue (2009). "P2Y1 receptor signaling enhances neuroprotection by astrocytes against oxidative stress via IL-6 release in hippocampal cultures." Glia **57**(3): 244-257.

Ghosh, T. K., J. Bian and D. L. Gill (1994). "Sphingosine 1-phosphate generated in the endoplasmic reticulum membrane activates release of stored calcium." J Biol Chem **269**(36): 22628-22635.

Gombault, A., L. Baron and I. Couillin (2012). "ATP release and purinergic signaling in NLRP3 inflammasome activation." Front Immunol **3**: 414.

Goyal, M. S., M. Hawrylycz, J. A. Miller, A. Z. Snyder and M. E. Raichle (2014). "Aerobic glycolysis in the human brain is associated with development and neotenous gene expression." Cell Metab **19**(1): 49-57.

Grassi, S., L. Mauri, S. Prioni, L. Cabitta, S. Sonnino, A. Prinetti and P. Giussani (2019). "Sphingosine 1-Phosphate Receptors and Metabolic Enzymes as Druggable Targets for Brain Diseases." Front Pharmacol **10**: 807.

Hagen-Euteneuer, N., S. Alam, H. Rindsfuesser, D. Meyer Zu Heringdorf and G. van Echten-Deckert (2020). "S1P-lyase deficiency uncouples ganglioside formation - Potential contribution to tumorigenic capacity." Biochim Biophys Acta Mol Cell Biol Lipids **1865**(8): 158708.

Hagen-Euteneuer, N., D. Lutjohann, H. Park, A. H. Merrill, Jr. and G. van Echten-Deckert (2012). "Sphingosine 1-phosphate (S1P) lyase deficiency increases sphingolipid formation via recycling at the expense of de novo biosynthesis in neurons." J Biol Chem **287**(12): 9128-9136.

Hagen, N., M. Hans, D. Hartmann, D. Swandulla and G. van Echten-Deckert (2011). "Sphingosine-1-phosphate links glycosphingolipid metabolism to neurodegeneration via a calpain-mediated mechanism." Cell Death Differ **18**(8): 1356-1365.

Halassa, M. M., T. Fellin and P. G. Haydon (2007). "The tripartite synapse: roles for gliotransmission in health and disease." Trends Mol Med **13**(2): 54-63.

Halassa, M. M., T. Fellin and P. G. Haydon (2009). "Tripartite synapses: roles for astrocytic purines in the control of synaptic physiology and behavior." Neuropharmacology **57**(4): 343-346.

Halim, N. D., T. McFate, A. Mohyeldin, P. Okagaki, L. G. Korotchkina, M. S. Patel, N. H. Jeoung, R. A. Harris, M. J. Schell and A. Verma (2010). "Phosphorylation status of pyruvate dehydrogenase distinguishes metabolic phenotypes of cultured rat brain astrocytes and neurons." Glia **58**(10): 1168-1176.

Han, R., J. Liang and B. Zhou (2021). "Glucose Metabolic Dysfunction in Neurodegenerative Diseases-New Mechanistic Insights and the Potential of Hypoxia as a Prospective Therapy Targeting Metabolic Reprogramming." Int J Mol Sci **22**(11).

Hannun, Y. A. and R. M. Bell (1989). "Regulation of protein kinase C by sphingosine and lysosphingolipids." Clin Chim Acta **185**(3): 333-345.

Hannun, Y. A. and L. M. Obeid (2008). "Principles of bioactive lipid signalling: lessons from sphingolipids." Nat Rev Mol Cell Biol **9**(2): 139-150.

He, X., Y. Huang, B. Li, C. X. Gong and E. H. Schuchman (2010). "Deregulation of sphingolipid metabolism in Alzheimer's disease." Neurobiol Aging **31**(3): 398-408.

Hostenbach, S., M. Cambron, M. D'Haeseleer, R. Kooijman and J. De Keyser (2014). "Astrocyte loss and astrogliosis in neuroinflammatory disorders." Neurosci Lett **565**: 39-41.

Howarth, C., P. Gleeson and D. Attwell (2012). "Updated energy budgets for neural computation in the neocortex and cerebellum." J Cereb Blood Flow Metab **32**(7): 1222-1232.

Iglesias, J., L. Morales and G. E. Barreto (2017). "Metabolic and Inflammatory Adaptation of Reactive Astrocytes: Role of PPARs." Mol Neurobiol **54**(4): 2518-2538.

Ihlefeld, K., R. F. Claas, A. Koch, J. M. Pfeilschifter and D. Meyer Zu Heringdorf (2012). "Evidence for a link between histone deacetylation and Ca(2)+ homoeostasis in sphingosine-1-phosphate lyase-deficient fibroblasts." Biochem J **447**(3): 457-464.

Iommarini, L., A. M. Porcelli, G. Gasparre and I. Kurelac (2017). "Non-Canonical Mechanisms Regulating Hypoxia-Inducible Factor 1 Alpha in Cancer." Front Oncol **7**: 286.

Jha, M. K., S. Jeon and K. Suk (2012). "Glia as a Link between Neuroinflammation and Neuropathic Pain." Immune Netw **12**(2): 41-47.

Jin, Y., H. J. Sui, Y. Dong, Q. Ding, W. H. Qu, S. X. Yu and Y. X. Jin (2012). "Atorvastatin enhances neurite outgrowth in cortical neurons in vitro via up-regulating the Akt/mTOR and Akt/GSK-3beta signaling pathways." Acta Pharmacol Sin **33**(7): 861-872.

Karunakaran, I., S. Alam, S. Jayagopi, S. J. Frohberger, J. N. Hansen, J. Kuehlwein, B. V. Holbling, B. Schumak, M. P. Hubner, M. H. Graler, A. Halle and G. van Echten-Deckert (2019). "Neural sphingosine 1-phosphate accumulation activates microglia and links impaired autophagy and inflammation." Glia **67**(10): 1859-1872.

Karunakaran, I. and G. van Echten-Deckert (2017). "Sphingosine 1-phosphate - A double edged sword in the brain." Biochim Biophys Acta Biomembr **1859**(9 Pt B): 1573-1582.

Kelley, N., D. Jeltema, Y. Duan and Y. He (2019). "The NLRP3 Inflammasome: An Overview of Mechanisms of Activation and Regulation." Int J Mol Sci **20**(13).

Kesavardhana, S., P. Samir, M. Zheng, R. K. S. Malireddi, R. Karki, B. R. Sharma, D. E. Place, B. Briard, P. Vogel and T. D. Kanneganti (2021). "DDX3X coordinates host defense against influenza virus by activating the NLRP3 inflammasome and type I interferon response." J Biol Chem **296**: 100579.

Khakh, B. S. (2001). "Molecular physiology of P2X receptors and ATP signalling at synapses." Nat Rev Neurosci **2**(3): 165-174.

Kim, S., J. Bielawski, H. Yang, Y. Kong, B. Zhou and J. Li (2018). "Functional antagonism of sphingosine-1-phosphate receptor 1 prevents cuprizone-induced demyelination." Glia **66**(3): 654-669.

Kim, S. H. and K. H. Baek (2021). "Regulation of Cancer Metabolism by Deubiquitinating Enzymes: The Warburg Effect." Int J Mol Sci **22**(12).

Kohama, T., A. Olivera, L. Edsall, M. M. Nagiec, R. Dickson and S. Spiegel (1998). "Molecular cloning and functional characterization of murine sphingosine kinase." J Biol Chem **273**(37): 23722-23728.

Koizumi, S. (2010). "Synchronization of Ca2+ oscillations: involvement of ATP release in astrocytes." FEBS J **277**(2): 286-292.

Ku, Y. C., M. H. Lai, C. C. Lo, Y. C. Cheng, J. T. Qiu, W. Y. Tarn and M. C. Lai (2019). "DDX3 Participates in Translational Control of Inflammation Induced by Infections and Injuries." Mol Cell Biol **39**(1).

Kuboyama, K., H. Harada, H. Tozaki-Saitoh, M. Tsuda, K. Ushijima and K. Inoue (2011). "Astrocytic P2Y(1) receptor is involved in the regulation of cytokine/chemokine transcription and cerebral damage in a rat model of cerebral ischemia." J Cereb Blood Flow Metab **31**(9): 1930-1941.

Lalo, U., W. Koh, C. J. Lee and Y. Pankratov (2021). "The tripartite glutamatergic synapse." Neuropharmacology **199**: 108758.

Laplante, M. and D. M. Sabatini (2009). "mTOR signaling at a glance." J Cell Sci **122**(Pt 20): 3589-3594.

Laplante, M. and D. M. Sabatini (2012). "mTOR signaling in growth control and disease." Cell **149**(2): 274-293.

Lavieu, G., F. Scarlatti, G. Sala, S. Carpentier, T. Levade, R. Ghidoni, J. Botti and P. Codogno (2006). "Regulation of autophagy by sphingosine kinase 1 and its role in cell survival during nutrient starvation." J Biol Chem **281**(13): 8518-8527.

Lei, M., A. Shafique, K. Shang, T. A. Couttas, H. Zhao, A. S. Don and T. Karl (2017). "Contextual fear conditioning is enhanced in mice lacking functional sphingosine kinase 2." Behav Brain Res **333**: 9-16.

Lepine, S., J. C. Allegood, M. Park, P. Dent, S. Milstien and S. Spiegel (2011). "Sphingosine-1-phosphate phosphohydrolase-1 regulates ER stress-induced autophagy." Cell Death Differ **18**(2): 350-361.

Li, H. and R. J. b. Durbin (2009). "Fast and accurate short read alignment with Burrows–Wheeler transform." **25**(14): 1754-1760.

Liddelow, S. A. and B. Barres (2017). "Reactive Astrocytes: Production, Function, and Therapeutic Potential." Immunity **46**(6): 957-967.

Linnerbauer, M. and V. Rothhammer (2020). "Protective Functions of Reactive Astrocytes Following Central Nervous System Insult." Front Immunol **11**: 573256.

Love, M. I., W. Huber and S. J. G. b. Anders (2014). "Moderated estimation of fold change and dispersion for RNA-seq data with DESeq2." **15**(12): 1-21.

Luo, Y., W. Yan, Z. Zhou, B. Liu, Z. Wang, J. Chen and H. Wang (2019). "Elevated Levels of NLRP3 in Cerebrospinal Fluid of Patients With Autoimmune GFAP Astrocytopathy." Front Neurol **10**: 1019.

Maceyka, M., K. B. Harikumar, S. Milstien and S. Spiegel (2012). "Sphingosine-1-phosphate signaling and its role in disease." Trends Cell Biol **22**(1): 50-60.

Magistretti, P. J. and I. Allaman (2015). "A cellular perspective on brain energy metabolism and functional imaging." Neuron **86**(4): 883-901.

Magistretti, P. J. and L. Pellerin (1999). "Astrocytes Couple Synaptic Activity to Glucose Utilization in the Brain." News Physiol Sci **14**: 177-182.

Manning, B. D. and L. C. Cantley (2007). "AKT/PKB signaling: navigating downstream." Cell **129**(7): 1261-1274.

Martinon, F., K. Burns and J. Tschopp (2002). "The inflammasome: a molecular platform triggering activation of inflammatory caspases and processing of proIL-beta." Mol Cell **10**(2): 417-426.

Menzies, F. M., A. Fleming and D. C. Rubinsztein (2015). "Compromised autophagy and neurodegenerative diseases." Nat Rev Neurosci **16**(6): 345-357.

Mergenthaler, P., U. Lindauer, G. A. Dienel and A. Meisel (2013). "Sugar for the brain: the role of glucose in physiological and pathological brain function." Trends Neurosci **36**(10): 587-597.

Mitroi, D. N., A. U. Deutschmann, M. Raucamp, I. Karunakaran, K. Glebov, M. Hans, J. Walter, J. Saba, M. Graler, D. Ehninger, E. Sopova, O. Shupliakov, D. Swandulla and G. van Echten-Deckert (2016). "Sphingosine 1-phosphate lyase ablation disrupts presynaptic architecture and function via an ubiquitin- proteasome mediated mechanism." Sci Rep **6**: 37064.

Mitroi, D. N., I. Karunakaran, M. Graler, J. D. Saba, D. Ehninger, M. D. Ledesma and G. van Echten-Deckert (2017). "SGPL1 (sphingosine phosphate lyase 1) modulates neuronal autophagy via phosphatidylethanolamine production." Autophagy **13**(5): 885-899.

Mizushima, N., B. Levine, A. M. Cuervo and D. J. Klionsky (2008). "Autophagy fights disease through cellular self-digestion." Nature **451**(7182): 1069-1075.

Moruno-Manchon, J. F., N. E. Uzor, C. R. Ambati, V. Shetty, N. Putluri, C. Jagannath, L. D. McCullough and A. S. Tsvetkov (2018). "Sphingosine kinase 1-associated autophagy differs between neurons and astrocytes." Cell Death Dis **9**(5): 521.

Moruno Manchon, J. F., N. E. Uzor, Y. Dabaghian, E. E. Furr-Stimming, S. Finkbeiner and A. S. Tsvetkov (2015). "Cytoplasmic sphingosine-1-phosphate pathway modulates neuronal autophagy." Sci Rep **5**: 15213.

Neal, M. and J. R. Richardson (2018). "Epigenetic regulation of astrocyte function in neuroinflammation and neurodegeneration." Biochim Biophys Acta Mol Basis Dis **1864**(2): 432-443.

Nedergaard, M., B. Ransom and S. A. Goldman (2003). "New roles for astrocytes: redefining the functional architecture of the brain." Trends Neurosci **26**(10): 523-530.

Nixon, R. A. (2004). "Niemann-Pick Type C disease and Alzheimer's disease: the APP-endosome connection fattens up." Am J Pathol **164**(3): 757-761.

Nixon, R. A. (2013). "The role of autophagy in neurodegenerative disease." Nat Med **19**(8): 983-997.

Nixon, R. A., D. S. Yang and J. H. Lee (2008). "Neurodegenerative lysosomal disorders: a continuum from development to late age." Autophagy **4**(5): 590-599.

Olivera, A. and S. Spiegel (1993). "Sphingosine-1-phosphate as second messenger in cell proliferation induced by PDGF and FCS mitogens." Nature **365**(6446): 557-560.

Olsen, A. S. B. and N. J. Faergeman (2017). "Sphingolipids: membrane microdomains in brain development, function and neurological diseases." Open Biol **7**(5).

Owen, L. and S. I. Sunram-Lea (2011). "Metabolic agents that enhance ATP can improve cognitive functioning: a review of the evidence for glucose, oxygen, pyruvate, creatine, and L-carnitine." Nutrients **3**(8): 735-755.

Pattingre, S., A. Tassa, X. Qu, R. Garuti, X. H. Liang, N. Mizushima, M. Packer, M. D. Schneider and B. Levine (2005). "Bcl-2 antiapoptotic proteins inhibit Beclin 1-dependent autophagy." Cell **122**(6): 927-939.

Pavlova, N. N. and C. B. Thompson (2016). "The Emerging Hallmarks of Cancer Metabolism." Cell Metab **23**(1): 27-47.

Pekny, M. and M. Nilsson (2005). "Astrocyte activation and reactive gliosis." Glia **50**(4): 427-434.

Peng, Y., Y. Wang, C. Zhou, W. Mei and C. Zeng (2022). "PI3K/Akt/mTOR Pathway and Its Role in Cancer Therapeutics: Are We Making Headway?" Front Oncol **12**: 819128.

Perea, G., M. Navarrete and A. Araque (2009). "Tripartite synapses: astrocytes process and control synaptic information." Trends Neurosci **32**(8): 421-431.

Piazzesi, A., S. Y. Afsar and G. van Echten-Deckert (2021). "Sphingolipid metabolism in the development and progression of cancer: one cancer's help is another's hindrance." Mol Oncol **15**(12): 3256-3279.

Rassendren, F. and E. Audinat (2016). "Purinergic signaling in epilepsy." **94**(9): 781-793.

Ravi, K., M. J. Paidas, A. Saad and A. R. Jayakumar (2021). "Astrocytes in rare neurological conditions: Morphological and functional considerations." J Comp Neurol **529**(10): 2676-2705.

Ren, H., D. Accili and C. Duan (2010). "Hypoxia converts the myogenic action of insulin-like growth factors into mitogenic action by differentially regulating multiple signaling pathways." Proc Natl Acad Sci U S A **107**(13): 5857-5862.

Rivkees, S. A. and C. C. Wendler (2011). "Adverse and protective influences of adenosine on the newborn and embryo: implications for preterm white matter injury and embryo protection." Pediatr Res **69**(4): 271-278.

Rodrigues, R. J., A. R. Tome and R. A. Cunha (2015). "ATP as a multi-target danger signal in the brain." Front Neurosci **9**: 148.

Rodrigues, R. J., A. R. Tomé and R. A. Cunha (2015). "ATP as a multi-target danger signal in the brain." **9**.

Rossi, S., E. R. Zanier, I. Mauri, A. Columbo and N. Stocchetti (2001). "Brain temperature, body core temperature, and intracranial pressure in acute cerebral damage." J Neurol Neurosurg Psychiatry **71**(4): 448-454.

Samir, P., S. Kesavardhana, D. M. Patmore, S. Gingras, R. K. S. Malireddi, R. Karki, C. S. Guy, B. Briard, D. E. Place, A. Bhattacharya, B. R. Sharma, A. Nourse, S. V. King, A. Pitre, A. R. Burton, S. Pelletier, R. J. Gilbertson and T. D. Kanneganti (2019). "DDX3X acts as a live-or-die checkpoint in stressed cells by regulating NLRP3 inflammasome." Nature **573**(7775): 590-594.

Schmahl, J., C. S. Raymond and P. Soriano (2007). "PDGF signaling specificity is mediated through multiple immediate early genes." Nat Genet **39**(1): 52-60.

Schmeisser, K. and J. A. Parker (2019). "Pleiotropic Effects of mTOR and Autophagy During Development and Aging." Front Cell Dev Biol **7**: 192.

Semenza, G. L. (2001). "Hypoxia-inducible factor 1: control of oxygen homeostasis in health and disease." Pediatr Res **49**(5): 614-617.

Sheng, R., T. T. Zhang, V. D. Felice, T. Qin, Z. H. Qin, C. D. Smith, E. Sapp, M. Difiglia and C. Waeber (2014). "Preconditioning stimuli induce autophagy via sphingosine kinase 2 in mouse cortical neurons." J Biol Chem **289**(30): 20845-20857.

Sofroniew, M. V. (2009). "Molecular dissection of reactive astrogliosis and glial scar formation." Trends Neurosci **32**(12): 638-647.

Sofroniew, M. V. (2014). "Astrogliosis." Cold Spring Harb Perspect Biol **7**(2): a020420.

Sofroniew, M. V. (2015). "Astrocyte barriers to neurotoxic inflammation." Nature Reviews Neuroscience **16**(5): 249-263.

Sofroniew, M. V. and H. V. Vinters (2010). "Astrocytes: biology and pathology." Acta Neuropathologica **119**(1): 7-35.

Song, S., H. Huang, X. Guan, V. Fiesler, M. I. H. Bhuiyan, R. Liu, S. Jalali, M. N. Hasan, A. K. Tai, A. Chattopadhyay, S. Chaparala, M. Sun, D. B. Stolz, P. He, D. Agalliu, D. Sun and G. Begum (2021). "Activation of endothelial Wnt/beta-catenin signaling by protective astrocytes repairs BBB damage in ischemic stroke." Prog Neurobiol **199**: 101963.

Spiegel, S. and S. Milstien (2000). "Sphingosine-1-phosphate: signaling inside and out." FEBS Lett **476**(1-2): 55-57.

Spiegel, S. and S. Milstien (2003). "Sphingosine-1-phosphate: an enigmatic signalling lipid." Nat Rev Mol Cell Biol **4**(5): 397-407.

Spiegel, S. and S. Milstien (2011). "The outs and the ins of sphingosine-1-phosphate in immunity." Nat Rev Immunol **11**(6): 403-415.

Swanson, K. V., M. Deng and J. P. Ting (2019). "The NLRP3 inflammasome: molecular activation and regulation to therapeutics." Nat Rev Immunol **19**(8): 477-489.

Taha, T. A., T. D. Mullen and L. M. Obeid (2006). "A house divided: ceramide, sphingosine, and sphingosine-1-phosphate in programmed cell death." Biochim Biophys Acta **1758**(12): 2027-2036.

Takasugi, N., T. Sasaki, K. Suzuki, S. Osawa, H. Isshiki, Y. Hori, N. Shimada, T. Higo, S. Yokoshima, T. Fukuyama, V. M. Lee, J. Q. Trojanowski, T. Tomita and T. Iwatsubo (2011). "BACE1 activity is modulated by cell-associated sphingosine-1-phosphate." J Neurosci **31**(18): 6850-6857.

Thudichum, J. L. W. (1884). " A treatise on the Chemical Constitution of the Brain. Archon Books." Glasgow Med J. **22(5)**: 363–364.

Thuy, A. V., C. M. Reimann, N. Y. Hemdan and M. H. Graler (2014). "Sphingosine 1-phosphate in blood: function, metabolism, and fate." Cell Physiol Biochem **34**(1): 158-171.

Ullian, E. M., S. K. Sapperstein, K. S. Christopherson and B. A. Barres (2001). "Control of synapse number by glia." Science **291**(5504): 657-661.

Van Doorn, R., J. Van Horssen, D. Verzijl, M. Witte, E. Ronken, B. Van Het Hof, K. Lakeman, C. D. Dijkstra, P. Van Der Valk, A. Reijerkerk, A. E. Alewijnse, S. L. Peters and H. E. De Vries (2010). "Sphingosine 1-phosphate receptor 1 and 3 are upregulated in multiple sclerosis lesions." Glia **58**(12): 1465-1476.

van Echten-Deckert, G. (2020). "Special Issue on "Sphingolipids: From Pathology to Therapeutic Perspectives"." Cells **9**(11).

van Echten-Deckert, G. (2023). "The role of sphingosine 1-phosphate metabolism in brain health and disease." Pharmacol Ther **244**: 108381.

van Echten-Deckert, G. and S. Alam (2018). "Sphingolipid metabolism - an ambiguous regulator of autophagy in the brain." Biol Chem **399**(8): 837-850.

van Echten-Deckert, G. and T. Herget (2006). "Sphingolipid metabolism in neural cells." Biochim Biophys Acta **1758**(12): 1978-1994.

van Kruining, D., Q. Luo, G. van Echten-Deckert, M. M. Mielke, A. Bowman, S. Ellis, T. G. Oliveira and P. Martinez-Martinez (2020). "Sphingolipids as prognostic biomarkers of neurodegeneration, neuroinflammation, and psychiatric diseases and their emerging role in lipidomic investigation methods." Adv Drug Deliv Rev **159**: 232-244.

Vander Heiden, M. G., L. C. Cantley and C. B. Thompson (2009). "Understanding the Warburg effect: the metabolic requirements of cell proliferation." Science **324**(5930): 1029-1033.

Vardjan, N., H. H. Chowdhury, A. Horvat, J. Velebit, M. Malnar, M. Muhic, M. Kreft, S. G. Krivec, S. T. Bobnar, K. Mis, S. Pirkmajer, S. Offermanns, G. Henriksen, J. Storm-Mathisen, L. H. Bergersen and R. Zorec (2018). "Enhancement of Astroglial Aerobic Glycolysis by Extracellular Lactate-Mediated Increase in cAMP." Front Mol Neurosci **11**: 148.

Vogel, P., M. S. Donoviel, R. Read, G. M. Hansen, J. Hazlewood, S. J. Anderson, W. Sun, J. Swaffield and T. Oravecz (2009). "Incomplete inhibition of sphingosine 1-phosphate lyase modulates immune system function yet prevents early lethality and non-lymphoid lesions." PLoS One **4**(1): e4112.

Volterra, A. and J. Meldolesi (2005). "Astrocytes, from brain glue to communication elements: the revolution continues." Nat Rev Neurosci **6**(8): 626-640.

Wang, G. and E. Bieberich (2018). "Sphingolipids in neurodegeneration (with focus on ceramide and S1P)." Adv Biol Regul **70**: 51-64.

Yamagata, K. (2021). "Astrocyte-induced synapse formation and ischemic stroke." J Neurosci Res **99**(5): 1401-1413.

Yan, H., D. W. Parsons, G. Jin, R. McLendon, B. A. Rasheed, W. Yuan, I. Kos, I. Batinic-Haberle, S. Jones, G. J. Riggins, H. Friedman, A. Friedman, D. Reardon, J. Herndon, K. W. Kinzler, V. E. Velculescu, B. Vogelstein and D. D. Bigner (2009). "IDH1 and IDH2 mutations in gliomas." N Engl J Med **360**(8): 765-773.

Zhu, A., R. Romero and H. R. Petty (2011). "An enzymatic colorimetric assay for glucose-6-phosphate." Anal Biochem **419**(2): 266-270.

8. ABBREVIATIONS

AD	Alzheimer's disease
ADP	Adenosine diphosphate
Akt	serine/threonine kinase
ALS	myotrophic lateral sclerosis
AMP	adenosine monophosphate
ANLS	astrocyte-neuronal lactate shuttle
APOE	apolipoprotein E
APP	amyloid precursor protein
APS	ammonium peroxydisulfate
ASM	acid sphingomyelinase
ATG	autophagy related protein
ATP	adenosine triphosphate
BSA	bovine serum albumin
cDNA	complementary deoxyribonucleic acid
CDase	ceramidase
CMA	chaperone-mediated autophagy
CerS	ceramide synthase
CNS	central nervous system
DAMP	damage- or danger-associated molecular pattern
DDX3X	DEAD–box helicase 3 X–linked
DMEM	Dulbecco's modified eagle medium
DMSO	dimethyl sulfoxide
EAP	ethanolamine phosphate
EDTA	ethylenediaminetetraacetate
EGF	epidermal growth factor
ER	endoplasmic reticulum
FBS	fetal bovine serum
GAPDH	glyceraldehyde 3-phosphate dehydrogenase
GFAP	glial fibrillary acidic protein
GFP	green fluorescent protein

IFN	interferon
IGF	insulin-like growth factor
HD	huntingtin’s disease
HAT	histone acetyltransferase
HDAC	histone deacetylase
HRP	horseradish peroxidase
IHC	immunohistochemistry
IHF	immunohistofluorescence
IL	interleukin
kDa	kilodalton
LC3	microtubule-associated protein 1A/1B-light chain 3
LPS	lipopolysaccharide
MAPK	mitogen-activated protein kinase
mM	millimolar
mRNA	messenger ribonucleic acid
mTOR	mammalian target of rapamycin
nM	nanomolar
NO	Nitric oxide
PBS	phosphate buffer saline
PCR	polymerase chain reaction
PD	Parkinson’s disease
PDH	pyruvate dehydrogenase
PE	phosphatidylethanolamine
PFA	paraformaldehyde
PFK	Phosphofructokinase
PGE	prostaglandin E2
PI3K	phosphatidylinositol-4,5-biphosphate 3-kinase
P2X	
P2Y1R	purinergic receptor 1
ROS	reactive oxygen species
S1P	sphingosine 1-phosphate
S1PR	sphingosine 1-phosphate receptor
SK	sphingosine kinase

SL	sphingolipid
SM	sphingomyelin
SMase	sphingomyelinase
SMS	sphingomyelin synthase
SNCA	synuclein alpha
Sph	sphingosine
SGPL1	sphingosine 1-phosphate lyase
SPP	sphingosine 1-phosphate phosphohydrolase
SPT	serine palmitoyl transferase
TCA	tri carboxylic acid
TNF	tumor necrosis factor
µl	microliter
µg	microgram
µm	micrometer
µM	micromole

9. ACKNOWLEDGMENT

The success of worthy discoveries relies on the guidance and direction provided and for this I am deeply grateful and hold utmost respect for my supervisor, **P.D. Dr. Gerhild van Echten Deckert**. Her unwavering support, invaluable guidance, and determination have made this research possible. Dr. Gerhild has consistently been available to assist me with any difficulties I encountered during my work, always pointing me in the right direction. Working on such an intriguing topic under her guidance has been a privilege.

I would also like to extend my gratitude to **Prof. Dr. Dirk Menche** for agreeing to act as the second referee for my thesis. I am also grateful for the collaborative project I had the privilege of working on during my initial research period at the University of Bonn.

My special thanks also go to **Prof. Dr. Lukas Schreiber** and **Prof. Dr. Dieter O. Fürst** for their participation as referees for the thesis dissertation. Their expertise and feedback will be invaluable.

I am thankful to the LIMES Institute and the University of Bonn for providing a good research environment and necessary resources for conducting my research. It has been enriching to discuss my work with individuals from various fields, and for that I would like to express my appreciation to the organizers of the BIGS retreats for facilitating such opportunities.

I would like to express my deepest gratitude to my husband, Shah Alam, for being an incredibly supportive and patient partner throughout my Ph.D. journey. His unwavering help and understanding have played a crucial role in my success.

I would also like to thank my friends and colleagues at the University of Bonn for creating a pleasant and collaborative atmosphere during my stay. Their companionship and support have made my academic journey all the more enjoyable.

Lastly, I want to convey my heartfelt gratitude to my parents and my brothers for their love and support throughout my academic journey and their belief in me has been a constant source of inspiration.

10. PUBLICATIONS

Parts of the dissertation that have been published:

1. Alam, S., **Afsar, S.Y.,** van Echten-Deckert, G. "S1P Released by SGPL1-Deficient Astrocytes Enhances Astrocytic ATP Production via S1PR2,4, Thus Keeping Autophagy in Check: Potential Consequences for Brain Health" IJMS (2023) https://doi.org/10.3390/ijms24054581
2. **Afsar, S.Y.,** Alam, S., Fernandez Gonzales, C., van Echten-Deckert, G. "Sphingosine-1-phosphate-lyase deficiency affects glucose metabolism in a way that abets oncogenesis" Mol. Oncol. 16, 3642 - 3653 (2022) http://doi.org/10.1002/1878-0261.13300
3. Piazzesi, A., **Afsar, S.Y.,** van Echten-Deckert, G. "Sphingolipid metabolism in the development and progression of cancer: one cancer's help is another's hindrance". Mol. Oncol. 15, 3256-79 (2021) https://doi.org/10.1002/1878-0261.13063

Publications submitted:

4. Alam, S., **Afsar, S.Y.,** Wolter, M., Volk, L., Mitroi, D.N., Heringdorf, D.M., van Echten-Deckert, G. SGPL1 Deficiency Promotes Astrogliosis and NLRP3 Inflammasome Activation Triggered by Purinergic Stimulation in the Brain (2023)
5. Philipp Wollnitzke, Raphael Wagner, **Sumaiya Yasmeen Afsar**, Christa Müller, Oliver Werz, Gerhild van Echten-Deckert, and Dirk Menche. “Total synthesis and biological evaluation of simplified ajudazol derivatives reveal potent anti-inflammatory efficiency and high apoptotic activity in neuroblastoma cells” (2023)